The conformational dynamics of BsoBI, analyzed by fluorescence spectroscopy down to the single molecule level

Inauguraldissertation

zur Erlangung des Grades
Doktor der Naturwissenschaften
Dr. rer. nat.
Im Fachbereich Biologie und Chemie
der Justus-Liebig-Universität Gießen

vorgelegt von

Dipl. Molekularbiologin und Physiologin
Jasmina Dikić

Gießen, 2009

The present study has been carried out within the Marie Curie Research Training Network "DNA enzymes", at the Institute of Biochemistry, Justus-Liebig-University Giessen, between April 2006 and October 2009, under the supervision of Prof. Dr. Alfred Pingoud.

Advisor	Prof. Dr. Alfred Pingoud Institut für Biochemie Justus-Liebig-Universität Heinrich-Buff-Ring 58 35392 Gießen
Co-Advisor	Prof. Dr. Michael U. Martin Institut für Immunologie Justus-Liebig-Universität Winchesterstraße 2 35394 Gießen

Erklärung

Hiermit versichere ich, die vorliegende Arbeit selbständig verfasst und keine anderen als die angegebenen Hilfsmittel benutzt zu haben. Stellen, die ich anderen Arbeiten und Veröffentlichungen dem Wortlaut oder Sinn entsprechend entnommen habe, sind durch Quellenangaben gekennzeichnet.

Gießen, den 9.11.2009

Acknowledgements

I would like to thank:

Prof. Dr. Alfred Pingoud, for invaluable discussions, ideas, motivation, and great knowledge which inspired me to learn more and work better every day. Thank You for the opportunity to be the part of the Institute of Biochemistry.

Prof. Dr. Michael U. Martin, for taking over the reading of this manuscript.

Dr. Wolfgang Wende, for constant help, great patience, productive discussions, helpful criticisms, and for supporting and encouraging me all the time. Above all, thank You for teaching me to enjoy my work, even when it didn't go as planned.

My friends all over Europe, whose diverse life experiences and cultures made me a better person:

Michele, my single-molecule fellow, for helpful discussions and a great time together, in Giessen, Düsseldorf and all other places we had fun at.

George, for your experience, knowledge and passion for science, and Silke, for your great spirit and fun times together.

Jadranka, Laura, Daniel, Lena, Ines W, thank you for all the fun we had, in different periods of my life in Giessen; you were all an important part of it.

My labmates, Ines F. for nice working atmosphere, and Dr. Vera Pingoud for all helpful advices.

All the people at the Institute of Biochemistry, for always creating an exciting working atmosphere.

My friends from the Marie Curie Network, for great scientific discussions and amazing fun we had in the past three years.

Our collaboration partners, Prof. Dr. Claus Seidel, for introducing me to single-molecule world, Dr. Paul Rothwell and Evangelos Sisamakis, for their help and patience, and all the people at the Institute of Molecular Physical Chemistry in Düsseldorf, who made my long days in their lab much easier.

I would especially like to thank my parents and my sister, for their constant support for everything I did, for their love, encouragement, sacrifice, and for understanding my decision to continue my scientific life in Germany.

I would like to thank the Marie Curie Research Training Network "DNA Enzymes" for funding my work.

Abbreviations

2-ME	2-Mercaptoethanol
A	Ampere
a.u.	Arbitrary unit
APS	Ammoniumpersulfate
ATP	Adenosine triphosphate
bp	Base pair(s)
BSA	Bovine serum albumin
dATP	Deoxyadenosine triphosphate
DNA	Deoxyribonucleic acid
DTT	1,4-dithiothreitol
EDTA	Ethylene diamine tetraacetate
e.g.	Exempli gratia; for example
EMSA	Electrophoretic mobility shift assay
FPLC	Fast protein liquid chromatography
FRET	Fluorescence resonance energy transfer
g	Gram
i.e.	Id est; that is
IPTG	Isopropyl-β-D-1-thiogalactopyranoside
l	Liter
LB	Luria-Bertani
m	Milli
M	Molar
MFD	Multiparameter fluorescence detection
min	Minute
MW	Molecular weight
n	Nano
NaOAc	Sodium acetate
o/n	Overnight
OD	Optical density
p	pico
PAGE	Polyacrylamide gel electrophoresis
PCR	Polymerase chain reaction
rpm	Rotations per minute
SDS	Sodium dodecyl sulfate
sec	Second
TCEP	Tris(2-carboxyethyl)phosphine
TEMED	Tetramethylethylenediamine
UV	Ultraviolet
vs.	versus
v/v	Volume/volume
w/v	Weight/volume
µ	Micro

Table of Contents

Abbreviations 5
1. Introduction 9
1.1. Restriction-modification systems in bacteria 9
1.2. Type II restriction enzymes 11
1.3. BsoBI restriction enzyme 14
1.4. Fluorescence spectroscopy of single molecules in solution 16
1.5. Structural dynamics of proteins probed by single-molecule techniques 18
1.6. Aim 20
2. Materials and methods 21
2.1. Materials 21
2.1.1. Chemicals and biochemicals 21
2.1.2. Plasmids 22
2.1.3. Bacterial strains 22
2.1.4. Buffers 22
2.1.5. Enzymes 23
2.1.6. Markers 24
2.1.7. Fluorophores 24
2.2. Methods 25
2.2.1. Microbiological methods 25
2.2.1.1. Culture media 25
2.2.1.2. Preparation of electrocompetent cells 25
2.2.1.3. Electroporation 25
2.2.2. Molecular biology methods 25
2.2.2.1. Electrophoresis 25
2.2.2.1.1. SDS-PAGE 26
2.2.2.1.2. Polyacrylamide gel electrophoresis 26
2.2.2.1.3. Agarose gel electrophoresis 26
2.2.2.1.4. EMSA 26
2.2.2.1.5. Denaturing polyacrylamide gel electrophoresis 27
2.2.2.2. Isolation of DNA 27
2.2.2.2.1. Minipreparation 27
2.2.2.2.2. Midipreparation 27
2.2.2.2.3. PCR purification 27
2.2.3. Creating single-cysteine BsoBI variants 27
2.2.3.1. Site-directed mutagenesis 27
2.2.3.2. Screening 28
2.2.3.3. Overexpression of BsoBI 28
2.2.3.4. Purification of BsoBI 29

2.2.3.5. Determination of protein concentration 29
2.2.3.6. Determination of protein binding and cleavage activity 30
2.2.3.6.1. Determination of binding activity 30
2.2.3.6.2. Determination of cleavage activity 30
2.2.4. Michaelis-Menten kinetics 30
2.2.5. Site-specific fluorescent labeling of single-cysteine variants 31
2.2.5.1. Labeling and purification of proteins used in steady-state and stopped-flow experiments 32
2.2.5.2. Labeling and purification of proteins used in single-molecule experiments 33
2.2.5.3. Determination of labeling efficiency 35
2.2.5.4. Determination of binding and cleavage activity 35
2.2.6. Fluorescence methods 35
2.2.6.1. Introduction to fluorescence 35
2.2.6.2. Fluorescence Resonance Energy Transfer (FRET) 36
2.2.6.3. Steady-state ensemble FRET experiments 38
2.2.6.4. Fluorescence stopped-flow experiments 39
2.2.6.5. Multiparameter single-molecule fluorescence spectroscopy 41
3. Results 44
3.1. Determination of binding and cleavage activity of different single-cysteine BsoBI variants 44
3.2. Michaelis-Menten kinetics 46
3.3. Site-specific labeling of BsoBI 48
3.3.1. Random double labeling of BsoBI used in ensemble experiments 49
3.3.2. Double labeling of BsoBI used in single-molecule experiments 52
3.4. DNA binding induces conformational changes in the catalytic domain of BsoBI 55
3.5. Ca^{2+} and Mg^{2+} ions have a different influence on the catalytic domain of BsoBI 57
3.6. Pre-steady state experiments reveal different enzyme kinetics in the presence of Ca^{2+} and Mg^{2+} ions 59
3.6.1. Kinetics of conformational changes induced by DNA binding to the double labeled BsoBI A153C variant 59
3.6.2. Kinetics of DNA binding to the BsoBI A153C variant using fluorescently labeled DNA and labeled protein 61
3.6.3. Kinetics of DNA binding and cleavage in the presence of Mg^{2+} ions 62
3.6.4. Influence of Ca^{2+} and Mg^{2+} ions on the conformation of the catalytic domain of BsoBI 63
3.6.5. Influence of Ca^{2+} and Mg^{2+} ions on the catalytic activity of BsoBI 69
3.7. Single-molecule experiments reveal the existence of two conformations of free BsoBI 72
3.7.1. Conformational changes during DNA binding in the presence of Ca^{2+} ions 73
3.7.2. Conformational changes during DNA binding and cleavage in the presence of Mg^{2+} ions 77

4. Discussion 81
4.1. Creating catalytically inactive single-cysteine BsoBI variants 81
4.2. Michaelis-Menten kinetics 82
4.3. Site-specific fluorescent labeling of selected single-cysteine BsoBI variants 82
4.4. DNA binding induces conformational change in the catalytic domain of BsoBI 84
4.5. Kinetic studies of BsoBI substrate binding and cleavage – influence of Ca^{2+} and Mg^{2+} ions 85
4.6. Conformational changes in BsoBI during DNA binding and cleavage studied on the single-molecule level 89
5. Summary 93
6. Zusammenfassung 95
7. References 98
Supplementary information 102

1. Introduction

1.1. Restriction-modification systems in bacteria

The phenomenon of restriction was first observed in the early 1950s, when some bacterial strains were observed to show the property of inhibiting the reproduction of viruses previously grown on different strains [1, 2]. This effect was connected to sequence-specific endonucleases [2]. Restriction-modification (R-M) systems consist of pairs of opposing enzyme activities: restriction endonuclease and methyltransferase activity [3], and their main function is the defence of the host organism against foreign DNA [4]. The mechanism of defence consists of the recognition of the incoming foreign DNA and cleaving at defined recognition sites [5]. Foreign DNA lacks specific modification within the recognition site, while the host DNA is modified by its methyltransferase at these sites, and thus is resistant to cleavage [5] (Figure 1.1). Recognition sequences are usually 4 to 8 bp long, continuous or interrupted, symmetric or asymmetric, unique or degenerate [3]. Restriction endonucleases and methyltransferases from the same system recognize the same sequence.

Methyltransferases add one methyl group to adenine or cytosine in each strand of the recognition sequence, which sterically blocks restriction enzyme:DNA binding, and prevents host genome cleavage by the restriction enzyme [3].

Restriction endonucleases catalyze double strand breaks in DNA, within or close or at a random distance (depending on the type) to the recognition sequence, requiring (with few exceptions) the presence of Mg^{2+} [3, 6].

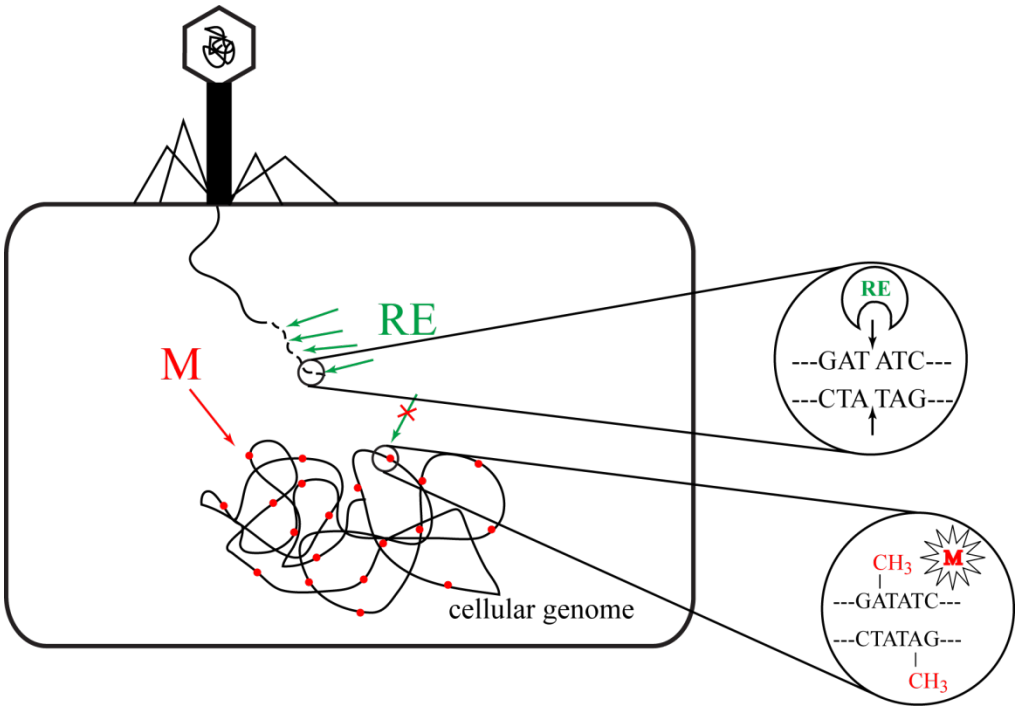

Figure 1.1 Schematic view of bacteriophage infection and host defence. *RE – restriction enzyme (here EcoRV as an example), M – modification enzyme. Detailed explanation in the text.*

Restriction modification systems occur in archaea, bacteria [7, 8] and certain viruses [9]. Up to date, almost 4000 different R-M systems have been identified [10]. Also, many different R-M systems can be present in one species: *Neisseria gonorrhoeae* has 16 biochemically identified R-M systems [11]. *Helicobacter pylori* and *Methanococcus jannaschii* have 30 and 13 genes for methyltransferase identified, respectively, that could belong to R-M systems [12].

Although most of restriction endonucleases and methyltransferases are coded together in the genome, there are some exceptions. *Escherichia coli* has two methyltransferases unlinked to the respective endonucleases, Dam (DNA-adenine methyltransferase) and Dcm (DNA-cytosine methyltransferase) [13]. Dam is involved in Dam-directed mismatch repair [14], as well as in gene regulation [13], while Dcm is required for very short patch (VSP) mismatch repair [15, 16].

Restriction endonucleases differ in structure, recognition site, cleavage site and required cofactors, and based on these differences they are classified into 4 types: Type I, Type II, Type III and Type IV [17].

Type I restriction enzymes have three different subunits, HsdM (responsible for modification), HsdR (responsible for restriction) and HsdS (responsible for sequence recognition) [18]. The holoenzyme consists of two modification subunits, two restriction

subunits and one sequence recognition subunit. They require ATP, Mg^{2+} and AdoMet (S-Adenosylmethionine) for activity, and recognize two asymmetric bi-partite recognition sites, cleaving approximately half way between the sites [19].

Type III restriction enzymes have two different subunits, Mod (responsible for DNA recognition and modification) and Res (responsible for cleavage), in Mod_2Res_2 stoichiometry [18]. They require ATP and Mg^{2+} for activity, and recognize two copies of head-to-head oriented recognition sequences, cleaving close to one of them [20].

Type IV restriction enzymes are not part of R-M systems, since they recognize and cleave only methylated DNA [17]. A typical representative of this group is McrBC, which consists of two subunits, McrB (responsible for DNA recognition) and McrC (responsible for cleavage) [21]. It requires GTP and Mg^{2+} for activity, and at least two RmC sequences (purine followed by methylated cysteine), cleaving close to one of the recognition sites [18, 22].

Since BsoBI is a Type II restriction enzyme, this group of enzymes will be discussed in more details.

1.2. Type II restriction enzymes

Type II restriction enzymes are well studied, with many reviews available [5, 6, 23, 24]. Type II REases are very powerful tools for genetic engineering, and thus very well genetically and biochemically characterized (there are more than 3500 Type II REases in the REBASE database from 2007) [10]. The orthodox Type II REase recognizes 4 to 8 bp long sequences, and cleaves both DNA strands within or close to the recognition site, leaving 3'-OH and 5'-phosphate ends (Figure 1.2). The catalytic mechanism shown in Figure 1.2 is also known as associative mechanism, in which the transition bypyramidal state is formed before the bond cleavage. However, the latest computational studies on the EcoRV restriction enzyme suggest that the most probable catalytic mechanism is dissociative, and that Mg^{2+} ions might have the role of activating the water molecule involved in nucleophilic attack [25]. Type II REases are usually homodimeric or homotetrameric, and do not require ATP or GTP, but usually (with some exceptions) only Mg^{2+} as cofactor.

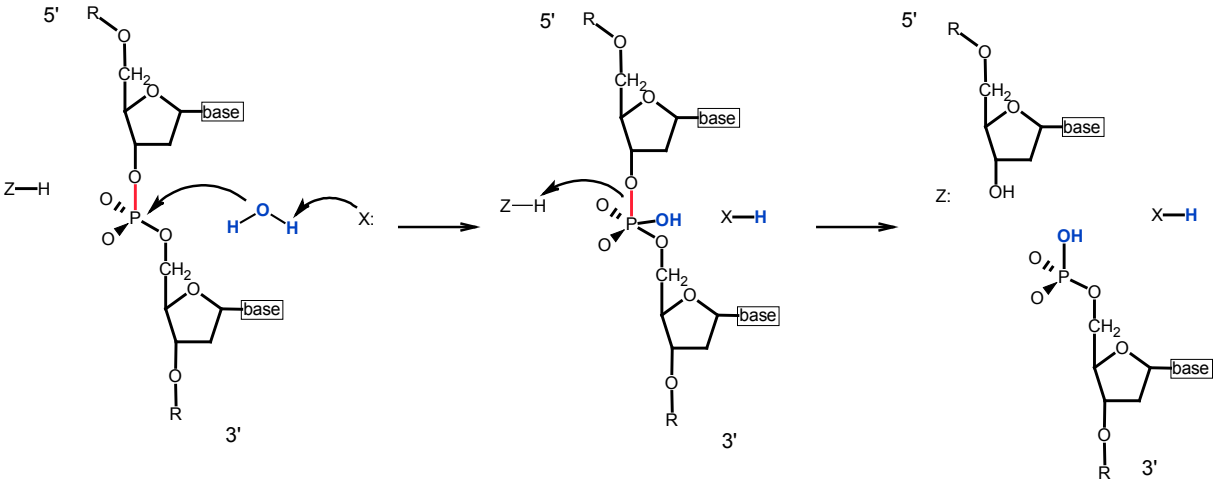

Figure 1.2 Hydrolysis of a phosphodiester bond. *General base (X) activates hydroxyl from water molecule which makes a nucleophilic attack at the phosphorus atom in the phosphodiester bond, leaving the phosphoryl group attached to the 5' end. The negatively charged leaving group is protonated by a general acid (Z). The bond that is cleaved is shown in red.*

Many Type II REases do not have these orthodox characteristics, so the division into subgroups was necessary, based on cleaved sequence or the structure of the enzymes [17]. However, due to the great diversity among Type II REases, overlaps cannot be avoided. The subgroups of Type II enzymes are listed below, and for a more detailed description see references [5, 17, 26].

Type IIA enzymes recognize an **a**symmetric sequence, and cleave within or a few base pairs away from the sequence. Typical representatives of this group are: FokI, Bpu10I and AciI.

Type IIB enzymes cleave both strands of DNA at both sides of the recognition sequence. Typical representatives are BplI and BcgI.

Type IIC enzymes are all Type II enzymes that have both cleavage and modification domains within one polypeptide. Due to this structural characteristic, many Type IIB, Type IIG and Type IIH enzymes are classified also as Type IIC enzymes (e.g. BcgI, HaeIV). They recognize both symmetric and asymmetric target sequences.

Type IIE enzymes interact with two copies of the recognition sequence, where one copy is the target for cleavage, and the other, in *cis* or *trans*, is serving as the allosteric effector. Typical examples and well studied Type IIE enzymes are EcoRII and NaeI.

Type IIF enzymes are usually homotetramers and interact with two copies of recognition sequence, cleaving both of them. Typical examples are SfiI and NgoMIV.

Type IIG enzymes are very similar to Type IIC enzymes, having both cleavage and modification domains in a single polypeptide. The only difference is that they may be

stimulated by AdoMet, and thus they were previously classified as Type IV enzymes. Typical representatives are Eco57I and BsgI.

Type IIH enzymes have the same genetic organization as Type I enzymes, but biochemically behave as Type II enzymes. They can recognize symmetric or asymmetric sequences, and typical representatives are AhdI and PshAI.

Type IIM enzymes recognize specific **m**ethylated sequence and cleave at a fixed site. They should not be mixed up with Type IV REases, since those enzymes do not have a defined DNA cleavage site. The best studied representative is DpnI.

Type IIP enzymes are homodimeric and recognize symmetric (**p**alindromic) sequences and cleave at fixed symmetrical locations within or immediately adjacent to the sequence. Recognition sequences can be interrupted with segments of unspecified sequences, but specified length. The products can have "blunt" or "sticky" ends (with 3'- or 5'-overhangs). Most of the enzymes used for genetic engineering belong to this subgroup, and thus many of them are well studied, e.g. EcoRI and EcoRV.

Type IIS subgroup of enzymes is the earliest identified group of Type II REases. They recognize asymmetric sequences, similar to Type IIA enzymes, but cleave at least one DNA strand outside of the recognition sequence (the cleavage site is **s**hifted away from the recognition site). The best known representative of this group is FokI, whose structural information helped determining structural information of other enzymes from this group.

Type IIT enzymes are heterodimers and can recognize both symmetric and asymmetric sequences. Typical examples are Bpu10I and BslI.

Some Type II enzymes cleave only one DNA strand, and these enzymes are called nicking enzymes. Some of the examples include Nt.BstNBI, Nt.BstSEI and Nt.CviPII (where Nt stands for **n**icking the **t**op strand). Some of the nicking enzymes play a role in mismatch repair, where they nick the G/T mismatch resulting from deamination of 5mC within the recognition sequence of the accompanied MTase.

Although Type II REases are extensively studied, many of them have not been characterized in details, and for many of them it is not yet known to which group they belong. However, it can be concluded that the range of cleavage modes is much larger than previously expected, as has been shown in [27].

Although restriction enzymes and methyltransferases from the same RM system recognize the same DNA sequence, they do not have strong amino acid sequence similarity, and their target recognition domains are usually different [7, 28, 29]. However, different methyltransferases have strong amino acid sequence similarity, with the target recognition domain being the

largest variable region [30-34]. Based on these properties, it is assumed that restriction endonucleases and methyltranferases from Type II system are the result of independent evolution. Methyltransferases probably evolved as enzymes with important function in gene regulation or replication, providing a genetic background of methylated genome in which restriction endonucleases could evolve [7].

1.3. BsoBI restriction enzyme

BsoBI is a thermostable Type IIP restriction enzyme, purified from the thermophilic gram-positive bacterium *Bacillus stearothermophilus* [35]. It recognizes the 6 bp symmetric sequence 5'-CYCGRG-3' (where Y represents pyrimidine, and R represents purine), and cleaves between the first and the second base [36, 37]. It requires Mg^{2+} ions for double strand cleavage and has the optimal cleavage temperature of 65 °C [36]. Crystallographic studies had shown that BsoBI is a homodimer which completely encircles the DNA, so that the recognition sequence lies within a 20 Å long tunnel formed by the protein, which excludes water molecules form the solvent (Figure 1.3) [38]. Each subunit of BsoBI contains 323 amino acids and has a molecular weight of 36.7 kDa. The analysis of the crystal structure showed that protein-DNA interactions are symmetric and that there are no significant differences between the two active sites [38].

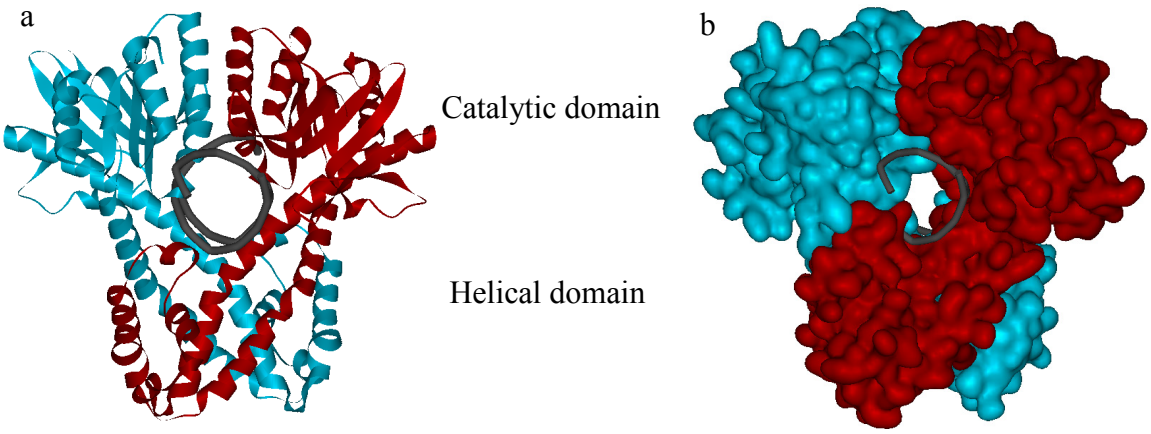

Figure 1.3 Structure of the BsoBI-DNA complex. *a) The protein subunits (shown in blue and red) encircle the DNA (shown in grey) b) Molecular surface of the protein, showing complete enclosure of DNA in the tunnel*

BsoBI belongs to the EcoRI family of restriction enzymes. This family shares the common PD…D/ExK motif in the catalytic site, where x represents a hydrophobic residue [39]. Three charged residues are arranged near the reactive phosphate group of the phosphodiester bond to

be cleaved, and an additional catalytic residue (acidic) is present at different positions in different REases (Figure 1.4) [39]. The three catalytic residues in BsoBI are D212, E240 and K242. Structurally equivalent to the fourth residue in BsoBI is D201, but it cannot be involved in catalysis since it is well removed from the active site [38]. Thus, H253 was proposed as putative catalytic residue, positioned to act as a general base during catalysis [38]. Apart from this His253, residue Glu252 was proposed as an important catalytic residue, which may be involved in metal ion binding [38]. Although histidines can be effective general bases, they were not seen in restriction endonucleases so far, and BsoBI could be the first enzyme that has histidine-mediated catalysis.

Figure 1.4 Catalytic sites of EcoRI (a) and BsoBI (b). *DNA is shown in black, and bases between which the cleavage occurs are shown in red. The putative BsoBI catalytic residue His253 is shown in green. Detailed explanation in the text.*

Putative catalytic residues of BsoBI were also analyzed by random mutagenesis [36]. Mutations in residues D124, D212, D246 and E252 led to the loss of catalytic activity, but not binding activity, thus these residues were proposed to be located near or within the active site [36]. In the same study histidine residue 253 was found to be an important catalytic residue.

The helical domain of BsoBI (see Figure 1.3) forms a compact structure with an important role in dimerization, but it also makes several contacts with DNA, especially with the uncleaved strand [38]. The catalytic domain is less compact and has a similar topology as the other enzymes from the EcoRI family. The gap between subunits is too small to allow DNA entry, so there must be large conformational changes prior to DNA binding. So far, only the structure of BsoBI with bound specific DNA was solved, and all attempts to crystallize the enzyme without DNA failed, which suggested a high mobility structure in the absence of DNA [38]. Based on the available crystal structure, it can be seen that the interface between the catalytic domains is much weaker than the one between the helical domains, so it could be

expected to see conformational changes in this part of the molecule. Determination of these conformational changes was one of the main questions of this work.

1.4. Fluorescence spectroscopy of single molecules in solution

Fluorescence spectroscopy methods were considered as primary methods in biophysics and biochemistry, but recently their use is expanding to other areas of research, e.g. biotechnology or cellular and molecular imaging. The reason is the fact that fluorescence is highly sensitive, it can cover a wide range of timescales (from femtoseconds to seconds, or longer), and it can be used to selectively examine certain molecules in complex mixtures, when it is combined with different single-molecule techniques [40-44].

Single-molecule experiments allow for separating subpopulations of macromolecules in solution, which would otherwise be hidden in ensemble experiments. They can provide information about time trajectories and distributions of these subpopulations, identify and sort them based on their properties [43, 45].

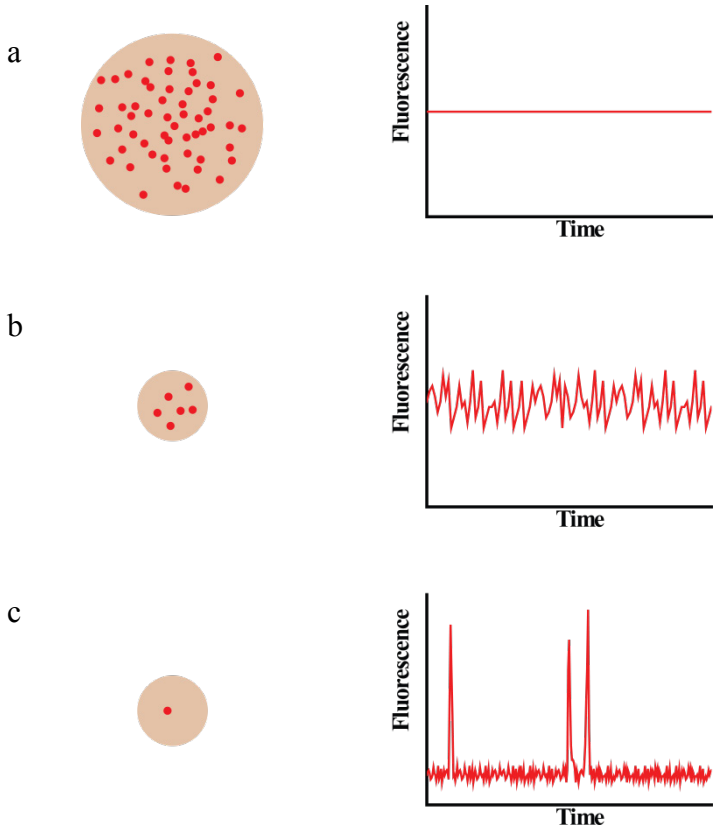

Figure 1.5 The difference between ensemble and single-molecule experiments. *a) Ensemble experiment where a large volume of highly concentrated molecules is observed, b) "Small ensemble" experiment where a smaller volume of diluted molecules is observed, c) Single-molecule experiment where a small volume of highly diluted molecules is observed, and single fluorescence bursts can be seen (adapted from Mukhopadhyay et al. [42]).*

Despite these advantages, certain criteria have to be fulfilled, and Figure 1.5 represents the transition between ensemble and single-molecule experiments, as well as the necessary conditions for a successful single-molecule setup.

In ensemble experiments, the output signal represents the average of all different subpopulations of molecules present in the solution. Usually, the observation volume is large and the concentration of investigated species is high. Lowering the observation volume, as well as the solution concentration, enables observation of single fluorescence bursts derived from single fluorescent molecule. In the setup used in this study, the observation volume was in the range of femtoliters, and the protein concentration used was 40-80 pM, conditions that allowed only one molecule at a time to pass through the observation volume.

The extent of energy transfer between donor and acceptor fluorophore in fluorescence resonance energy transfer (FRET) gives information about distances between those two fluorophores. Optimal distances that could be investigated using FRET are between 10 and 100 Å, which are typical distances in biomolecules. This fact makes FRET a very useful technique for the investigation of protein and DNA dynamics, protein folding, replication, transcription, translation and many other fundamental biological processes [46]. Typical FRET setups use one donor fluorophore and one acceptor fluorophore (so-called single-pair FRET), which allows the examination of biomolecules in one dimension (Figure 1.6).

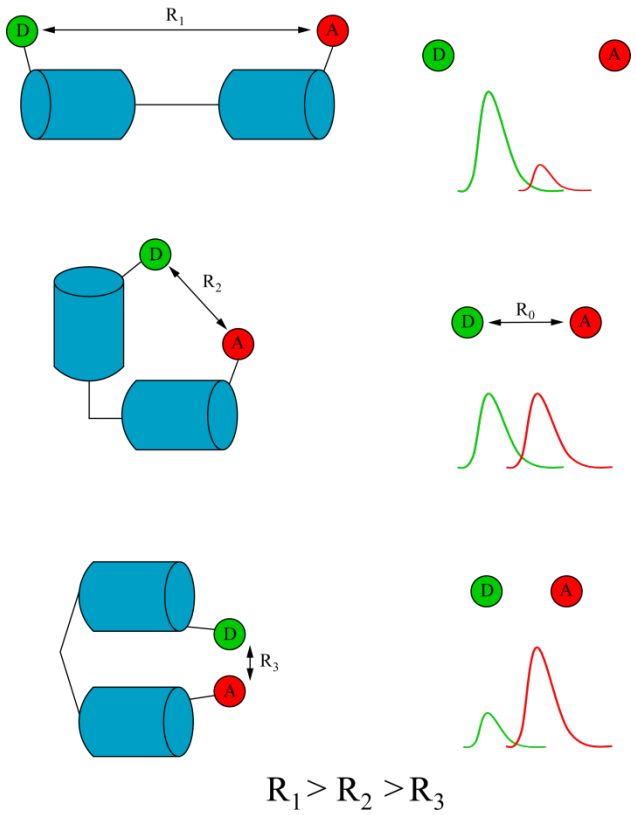

Figure 1.6 Schematic representation of intramolecular FRET. *The FRET efficiency depends strongly on the distance between two fluorophores. The distance equal to the R_0 value for certain donor/acceptor pair leads to 50 % of FRET efficiency; longer distance leads to lower FRET, while shorter distance leads to higher FRET efficiency. D – donor fluorophore; A – acceptor fluorophore.*

1.5. Structural dynamics of proteins probed by single-molecule techniques

For more than 30 years it is known that enzymes are not static but flexible structures [47-49] and this flexibility was shown to be crucial for various enzymatic functions, such as catalysis, allosteric regulation or ligand binding induced conformational changes [50-52]. Conformational rearrangements have wide range of timescales (from femtosecond timescale for bond vibrations to second timescale for large conformational rearrangements [Figure 1.7]) and are considered intrinsic features of all proteins. Although X-ray crystallography has provided important insight into different conformations one enzyme can have [53-55], it gives only a snapshot of the complex life cycle of the protein.

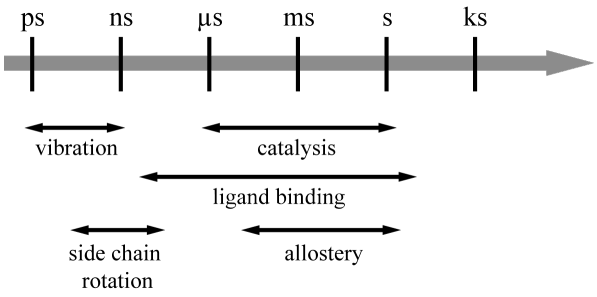

Figure 1.7 Timescale range of dynamic events in enzymes. *Adapted from Boehr et al. [56].*

Ensemble FRET has been used extensively to measure static distances in the range of 10-100 Å [57-60]. However, ensemble measurements record only the average responses, and rare events usually escape notice because they are buried in the average properties of the system. The first reported observation of FRET between a single donor and a single acceptor fluorophore [61] pointed out the potential of the single-molecule techniques and motivated further developments towards biological applications. The technique can now be used to study intramolecular conformational changes, when both fluorophores are attached to the same molecule, or intermolecular interactions, when two fluorophores are attached to different molecules. Intramolecular labeling can provide information about enzyme structural changes during catalysis, folding/unfolding of macromolecules as well as fluctuation and stability of macromolecules.

Single-molecule FRET can be observed in two different experimental setups: surface immobilization or free diffusion through the solution. Immobilized molecules can be observed for longer periods of time, providing information about several reaction cycles, but the proximity of the surface can cause artifacts. Molecules freely diffusing through the solution can be observed only for a short period of time while traveling through the observation volume (Figure 1.8), but this setup excludes surface artifacts, and can provide information about diffusion properties.

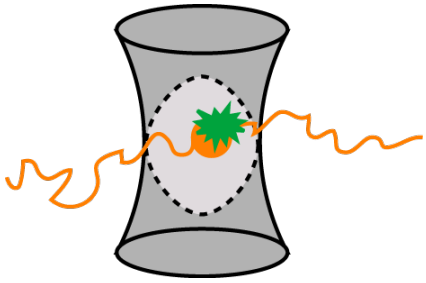

Figure 1.8 Single molecule diffusing through the optically defined observation volume. *Fluorescent molecules cause a rise of the detected fluorescent signal while passing through the observation volume.*

Many of the molecular machines essential for cell function and survival have complex kinetic pathways and intermediates, and also consist of several interacting components. The ability of different single-molecule techniques to follow structural dynamics of macromolecules is proving to be important for studies of many important processes (e.g. protein folding, replication, transcription). Although recent advances in single-molecule fluorescence spectroscopy allow for real-time observations of conformational changes on biologically relevant timescales [40, 43, 45, 62-65, and reviewed in 66], all experiments are performed under *in vitro* conditions. The real challenge will be to measure conformational dynamics *in vivo*, which will enable the studies of enzymes and multicomponent molecular machines in their natural environment.

1.6. Aim

The most striking feature of the restriction enzyme BsoBI is the complete encirclement of specific DNA inside the tunnel formed by two protein subunits. The gap between subunits is too small to allow DNA entry, and large conformational changes during substrate binding were suggested. The main goal of this study was to determine the nature and dynamics of these conformational changes. For this purpose, a set of single-cysteine variants had to be created, and labeled with different fluorescent dyes, and the ability of fluorescence resonance energy transfer (FRET) to monitor distance changes of biomolecules was used. The combination of the results obtained from different fluorescent techniques (ensemble steady-state and pre-steady state, as well as single molecule techniques) will allow the description of the catalytic cycle of BsoBI as well as the dynamics of this process.

2. Materials and methods

2.1. Materials

2.1.1. Chemicals and biochemicals

All chemicals and biochemicals used were of high purity grade and are listed in Table 1. All buffers were prepared using water from the Milli-Q Synthesis (Millipore) water purification system.

Table 1

Chemical	Company
Acetic acid	Roth
40% Acrylamide:bisacrylamide solution29:1	AppliChem
40% Acrylamide:bisacrylamide solution19:1	AppliChem
Agar	AppliChem
Agarose Ultra Pure ™	Invitrogen
Ammoniumpersulfate	Merck
Ampicillin	AppliChem
[α-^{32}P] dATP	Hartmann Analytic
[γ-^{32}P] ATP	Hartmann Analytic
Boric acid	Merck
Bromphenol blue	Merck
BSA	NEB
Calcium chloride	Merck
κ-Casein	AppliChem
Chloramphenicol	AppliChem
Coomassie® Brilliant blue G250	AppliChem
DTT	AppliChem
EDTA	AppliChem
Ethanol	Merck
Ethidium bromide	Roth
Formamide	Merck
Glycerol	AppliChem
Glycine	Merck
Imidazole	Merck
IPTG	AppliChem
Lubrol	Sigma
Magnesium chloride	Merck
2-Mercaptoethanol	Merck
Ni^{2+}-NTA-agarose	Qiagen
Poly(dI-dC)	GE Healthcare
Potassium chloride	Merck
Potassium dihydrogen phosphate	Merck

di-Potassium hydrogen phosphate	Merck
Sodium chloride	Merck
SDS	AppliChem
TCEP	Pierce
TEMED	Merck
Tris	Merck
Tryptone	AppliChem
Urea	AppliChem
Yeast extract	AppliChem

2.1.2. Plasmids

The gene for the BsoBI wild type enzyme (see Supplementary information for the sequences), with a His-tag on the N-terminus (5 histidines), was cloned into the pQE2 vector (Qiagen). This newly created pQE2-HisBsoBI plasmid was used to produce the cysteine free variant, where 3 cysteines, C214, C218 and C317, were exchanged to alanine, serine and alanine, respectively, and thereby the pQE2-HisBsoBI-cf plasmid was created. This plasmid was used for producing different single-cysteine variants.

Plasmid pACYC M.BsoBI codes for the BsoBI methyltransferase, and protects the host genome from BsoBI cleavage.

For activity assays, two different plasmids were used: pAT153 triple, which contains two BsoBI recognition sites, and pDGS, which contains one BsoBI recognition site.

2.1.3. Bacterial strains

The *E. coli* K12 strain XL1-Blue MRF' (Stratagene Europe) was used for expression of different BsoBI variants. The genotype of this strain is: Δ(*mcrA*)*183* Δ(*mcrCB-hsdSMR-mrr*)*173 endA1 supE44 thi-1 recA1 gyrA96 relA1 lac* [F′*proAB lacIqZΔM15 Tn10* (Tetr)].

The *E. coli* strain DH5α was used for amplification of the plasmid pAT153 triple. The *E. coli* strain XL1-Blue was used for amplification of the plasmid pDGS.

2.1.4. Buffers

Buffers used for protein purification (chapter 2.2.3.4.) were:

Digest buffer: 10 mM Tris-HCl pH 8.0, 500 mM NaCl, 15 mM imidazole, 0.5 mM EDTA

Washing buffer: 10 mM Tris-HCl pH 8.0, 200 mM NaCl, 15 mM imidazole, 0.5 mM EDTA

Elution buffer: 10 mM Tris-HCl pH 8.0, 200 mM NaCl, 200 mM imidazole, 0.5 mM EDTA

Dialysis buffer: 30 mM KPi pH 7.2, 0.5 mM EDTA, 0.1 mM 2-mercaptoethanol, 0.01 % (w/v) lubrol, 300 mM NaCl, 50 % glycerol

The cleavage buffer used for activity assays was: 10 mM Tris-HCl, 50 mM NaCl, 10 mM $MgCl_2$, pH 7.9. For binding assays, $MgCl_2$ in the cleavage buffer was replaced by $CaCl_2$ (supports specific binding, but not cleavage of DNA substrate).

Buffers used for FPLC purification of labeled proteins (chapter 2.2.5.2.) were:
Start buffer: 20 mM KH_2PO_4, 20 mM K_2HPO_4, pH 8.0
Elution buffer: 20 mM KH_2PO_4, 20 mM K_2HPO_4, 500 mM KCl, pH 8.0

Buffers used for steady state, stopped-flow and single molecule experiments were:
$CaCl_2$ buffer: 10 mM Tris-HCl pH 7.9, 50 mM NaCl, 5.5 mM $CaCl_2$
$MgCl_2$ buffer: 10 mM Tris-HCl pH 7.9, 50 mM NaCl, 5.5 mM $MgCl_2$
EDTA buffer: 10 mM Tris-HCl pH 7.9, 50 mM NaCl, 0.5 mM EDTA

2.1.5. Enzymes

Several restriction enzymes were used, and they are listed alphabetically in Table 2.

Table 2

Name	Recognition sequence	Company
AclI	5' - A A ^ C G T T - 3'	NEB
BsaI	5' - G G T C T C $(N)_1$^ - 3' 3' - C C A G A G $(N)_5$^ - 5'	NEB
BsrDI	5' - G C A A T G N N ^ - 3' 3' - C G T T A C ^ N N - 5'	NEB
DpnI	3‘ - G A* ^ T C – 5‘	Fermentas
NaeI	5' - G C C ^ G G C - 3'	NEB
NdeI	5' - C A ^ T A T G - 3'	NEB
PstI	5' - C T G C A ^ G - 3'	Fermentas
SphI	5' - G C A T G ^ C - 3'	Fermentas

^ represents cleavage position; N: A, C, T or G; * methylation site

DNA modification enzymes are listed in Table 3.

Table 3

Name	Company
Taq DNA polymerase	Overexpressed and purified in our institute
Pfu DNA polymerase	Overexpressed and purified in our institute
T4 Polynucleotide kinase	Fermentas

2.1.6. Markers

Weight markers used for protein and DNA gels are listed in Table 4.

Table 4

Name	Company
PageRuler^{TM} Unstained protein ladder	Fermentas
GeneRuler^{TM} 1kb	Fermentas
pUC Mix marker, 8	Fermentas

2.1.7. Fluorophores

For labeling of single-cysteine BsoBI variants, Alexa fluorophores, with a maleimide functional group were used: Alexa488 C_5 maleimide, Alexa594 C_5 maleimide and Alexa647 C_2 maleimide (Figure 2.1). All fluorophores used were purchased from Invitrogen.

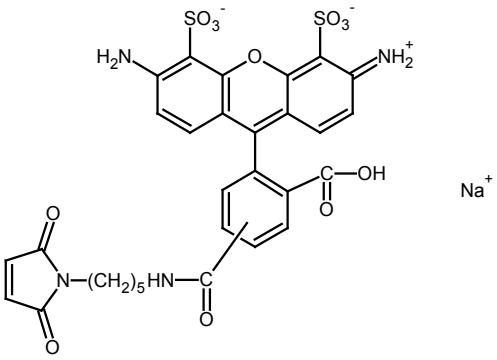

Alexa488 maleimide

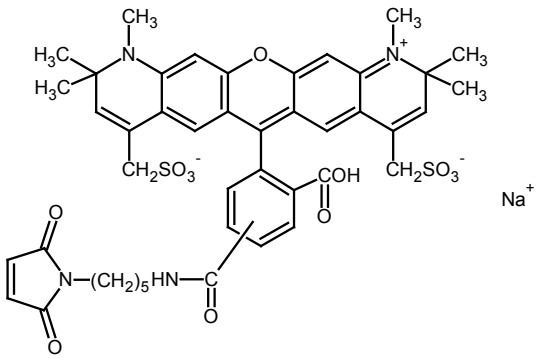

Alexa594 maleimide

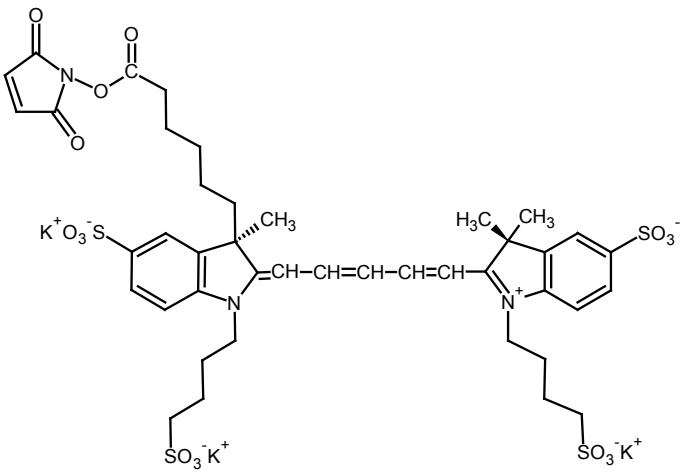

Alexa647 maleimide

Figure 2.1 Alexa fluorophores

2.2. Methods

2.2.1. Microbiological methods

2.2.1.1. Culture media

LB (Luria Bertani) medium was used for all bacterial cell growth.
LB medium: 10 g/l tryptone, 5 g/l yeast extract, 5 g/l NaCl
For making the agar plates, 1.5 % (w/v) of bacto-agar was added to the liquid medium.
Antibiotics were added to the media after sterilization, shortly before use.

2.2.1.2. Preparation of electrocompetent cells

500 ml of LB medium was inoculated with 10 ml of an overnight *E. coli* culture, and grown at 37 °C until an OD_{600} of 0.6-0.8 was reached. The culture was incubated on ice for 15 min and then centrifuged for 15 min at 4200 rpm, 4 °C (Beckman, J6-HC). The cell pellet was washed three times with ice cold 10 % (v/v) glycerol solution (250 ml, 150 ml and 20 ml, consecutively). After the last step of centrifugation, the cell pellet was resuspend in 2 ml of 10 % glycerol. The cells were separated into 80 µl aliquots, rapidly frozen in liquid nitrogen and stored at -80 °C.

2.2.1.3. Electroporation

Aliquots of frozen electrocompetent cells and plasmid for transformation were thawed on ice. The electroporation cuvette was cooled on ice. 4-10 ng of plasmid was mixed with an aliquot (80 µl) of electrocompetent cells, and incubated on ice for 5 minutes. The mixture was transferred into the cuvette, and electroporation was done in the electroporator (EasyjecT, EquiBio), with 1250 V, 25 mA and 25 ohm. The cells were immediately transferred into 900 µl of LB medium, and incubated at 37 °C for 1 h. After the incubation, 10-40 µl of cells was spread on an agar plate containing the necessary antibiotic, and the plate was incubated o/n at 37 °C until colonies were grown. Afterwards, the plate was kept at 4 °C.

2.2.2. Molecular biology methods

2.2.2.1. Electrophoresis

Characterization and analysis of different protein and DNA molecules was done using different electrophoresis techniques.

2.2.2.1.1. SDS-PAGE

Analysis and characterization of proteins were done using SDS-PAGE. The SDS-Polyacrylamide gel contained a stacking and a resolving gel. Stacking and resolving gels differ in polyacrylamide content (6 % stacking gel, 12 % resolving gel), and pH value (pH 6.8 stacking gel, pH 8.8 resolving gel). Protein samples were mixed with 0.2 x vol of 5 x concentrated loading buffer (160 mM Tris-HCl pH 6.8, 2 % (w/v) SDS, 5 % (v/v) 2-mercaptoethanol, 40 % (v/v) glycerol, 0.1 % (w/v) bromphenol blue) and loaded on the gel. The electrophoretic separation was done at 35 mA for approximately 1 h, in 1 x SDS buffer (25 mM Tris, 190 mM glycine, 0.1 % (w/v) SDS). After completion of the run, gels were washed 3x10 minutes with hot water, and then stained using the Coomassie Brilliant Blue staining solution (0.1 % (w/v) Coomassie Brilliant Blue G-250, 2 % (v/v) H_3PO_4, 5 % (w/v) Al_2O_3, 10 % (v/v) ethanol). Protein bands were visualized and documented using the gel documentation system BioDocAnalyze (Biometra).

2.2.2.1.2. Polyacrylamide gel electrophoresis

PCR products and smaller DNA fragments were analyzed using polyacrylamide gel electrophoresis. The gel contained 6 % polyacrylamide in 1 x TPE pH 8.2 (90 mM Tris-H_3PO_4, 2 mM EDTA), and the separation was done in 1 x TPE at 30 mA for approximately 1 h. DNA bands were stained using ethidium bromide, and visualized and documented using the gel documentation system BioDocAnalyze (Biometra).

2.2.2.1.3. Agarose gel electrophoresis

Analysis of plasmid DNA was done using agarose gel electrophoresis. The gel contained 0.8 % (w/v) agarose in 1 x TBE pH 8.3 (100 mM Tris-HCl, 100 mM H_3BO_3, 2.5 mM EDTA), and the separation was done in 1 x TBE at 90 V for approximately 1 h. DNA bands were stained using ethidium bromide, and visualized and documented using the gel documentation system BioDocAnalyze (Biometra).

2.2.2.1.4. EMSA

EMSA was used to determine binding activity of unlabeled and labeled BsoBI variants. The gel contained 6 % polyacrylamide in 20 mM Tris-Acetate pH 8.2, 5 mM $CaCl_2$, and the separation was done in 20 mM Tris-Acetate pH 8.2, 5 mM $CaCl_2$. Before loading the samples, the gel was prerun for 30’ at 80 V, and after the loading separation was done for approximately 2 h.

2.2.2.1.5. Denaturing polyacrylamide gel electrophoresis

For analyzing short oligonucleotides, products of BsoBI cleavage, denaturing polyacrylamide gels were used. These gels contain 7 M urea, and allow for separation of single DNA strands. In order to separate products of 39 bp oligonucleotide cleavage, 15 % gels were prepared, using the acrylamide:bis-acrylamide mix 19:1, in 1 x TBE buffer, with addition of 7 M urea. The mixture was heated for a few seconds in a microwave oven to dissolve urea, and then cooled down before adding APS and TEMED. The gels were prerun for 15' at 15 mA, and the separation of samples was done at the same current. This allowed for warming the gels while running, which, in addition to urea, helps denaturing the DNA. The samples were mixed in a 1:1 ratio with loading buffer containing 90 % (v/v) formamide diluted in 10 x TBE buffer. After mixing with loading buffer, tubes were heated up for 1' at 95 °C to denature the DNA, and then placed on ice to prevent reannealing.

2.2.2.2. Isolation of DNA

2.2.2.2.1. Minipreparation

Isolation of plasmids containing genes for different BsoBI variants was done using the commercially available QIAprep Spin Miniprep Kit (Qiagen), following the manufacturer's instructions.

2.2.2.2.2. Midipreparation

Isolation of plasmids used for cleavage assays (pAT153 triple, pDGS) was done using the commercially available QIAGEN Plasmid Midi Kit (Qiagen), following the manufacturer's instructions.

2.2.2.2.3. PCR purification

Purification of PCR fragments used for EMSA and site-directed mutagenesis was done using the commercially available QIAquick PCR Purification Kit (Qiagen).

2.2.3. Creating single-cysteine BsoBI variants

2.2.3.1. Site-directed mutagenesis

For creating different single-cysteine variants, the plasmid pQE2-HisBsoBI-cf was used as template, and primers were constructed to carry the desired mutation and an additional restriction enzyme recognition site. The list of primers used is presented in Table 12. PCR

was done with Pfu polymerase, and the program was: one-time denaturation at 95 °C 3 min, 30 cycles of denaturation (95 °C, 30 sec), annealing (58 °C, 30 sec) and elongation (68 °C, 90 sec), and final elongation 68 °C, 3 min. PCR fragments (ca. 300 bp long, so-called "megaprimers" [67]) were purified and used in a second PCR reaction, called "rolling circle" PCR, as primers (the template plasmid was the same). The program for this PCR reaction was: one-time denaturation at 93 °C, 5 min, 9 cycles of denaturation (93 °C, 1 min), annealing (60 °C, 50 sec) and elongation (68 °C, 15 min), and final elongation 68 °C, 20 min.

The "rolling circle" PCR product was digested with DpnI, which only cleaves the methylated template plasmid, lacking the mutation. The digested sample (in volume V) was precipitated on ice using the following procedure: 1/3 V 3 M NaOAc and 3 V 100 % (v/v) ethanol were added to precipitate DNA. The sample was then centrifuged at 13000 x g, 30 min, at 4 °C, and the precipitate was washed with 6 V of 70 % (v/v) ethanol. After drying, the precipitated plasmid was resuspended in water. The electrocompetent cells were transformed with this plasmid, and plated on agar plate containing ampicillin and chloramphenicol.

2.2.3.2. Screening

The clones obtained after mutagenesis were screened for the presence of the desired mutation(s). For each mutation 10 clones were picked, and PCR was performed to amplify the region with the putative mutation (using Taq polymerase), also containing the newly introduced recognition site for the selected marker enzyme. The PCR program was: one-time denaturation at 95 °C, 3 min, 30 cycles of denaturation (93 °C, 30 sec), annealing (52 °C, 30 sec) and elongation (72 °C, 90 sec), and final elongation 72 °C, 3 min. Primers used are listed in Table 14. PCR fragments were incubated with corresponding marker enzymes, and products of these reactions were analyzed on polyacrylamide gels (Chapter 2.2.2.1.2.).

Positive clones were selected, grown in liquid culture, plasmids were isolated using minipreparation, and sequenced to verify that the desired mutation was present and that the rest of the coding sequence for BsoBI does not contain any additional mutations.

2.2.3.3. Overexpression of BsoBI

Freshly transformed *E. coli* cells, containing the plasmid coding for BsoBI, were plated on an agar plate, and the plate was incubated at 37 °C until colonies had grown. A single colony was picked and a 25 ml liquid culture (containing Amp and Chl) was inoculated and incubated o/n at 37 °C in an air shaker. The 500 ml liquid culture was inoculated with 10-15 ml of this preculture, and the cells were grown under the same conditions until an OD_{600} of

0.7-0.9. The induction was started by adding IPTG to a final concentration of 1 mM, and the cells were grown at 37 °C for 2 h.

An aliquot of cells (1 ml) was collected before induction and 2 h after induction, and used to check the expression. The cells were harvested by a 1 min centrifugation (Eppendorf MiniSpin®), the pellet was resuspended in 30 µl of loading buffer, heated up to 95 °C for 10 min, and loaded onto an SDS gel. Based on OD_{600} measurements of samples before and after induction, the same amount of cells was loaded, allowing for comparison of BsoBI expression.

After 2 h of induction, the cells were harvested by a 15 min centrifugation at 4200 rpm, 4 °C (Beckman, J6-HC). The pellet was washed with 40 ml of STE buffer (100 mM NaCl, 10 mM Tris-HCl pH 8.0, 0.1 mM EDTA), and centrifuged again as described above. The pellet was stored at -20 °C or resuspended in digest buffer immediately for further steps of protein purification.

2.2.3.4. Purification of BsoBI

The cell pellet was thawed on ice and resuspended in 10 ml of digest buffer. The cells were transferred to a 25 ml beaker, and lysed by ultrasonification using a Branson sonifier (6 x 1 min, with 30 sec break, duty cycle 50 %, output control 5). The soluble fraction containing proteins was separated from cell debris by a 30 min centrifugation at 20000 rpm, 4 °C (Beckman, JA20).

All BsoBI variants used contain a His-tag which is used for reversible binding of the protein to Ni-NTA agarose via the imidazole group of the histidines. For this purpose, the resuspended volume of 500 µl of Ni-NTA was equilibrated with 10 ml of digest buffer. The supernatant containing BsoBI was added to the Ni-NTA agarose matrix, and incubated at 4 °C for 1 h. This was followed by the wash, twice with digest buffer (2 x 10 ml) and twice with wash buffer (2 x 10 ml). The protein was eluted with 2 ml of elution buffer and 4 fractions of 500 µl each were collected. Fractions containing protein were dialyzed o/n in the dialysis buffer at 4 °C, and stored at -20 °C.

2.2.3.5. Determination of protein concentration

Protein concentration was measured using the spectrophotometer NanoDrop® 1000 (Thermo Scientific), using the equation: $A = \varepsilon cl$, where A is the absorbance at 280 nm, ε is the extinction coefficient (49620 $M^{-1}cm^{-1}$ for BsoBI variants), c is the concentration (in M) and l is the length of the light pathway.

2.2.3.6. Determination of protein binding and cleavage activity

2.2.3.6.1. Determination of binding activity

The binding activity of purified BsoBI variants was determined using EMSA. PCR fragments (237 bp) used to test binding activity were prepared using the primers listed in Table 13 and plasmid pAT153 triple as template. The PCR program was: one-time denaturation at 95 °C, 3 min, 30 cycles of denaturation (93 °C, 30 sec), annealing (52 °C, 30 sec) and elongation (72 °C, 90 sec), and final elongation 72 °C, 3 min. To achieve radioactive labeling of PCR fragments, [α-^{32}P] dATP (with specific activity of 5000 Ci/mmol) was added to the reaction, to a final concentration of 0.04 μM. PCR products were purified as described in Chapter 2.2.2.2.3. and the concentration was determined by the UV-absorption at 280 nm using a UV spectrophotometer (U-3000 Spectrophotometer, Hitachi).

Protein concentrations used in the binding reaction were: 8 nM, 12 nM, 20 nM, 31 nM, 50 nM, 79 nM, 125 nM, 197 nM, 312 nM and 494 nM, while DNA concentration was 1 nM. The binding reaction was carried out at room temperature for 15 min, in binding buffer (Chapter 2.1.4.), with the addition of 1 μg Poly(dI-dC)·Poly(dI-dC) (GE Healthcare) as polynucleotide that blocks nonspecific binding. DNA fragments were analyzed on polyacrylamide gels, as described in Chapter 2.2.2.1.4. The amounts of bound and free DNA were determined using an Instant Imager (Packard).

2.2.3.6.2. Determination of cleavage activity

Purified BsoBI variants were incubated with pAT153 triple or pDGS plasmids at 37 °C for 1 h in cleavage buffer (with addition of 1 x BSA), to determine cleavage activity. Protein concentrations were: 195 pM, 390 pM, 780 pM, 1.56 nM, 3.125 nM, 6.25 nM, 12.5 nM, 25 nM, 50 nM and 100 nM, while DNA concentration was 6 nM (100 ng). After the reaction was completed, DNA fragments were analyzed on a 0.8 % agarose gel (2.2.2.1.3.).

2.2.4. Michaelis-Menten kinetics

Michaelis-Menten kinetics describe the rates of enzyme catalysed reactions. The equation represents the relation between the initial reaction rate (V_0) and the substrate concentration ([S]):

$$V_0 = \frac{V_{max} \cdot [S]}{K_M + [S]}$$

Where V_0 is the initial velocity, V_{max} is the maximum velocity, [S] is the substrate concentration and K_M is the Michaelis constant, which represents the substrate concentration at which the velocity reaches its half maximum, and it is a measure of the affinity of an enzyme for the substrate. The resulting graph is a hyperbola, which asymptotically approaches the maximum velocity (V_{max}).

The substrate for determining the cleavage rates was a 39 bp long oligonucleotide, 5' labeled with radioactive phosphorus ^{32}P. The labeling reaction was done following the protocol for labeling of 5' termini of DNA (available on www.fermentas.com) using T4 polynucleotide kinase (T4 PNK; Fermentas). Both strands of the oligonucleotide were labeled. The excess of free [γ-^{32}P] ATP was removed using Illustra MicroSpin^{TM} G-25 columns (GE Healthcare).

Initial rates were determined at three different temperatures: room temperature (25 °C), 37 °C and 65 °C. The protein concentration for experiments at room temperature was 100 pM, and DNA concentrations were 100 pM, 500 pM, 1000 pM, 5000 pM, 10000 pM, 15000 pM, 20000 pM and 25000 pM. For the experiments at 37 °C, the protein concentration was 10 pM, while the DNA concentrations were 100 pM, 200 pM, 500 pM, 1000 pM, 1500 pM, 2000 pM, 5000 pM and 10000 pM. Since BsoBI has the highest activity at 65 °C, the protein concentration for experiments at this temperature had to be lowered to 1 pM, and DNA concentrations used were 10 pM, 20 pM, 50 pM, 100 pM, 200 pM, 500 pM, 1000 pM and 2000 pM. In order to have the same radioactivity in all reactions, concentration of radioactive DNA was always 100 pM, and it was mixed with nonradioactive DNA (of the same sequence) to achieve the desired concentration. When DNA concentration was lower than 100 pM, only radioactive DNA was used, without mixing with nonradioactive DNA. Protein was diluted in cleavage buffer with the addition of 20 % (v/v) glycerol, to prevent adsorption to the tube walls.

First, the master mix containing cleavage buffer and DNA was prepared, and then the reaction was started by adding BsoBI. At time points 10 s, 30 s, 1 min, 2 min, 3 min, 5 min, 7 min and 10 min, 10 µl were taken, mixed with loading buffer and put on 95 °C for 1 min. The samples were loaded onto 15 % denaturing polyacrylamide gels. The amounts of cleaved and uncleaved DNA were determined using an Instant Imager (Packard).

2.2.5. Site-specific fluorescent labeling of single-cysteine variants

The most specific method for protein modification is the use of cysteine, through the nucleophilic attack of the maleimide group to the cysteine's sulfhydryl group (Figure 2.2). For

this purpose, the cysteines positioned on the surface of the protein have to be replaced by mutagenesis, and the desired position to be labeled must be changed to cysteine.

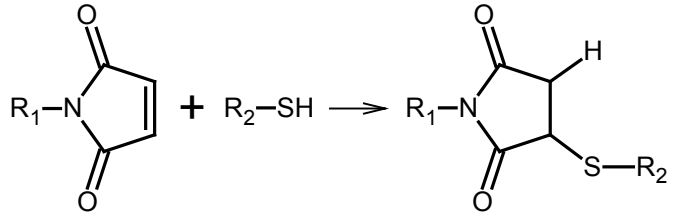

Figure 2.2 Chemical modification reaction of sulfhydryl with maleimide. *R_1 – fluorophore attached to maleimide, R_2 – polypeptide chain containing a free sulfhydryl group of cysteine. The result of the nucleophilic attack is a fluorophore covalently attached to the cysteine residue of the protein.*

To achieve complete labeling with fluorophore, cysteine introduced at the desired position must be kept in the reduced state. This was accomplished by incubation of protein with TCEP (tris(2-carboxyethyl) phosphine) for 10 min prior to the labeling reaction (Figure 2.3). TCEP is a reducing agent which is used instead of other reducing agents (like DTT or 2-mercaptoethanol) because of the advantage that it does not have to be removed before the labeling, since it does not react with maleimides. Also, the highest stability of maleimide groups is at pH 7.2, so the labeling reactions are usually done at this pH value.

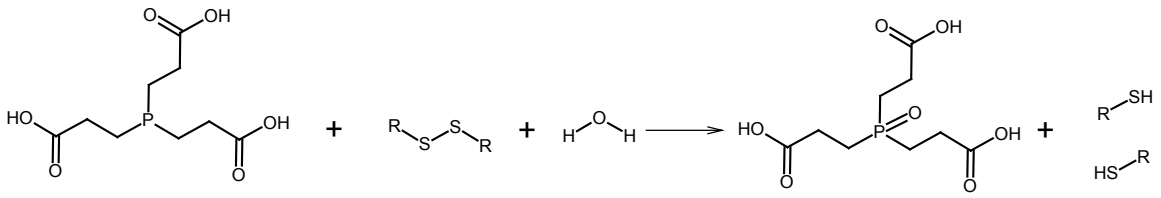

Figure 2.3 TCEP reaction.

2.2.5.1. Labeling and purification of proteins used in steady-state and stopped-flow experiments

Purified protein stored in buffer containing 2-mercaptoethanol (2-ME) was loaded onto a HiTrap™ Desalting column (GE Healthcare) connected to the ÄKTApurifier™ (GE Healthcare), to remove 2-ME and bring the protein into the buffer suitable for labeling. The list of buffers used is presented in Chapter 2.1.4. Chromatography steps are presented in Table 5.

Table 5

Equilibration	1 CV
Elution	3 CV
Concentration	1.3 % B
Fraction size	0.5 ml
Flow rate	0.8 ml/min

CV: column volume; % B: concentration of elution buffer

After removing 2-ME, the protein was incubated with a mixture of donor (Alexa488) and acceptor (Alexa594 or Alexa647) fluorophores (Chapter 2.1.7). The concentration of the donor fluorophore was in 1-fold molar excess over dimer protein, and acceptor fluorophore in 10-fold molar excess. The labeling reaction was done at room temperature for 30 min. The result of this labeling procedure is the dimer protein labeled randomly with donor and acceptor fluorophores on two cysteines. The excess of unreacted fluorophore was removed using a HiTrap^{TM} Desalting column, as previously described. Protein was labeled the same way using only donor fluorophore in excess, for use in control experiments. Labeled protein was dialysed o/n against storage buffer containing glycerol, and kept at -20 °C.

2.2.5.2. Labeling and purification of proteins used in single-molecule experiments

In order to obtain protein labeled with one donor fluorophore on one cysteine of the dimer, and one acceptor fluorophore on the other one, a different labeling and purification protocol was used. First, 2-ME was removed from the protein preparation as described in Chapter 2.2.5.1. Then, the protein was labeled with donor fluorophore in a 1-fold molar excess over dimer, and unreacted dye was removed as previously described. Donor labeled protein was then loaded onto a ResourceQ^{TM} column (GE Healthcare). The ResourceQ column is an anion exchange column, which enables separation of species according to their charge. Alexa fluorophores are negatively charged, and this property can be used to separate unlabeled, single labeled and double labeled protein. Chromatography steps are presented in Table 6, and concentration gradient in Figure 2.4.

Table 6

Equilibration	5 CV
Wash column	2 CV
Gradient segment 1	20 % B
Length of gradient	2 CV
Gradient segment 2	30 % B
Length of gradient	15 CV
Gradient segment 3	100 % B
Length of gradient	2 CV
Gradient delay	2 CV
Fraction size	1 ml
Flow rate	1 ml/min

CV: column volume; % B: concentration of elution buffer

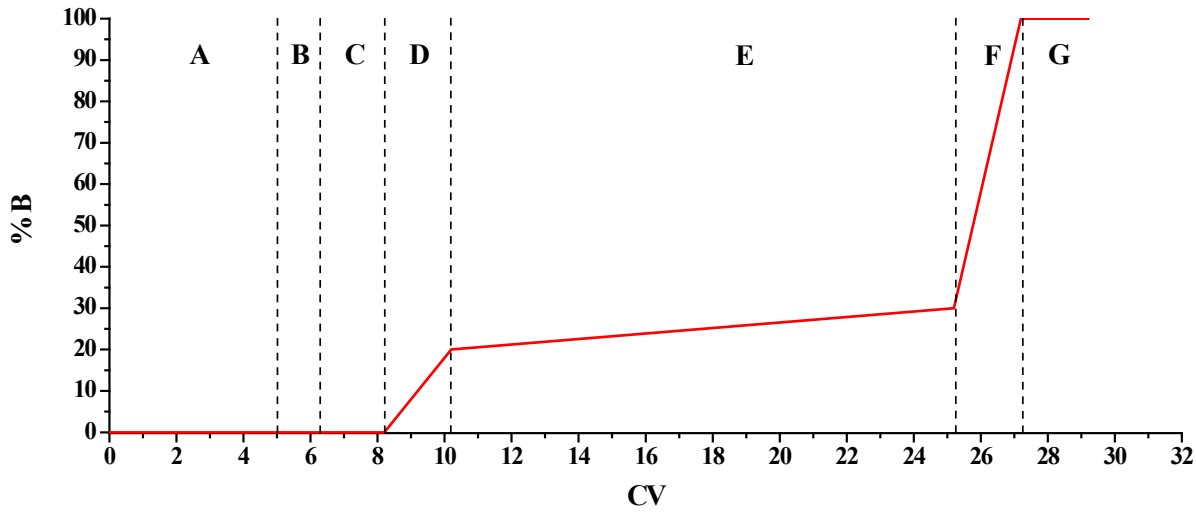

Figure 2.4 Concentration gradient used for separation with ResourceQ™. *CV: column volume, % B: concentration of elution buffer; A – column equilibration, B – sample loading, C – column washing, D – gradient segment 1, E – gradient segment 2, F – gradient segment 3, G – gradient delay*

The order of elution from the ResourceQ column is: unlabeled protein, single labeled protein (one donor fluorophore on one cysteine) and double labeled protein (two donor fluorophores on two cysteines). The fraction (1 ml) containing single labeled protein was collected, 200 µl was kept as donor only sample, and the rest was labeled with 10-fold molar excess of acceptor fluorophore. Unreacted acceptor dye was removed as described previously using a desalting column. Labeled protein was dialysed o/n into storage buffer containing glycerol, and kept at -20 °C.

2.2.5.3. Determination of labeling efficiency

The protein and the fluorophore concentration after labeling was determined by recording the absorbance spectrum between 220 nm and 750 nm using the spectrophotometer NanoDrop® 1000. Alexa fluorophores absorb also at 280 nm, so the protein concentration has to be calculated using specific correction factors. Correction factors for fluorophores used were provided by the supplier: Alexa488 0.11, Alexa594 0.56, Alexa647 0.03. The degree of labeling was calculated using the following equation:

$$DOL = \frac{A_{max} \cdot \varepsilon_{prot}}{(A_{280} - A_{max} \cdot CF) \cdot \varepsilon_{max}}$$

Where A_{max} is the absorbance of the fluorophore, ε_{prot} is the extinction coefficient of the protein, A_{280} is the absorbance of the protein, CF is the fluorophore correction factor and ε_{max} is the extinction coefficient of the fluorophore.

2.2.5.4. Determination of binding and cleavage activity

Binding and cleavage activity of all labeled proteins were determined as described in Chapter 2.2.3.6.

2.2.6. Fluorescence methods

2.2.6.1. Introduction to fluorescence

Luminescence is the optical phenomenon of emitting light after any type of excitation other than increasing the temperature. It can be divided into two categories, fluorescence and phosphorescence. During fluorescence, the substance absorbs a photon of high energy (lower wavelength), and emits a photon of lower energy (higher wavelength). The phenomenon of different wavelengths of absorption and emission was observed by George G. Stokes in 1852, and is now called Stokes shift. The electron in the excited state is paired with the electron in the ground state (by opposite spin), and this excited state is called excited singlet state. The return of the excited electron to the ground level is therefore spin allowed, and occurs rapidly (typically 10^8 s^{-1}). If the excited electron has the same spin as the ground state electron (triplet excited state), the return to the ground state is forbidden and therefore slower (10^3 to 10 s^{-1}). This phenomenon is called phosphorescence. Different electronic states and transitions between the absorption and emission of photons are represented in the Jablonski diagram (Figure 2.5) [41].

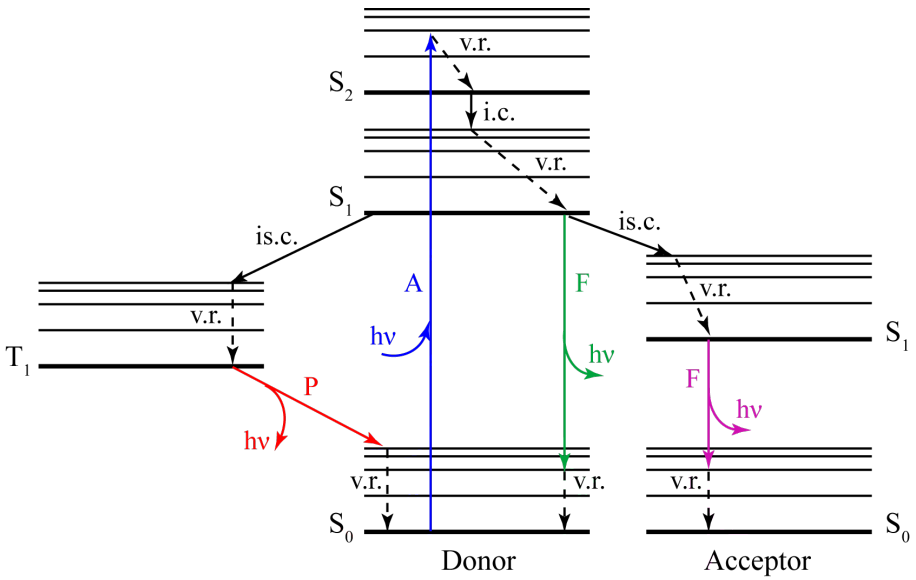

Figure 2.5 Jablonski diagram. *S_0 – singlet ground state, S_1, S_2 – singlet excited states, T_1 – triplet excited state, v.r. – vibrational relaxation (10^{-14} – 10^{-11} s), i.c. – internal conversion (10^{-14} – 10^{-11} s), is.c. intersystem crossing, A – absorbance (10^{-15} s), F – fluorescence (10^{-9} – 10^{-7} s), P – phosphorescence (10^{-3} – 10^{2} s)*

2.2.6.2. Fluorescence Resonance Energy Transfer (FRET)

FRET is the process that occurs when the emission spectrum of one fluorophore (called donor) overlaps with the absorption spectrum of another fluorophore (called acceptor) [Figure 2.6], and when two fluorophores are in close proximity.

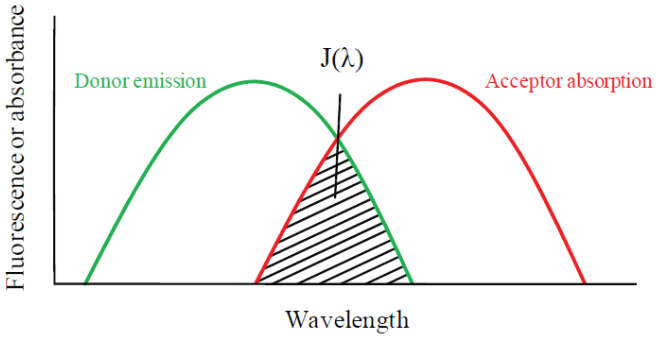

Figure 2.6 Spectral overlap [J(λ)] between donor emission spectrum and acceptor absorption spectrum

During FRET, donor and acceptor fluorophores are coupled by dipole-dipole interaction, and there is no photon transferred between the two fluorophores (Figure 2.5). The efficiency of energy transfer is determined by the spectral overlap and the distance between the donor and acceptor, and it is also dependent on the Förster distance. The Förster distance is defined as

the distance between two fluorophores when the energy efficiency is 50 %. The graphical relationship between fluorophore distance and FRET efficiency is presented in Figure 2.7.

$$E = \frac{R_0^6}{R_0^6 + r^6}$$

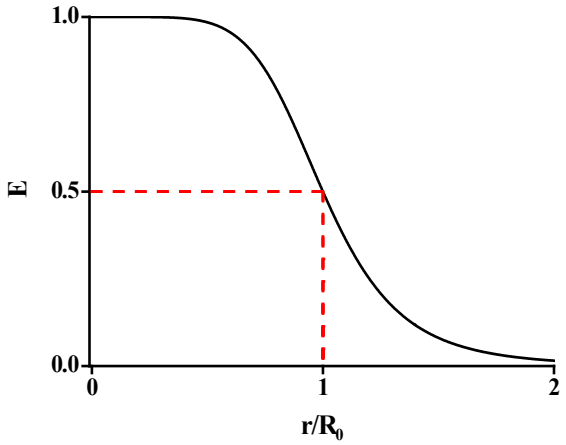

Figure 2.7 FRET efficiency (E) as a function of distance (r). *R_0 – Förster distance*

R_0 is characteristic for each fluorophore pair, and can be determined using the following equation:

$$R_0 = 0.211\ (\kappa^2 n^{-4} \Phi_D J(\lambda))^{1/6} \qquad \text{(in Å)}$$

Where κ^2 is the orientation factor between the dipoles of donor and acceptor, n is the refractive index of the medium, Φ_D is the quantum yield of the donor and J(λ) is the spectral overlap. The value of the orientation factor κ^2 is usually taken as 2/3, which assumes freely rotating donor and acceptor fluorophores. However, depending on the relative orientation of donor and acceptor, this factor can vary from 0 to 4. If the dipoles are in a head-to-tail parallel orientation κ^2 is 4, and if they are parallel κ^2 is 1. The variation from 1 to 4 would result in only 26 % change in R_0, since the sixth root is taken to calculate it. If the dipoles are perpendicular to one another κ^2 has the value 0, and the error would be much higher. By measuring the fluorescence anisotropy of donor and acceptor, which gives the information of their mobility, the errors in κ^2 values can be minimized.

The FRET efficiency was calculated using the method of Clegg [68]. For this purpose, the fluorescence of donor only labeled protein, and donor-acceptor labeled protein was measured, by exciting at the wavelength of 470 nm, and recording the emission from 490 nm to 700 nm. Then, the spectrum of donor only labeled protein was normalized to the maximum of donor fluorescence, and subtracted from the spectrum of double labeled protein. As the result, the

acceptor fluorescence, without donor fluorescence, is obtained. An example of different spectra is presented in Figure 2.8.

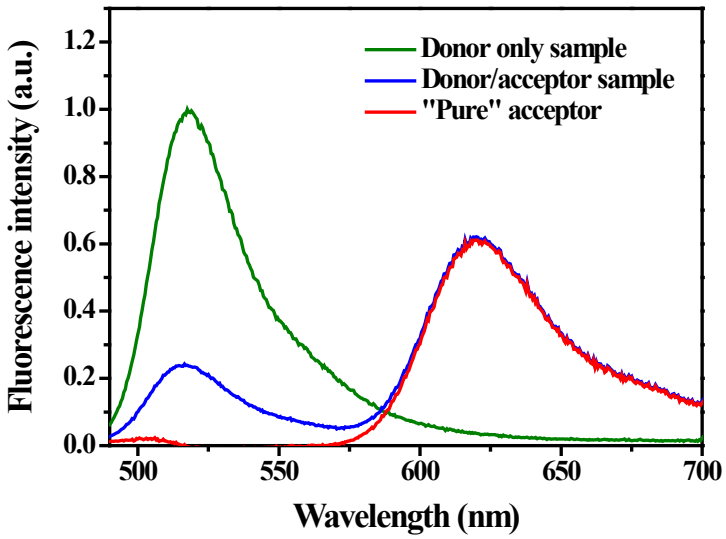

Figure 2.8 Calculation of FRET efficiency. *Fluorescence spectra of donor only sample (green line), donor/acceptor sample (blue line) and calculated "pure" acceptor spectrum (red line)*

The FRET efficiency (E) can be calculated using the following equation:

$$E = \left[\frac{F^*_{A,FRET}(\lambda_{exD}, \lambda_{emA})}{F_{A/dir}(\lambda_{exA}, \lambda_{emA})} - \frac{\varepsilon_A(\lambda_{exD})}{\varepsilon_A(\lambda_{exA})}\right] \cdot \frac{(c+c_A)}{c} \cdot \frac{1}{d} \cdot \frac{\varepsilon_A(\lambda_{exA})}{\varepsilon_D(\lambda_{exD})}$$

Where $F^*_{A,FRET}$ is the corrected ("pure") acceptor fluorescence in the donor/acceptor sample, $F_{A/dir}$ is the acceptor fluorescence in the donor/acceptor labeled sample, ε_A and ε_D are the extinction coefficients of acceptor and donor, respectively, at the wavelengths chosen, d is the degree of labeling, and c and c_A are concentrations of donor and acceptor fluorophores, respectively. λ_{ex} and λ_{em} of donor (D) and acceptor (A) represent maxima of the excitation and emission spectra, respectively. Assuming that the extinction coefficient of the acceptor is 0 at the donor excitation maximum, the ratio $\varepsilon_A(\lambda_{exD})/\varepsilon_A(\lambda_{exA})$ will have the value of 0, and can be omitted from the equation.

2.2.6.3. Steady-state ensemble FRET experiments

To analyze conformational changes in BsoBI upon DNA binding, steady-state ensemble measurements were carried out. The measurements were done in the FluoroMax®4

spectrofluorimeter (HORIBA Jobin-Yvon). For this purpose, the protein was labeled with Alexa488 fluorophore as donor and Alexa594 as acceptor, as described in chapter 2.2.5.1. Labeled protein was diluted to 50 nM dimer concentration, in appropriate buffer (chapter 2.1.4.), and fluorescence spectra were measured after excitation at 470 nm for Alexa488, and 575 nm for Alexa594. The emission of Alexa488 (in donor and donor/acceptor labeled sample) was monitored between 490 nm and 800 nm, while emission of Alexa594 was monitored between 595 nm and 800 nm. The excitation and emission slits were set at 2.5 nm, and spectra were corrected using the correction function provided by the spectrofluorimeter supplier. After recording the spectrum of protein alone, an excess of specific or unspecific DNA was added to the cuvette (Quartz Ultra-Micro Cell, Hellma), and the measurements were repeated.

2.2.6.4. Fluorescence stopped-flow experiments

In order to monitor fast reaction of DNA binding by BsoBI, starting from the moment of mixing, stopped-flow measurements were performed, using the SFM-300 stopped-flow instrument (Bio-Logic). The scheme of the instrument is shown in Figure 2.9. Main parts of the apparatus are: two syringes (containing the reaction species) driven by the motor, mixing device, observation cell, stopping syringe and detection system capable of rapid response. Two reaction species are added to different syringes, and the reaction is started by pushing the same volume of reactants from both syringes at the same time. The reactants are kept in the observation cell through a stop syringe, and excited by appropriate wavelength. The emission is measured and recorded, with a short delay (dead time) between the mixing and detection, which is in the order of ms.

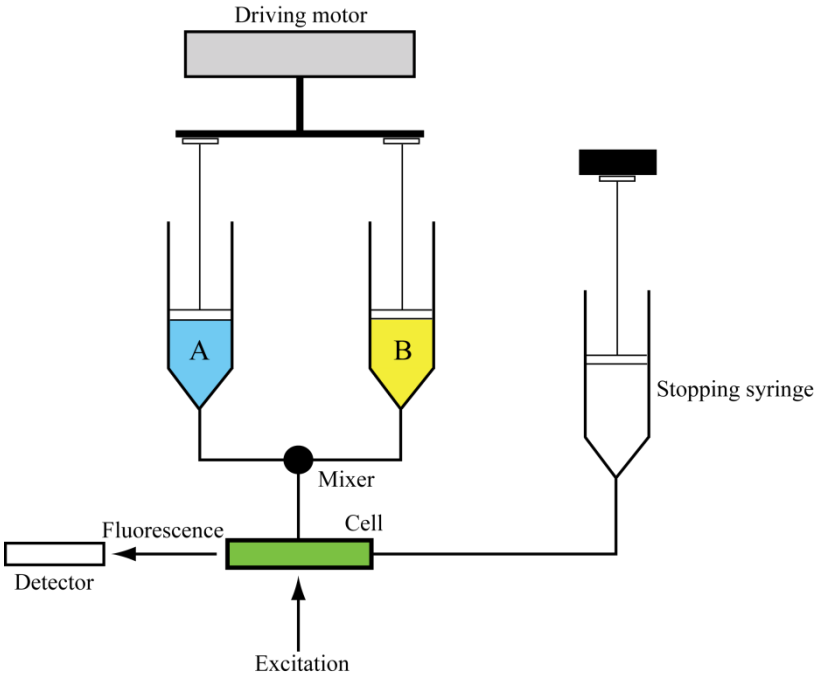

Figure 2.9 Stopped-flow instrument scheme. *Explanation in the text.*

The excitation wavelength used was 436 nm. At this wavelength, the lamp has a maximum energy output. The change in fluorescence signal was monitored using emission filters specific for donor or acceptor fluorophore. Bandpass filter D515/30m (LOT Oriel) was used for Alexa488 (central wavelength 515 nm, bandwidth 30 nm) and D630/30m (LOT Oriel) was used for Alexa594 (central wavelength 630 nm, bandwidth 30 nm). For all measurements, 100 µl of each reactant were mixed, and 10-20 curves were collected and averaged using Biokine 2.07 software. The fitting was done using Dynafit program (BioKin) [69]. All measurements were done at room temperature.

To monitor the kinetics of DNA binding by BsoBI, the protein was labeled with Alexa488 fluorophore and DNA was labeled with Alexa594 fluorophore. The protein was diluted to 100 nM concentration in buffer containing $CaCl_2$ (chapter 2.1.4.), to obtain 50 nM concentration in the mixture. DNA concentration (diluted in the same buffer) was varied from 25 nM to 400 nM (in the mixture). The change in fluorescence signal was monitored using donor emission filter, since the acceptor labeled component was varied. The signal was collected for 100 s, in three time intervals: 0-5 s every 10 ms, 5-50 s every 50 ms, 50-100 ms every 100 ms. Monitoring of DNA binding and cleavage was done in buffer containing $MgCl_2$ (chapter 2.1.4.), with the same protein and DNA concentrations, and measurement setup.

To monitor conformational changes in protein after DNA binding, protein labeled with both donor and acceptor fluorophore was mixed with unlabeled DNA.

The influence of different metal ions on the conformation of the protein was monitored by mixing double labeled protein with buffer containing excess of the metal ion of interest.

2.2.6.5. Multiparameter single-molecule fluorescence spectroscopy

The results obtained from ensemble steady-state and stopped-flow measurements represent the average of events happening in the sample of interest. In order to acquire information about subpopulations present in the sample, a series of single-molecule experiments was performed. The experimental setup allowed monitoring different fluorescence parameters (Figure 2.10) of labeled protein molecules in solution.

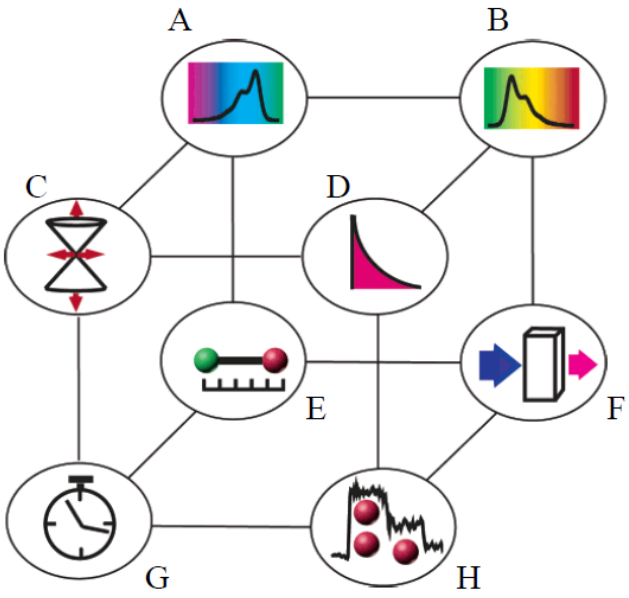

Figure 2.10 Multiple dimensions of fluorescence monitored. *A – Excitation spectrum, B – Fluorescence spectrum, C – Fundamental anisotropy, D – Fluorescence lifetime, E – Distance between fluorophores, F – Fluorescence quantum yield, G – Time, H – Fluorescence intensity (adapted from Widengren et al. [70])*

Single-molecule experiments were carried out on a confocal epi-illuminated setup. Labeled protein was diluted in 2 steps, in the measurement buffer, to a concentration of 40-80 pM (depending on the degree of labeling). The final dilution was done in a 50 µl droplet used for the experiment. To prevent protein adsorption, the glass cover slide was coated with 5 mg/ml κ-casein. A droplet of 50 µl of κ-casein was applied to the cover slide and left for 10 minutes. Then the droplet was removed, and the spot was carefully washed with water to remove excess of κ-casein, and leave only a thin layer at the surface.

The excitation was done at 497 nm using an Argon-ion laser (Sabre, Coherent, Palo Alto, CA, USA; APE, Berlin, Germany), focused into the solution. Labeled molecules freely diffusing in the solution create a burst of fluorescence photons while they travel through the detection volume (in the range of femtoliter, restricted by a pinhole of 100 µm in diameter, and the beam waist ω_0 of 0.56 µm). The objective was a 60 x water immersion lens (Olympus, UPlanApo, 60 x, 1.2 N.A). The excitation pulses had a width of 190 ps and a repetition rate of 73 MHz. The dual-band dichroic mirror separates the incoming excitation wavelength fluorescence signal (488/636PC, AHF Analysentechnik, Tübingen, Germany). The fluorescence signal is divided into its parallel and perpendicular components with respect to the linear polarised excitation beam by a polarising beam splitter cube (Olympus, UPlanApo, 60 x, 1.2 N.A), and then divided into red and green fluorescence components by further dichroic mirrors (DB: 595 DCRX, AHF), resulting in 4 signal paths: green parallel and green perpendicular, red parallel and red perpendicular (Figure 2.11).

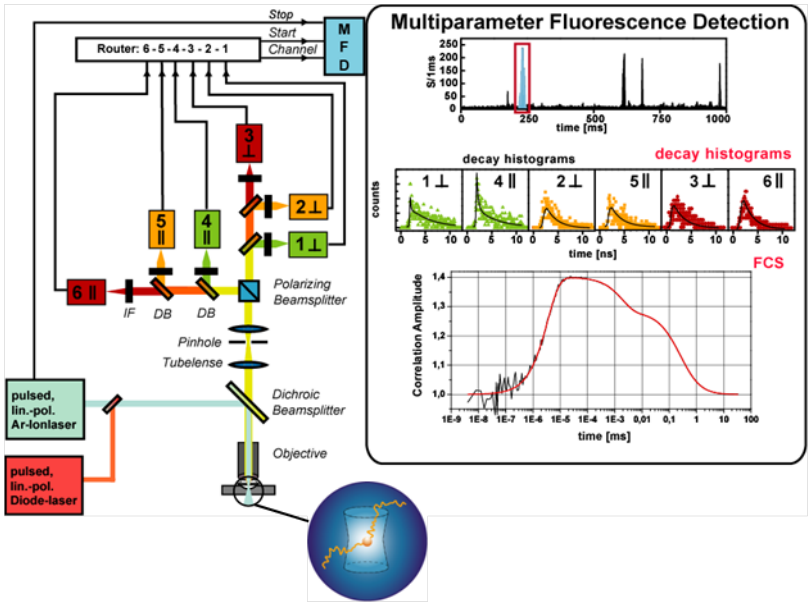

Figure 2.11 The setup for multiparameter fluorescence detection.

Band pass filters (HQ 533/46 and HQ 720/150, for donor and acceptor fluorophore, respectively) are finally used to separate the signal in spectral regions from background. Four avalanche photodiodes (SPCM-AQR-14, Laser Components, Germany) are used to monitor the photons. The PC-BIFL-card (SPC 132, Becker & Hickl GmbH Berlin, Germany) registers for each event the arrival time after the laser pulse, the interphoton time and the detector channel in which the photon arrives corresponding to spectral range and polarisation. Fluorescence bursts created by freely diffusing molecules are distinguished from the

background of 1-2 kHz by applying certain selection criteria (~50 μs interphoton time, minimum burst size 100 photons). Also, bursts which have acceptor bleaching were removed from the analysis by the criterion of the difference in macroscopic times, $-0.5\ s < T_G - T_R < 0.5\ s$, where T_G and T_R represent the average macroscopic time in which all photons are detected during one burst in the green and red channels, respectively. Without photobleaching T_G and T_R would be similar, and thus $T_G - T_R \approx 0$. Another selection criterion included choosing the bursts in the red channel that had more than 20 photons. This allowed for the exclusion of the red bursts not originating from FRET, but from crosstalk of green donor signal to red acceptor detection channel. In this way significant amount of the donor only species was also removed from the analysis.

First, double labeled protein in different buffers (chapter 2.1.4.) was measured, typically 1-1,5 h, i.e. until enough photons were collected to ensure good statistical result processing. Then, a new droplet with protein was prepared, and excess of specific or unspecific DNA (500 nM) was added, and the measurement was repeated.

3. Results

The dynamics of conformational changes in the restriction enzyme BsoBI was analyzed using different fluorescence techniques. For this purpose, the enzyme had to be labeled with donor and/or acceptor fluorophore, at defined positions. The modifications were done using fluorophores with the maleimide functional group, and different single-cysteine BsoBI variants.

3.1. Determination of binding and cleavage activity of different single-cysteine BsoBI variants

In order to specifically label BsoBI with different fluorophores, cysteine residues had to be introduced at certain positions of the protein. This was done by removing three naturally occurring cysteines from BsoBI, to produce a cysteine-free variant, and subsequently introducing single cysteines into specific positions. Using the plasmid containing the gene for cysteine-free BsoBI variant, and site-directed mutagenesis (as explained in Chapter 2.2.3.1), several single-cysteine BsoBI variants were produced, e.g. E100C, A153C, E290C. The presence of the newly introduced cysteines was determined by DNA sequencing. These new variants should not have impaired binding and cleavage activity compared to the wild type variant. The cleavage tests were done using a plasmid containing one BsoBI recognition site (CTCGAG), as described in chapter 2.2.3.6.2. Figure 3.1 shows cleavage assays for BsoBI wild type (wt) and the BsoBI A153C variant as one example of single-cysteine variants.

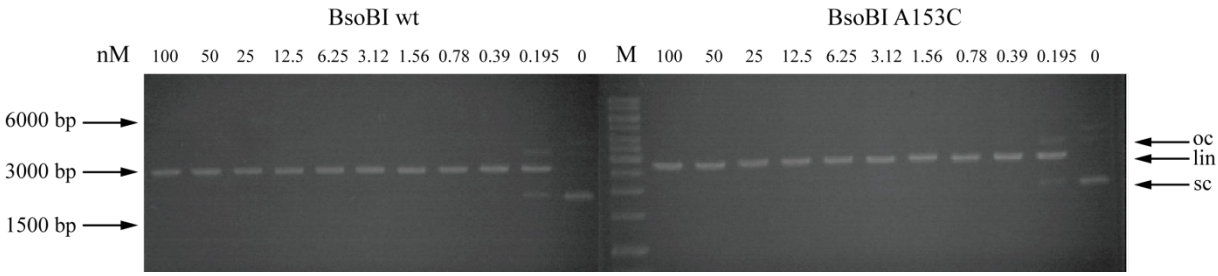

Figure 3.1 Activity test of the BsoBI wild type (wt) and the A153C variant. *Cleavage of the pDGS plasmid, with one BsoBI recognition site, results in appearance of linear DNA in the electropherogram. M: GeneRuler™ 1kb DNA ladder (Fermentas); oc: open circle; lin: linear plasmid DNA; sc: supercoiled plasmid DNA*

It can be seen that cleavage activities of both the wild type enzyme and the single-cysteine variant are the same (partial cleavage at 0.195 nM BsoBI, full cleavage at 0.39 nM BsoBI).

All single-cysteine variants used in this study were checked for cleavage activity, and neither of them showed any cleavage deficiency.

Based on available literature data [36], certain mutations were introduced into already existing single-cysteine variants in order to create binding efficient but cleavage inactive variants. The residues chosen were D212, which was exchanged to alanine or asparagine (creating D212A and D212N variants, respectively), and H253, which was exchanged to glutamine (creating H253Q variant). The amino acids were exchanged in genes coding for BsoBI A153C and E100C. First, the binding activity of newly created double variants was checked and compared with the binding activity of the wild-type protein and the single-cysteine variant from which the double mutant originated (Figure 3.2).

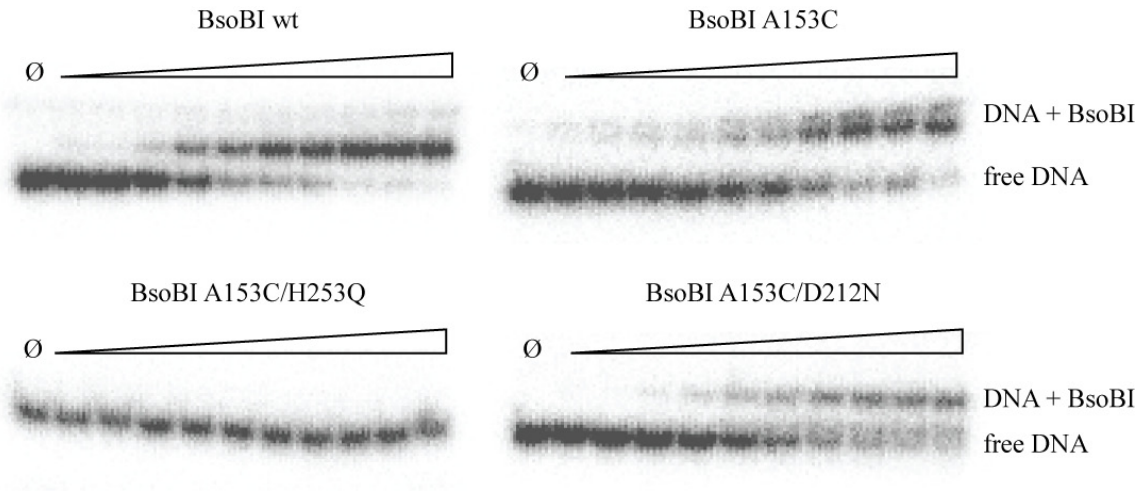

Figure 3.2 Binding activity of different BsoBI variants as determined by EMSA. *The substrate used in the experiments was a 237 bp long PCR product. The binding reaction was done in the presence of Poly(dI-dC)·Poly(dI-dC) (GE Healthcare), as polynucleotide that blocks unspecific binding. BsoBI concentrations used were: 8 nM, 12 nM, 20 nM,31 nM, 50 nM, 79 nM, 125 nM, 197 nM, 312 nM, 494 nM. Ø – control reaction without BsoBI.*

The binding activity was determined using 1 nM 237 bp long PCR product (with one BsoBI recognition site – CTCGAG), and different concentrations of BsoBI (ranging from 8 nM to 490 nM), as explained in chapter 2.2.3.6.1. The reaction was done in the presence of $CaCl_2$, which supports specific DNA binding, but not cleavage. Excess of Poly(dI-dC)·Poly(dI-dC) was also added to the reaction, in order to prevent unspecific binding. The introduction of cysteine instead of alanine at the position 153 did not cause a significant change in the binding efficiency compared to the wild type protein. Also, the exchange of residue D212 in the active site to asparagine did not significantly impair the binding activity (estimated K_D value for wild type was 40 nM, for A153C 65 nM and for A153C/D212N 57 nM). However,

the exchange of residue H253 to glutamine caused loss in binding activity. This mutation was shown to impair the binding activity also when it was introduced into the variant E100C.
In addition to checking the binding activity, the newly created double mutants were also checked for their cleavage activity (Figure 3.3). Variant A153C/H253Q showed no binding activity, and it was thus expected to see no cleavage activity either.

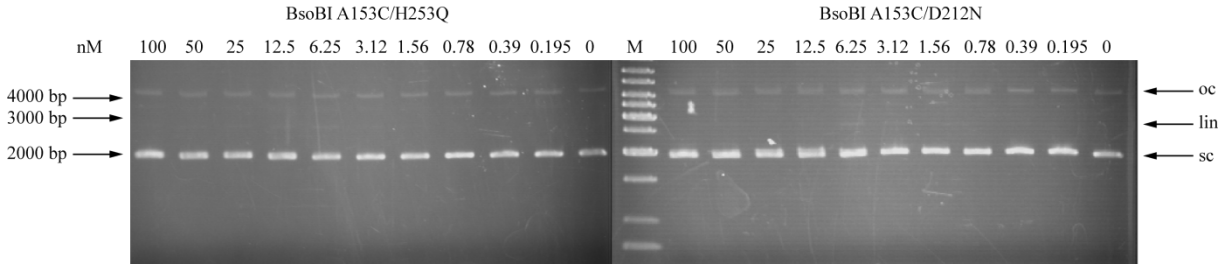

Figure 3.3 Activity test of BsoBI A153C/H253Q and A153C/D212N variants. *Cleavage of the pDGS plasmid, with one BsoBI recognition site, results in appearance of linear DNA in the electropherogram. M: GeneRuler™ 1kb DNA ladder (Fermentas); oc: open circle; lin: linear plasmid DNA; sc: supercoiled plasmid DNA*

As expected, the variant A153C/H253Q did not show cleavage activity. Although the variant A153C/D212N showed binding activity, it did not show any cleavage activity. The mutation of aspartic acid at the position 212 into asparagine caused loss of cleavage activity, but not in binding activity, also when introduced into the BsoBI variant E100C. Mutation of the histidine residue at position 253 caused loss of both binding and cleavage activities, regardless of into which single-cysteine variant it was introduced.

3.2. Michaelis-Menten kinetics

BsoBI is a thermostable restriction enzyme, purified from the thermophilic gram-positive bacterium *Bacillus stearothermophilus*, with an optimal catalytic activity at 65 °C. However, all pre-steady state ensemble experiments, as well as single-molecule experiments were carried out at room temperature. Thus, the kinetics of DNA cleavage was analyzed at three different temperatures, room temperature (25 °C), 37 °C and 65 °C, in order to compare the cleavage rates.

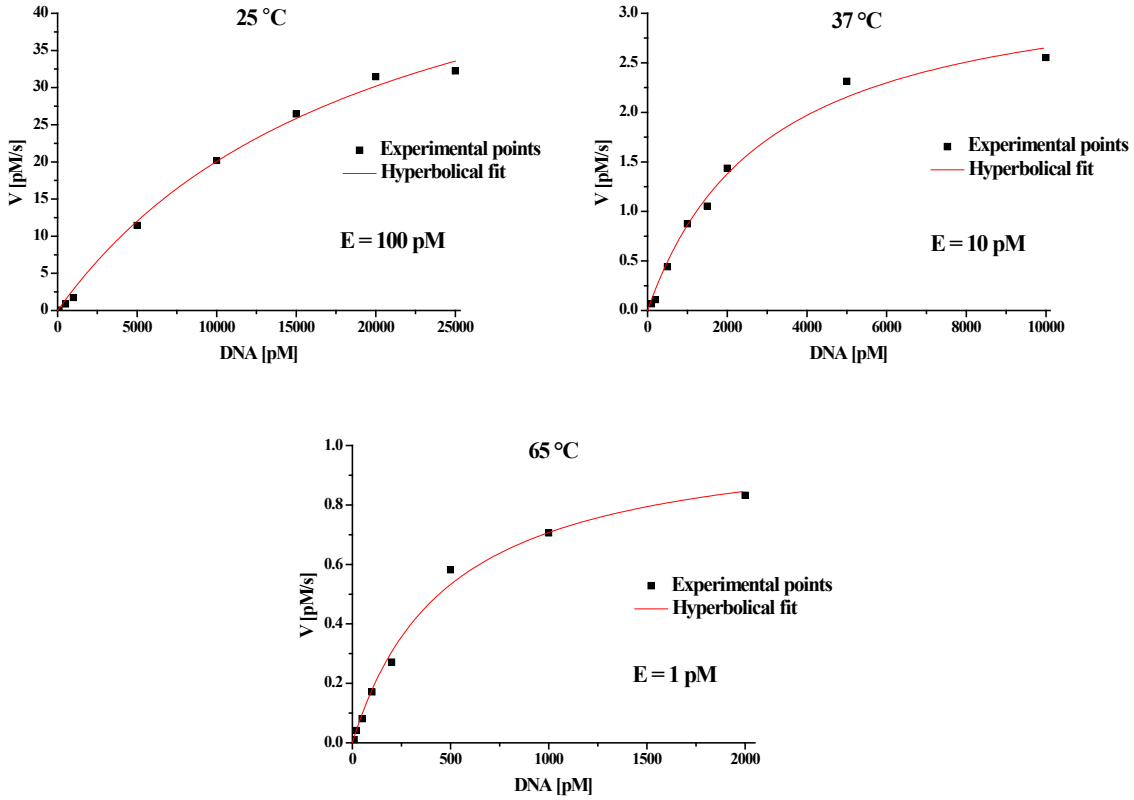

Figure 3.4 Michaelis-Menten analysis of DNA cleavage by BsoBI at different temperatures. *The initial rate constants were plotted as a function of substrate concentration, and the hyperbolic function was used to fit the data obtained.*

The collected data was analyzed using the GraphPad Prism software, in order to fit the experimental points to the hyperbolical function that describes the Michaelis-Menten kinetics. Figure 3.4 shows the dependence of initial rate constants on the substrate concentration used, at three different temperatures.

Using the Michaelis-Menten equation (Chapter 2.2.4), the values for V_{max} and K_M could be determined. The value for k_{cat} was calculated by dividing V_{max} by the total enzyme concentration. Table 7 represents the Michaelis-Menten parameters for DNA cleavage by BsoBI at three different temperatures.

Table 7

	25 °C	37 °C	65 °C
V_{max} [pM/s]	60.9	3.4	1.1
K_M [nM]	20.3	3.0	0.5
k_{cat} [s^{-1}]	0.6	0.3	1.1

It can be seen that an increase in the temperature causes a decrease of the K_M value, suggesting that BsoBI has a higher affinity for the substrate at higher temperatures. However, the values of the cleavage rates (k_{cat}) were not significantly affected by the change in temperatures. Although the optimal conditions for determining the Michaelis-Menten parameters were not achieved (Michaelis-Menten plots need to reach a plateau), it is clear that the temperature changes influence the K_M of BsoBI.

3.3. Site-specific labeling of BsoBI

In order to study conformational changes in BsoBI as well as the interaction between BsoBI and DNA using FRET, single-cysteine variants of BsoBI had to be labeled with one or two fluorophores, depending on the type of experiment. The labeling positions were chosen so that they do not interfere with the catalytic center of BsoBI, that they are surface exposed and that the distance between them is optimal for FRET studies. Three single-cysteine variants used in different fluorescence experiments are represented in Figure 3.5.

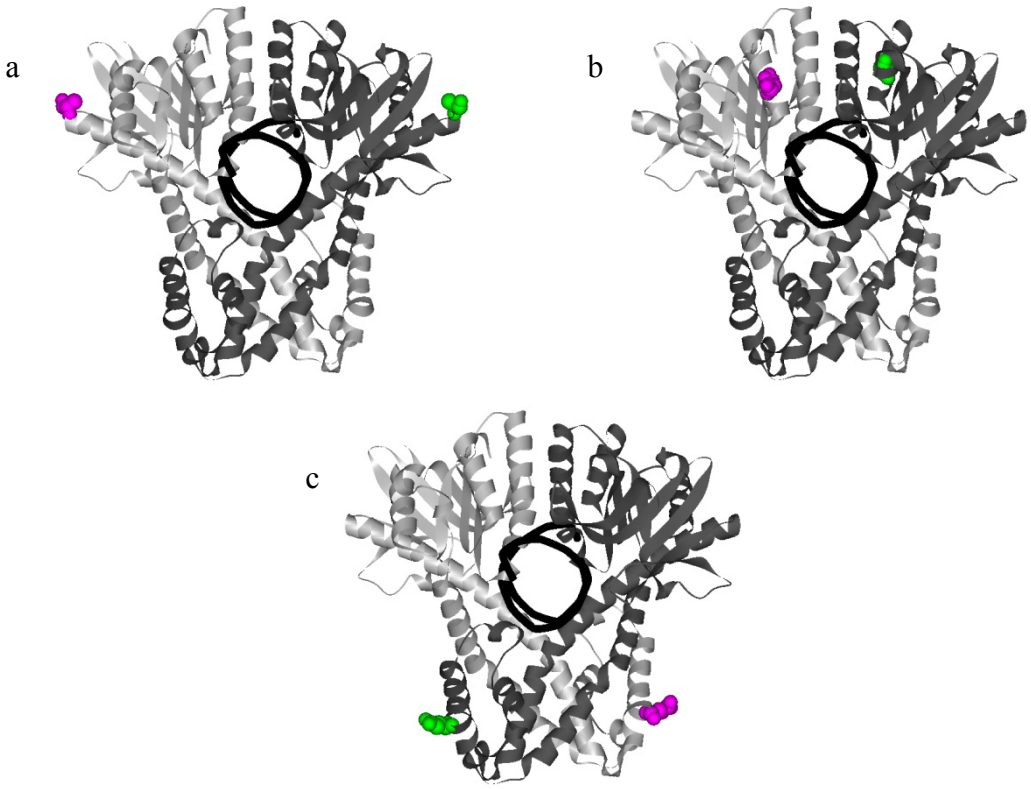

Figure 3.5 Position of the three single-cysteine substitutions chosen, represented in the co-crystal structure of the wt enzyme. *a) BsoBI A153C, b) BsoBI E290C, c) BsoBI E100C; Green and pink spheres represent residues that were mutated into cysteines and labeled with donor and acceptor fluorophores, respectively.*

3.3.1. Random double labeling of BsoBI used in ensemble experiments

Labeling of BsoBI used in pre-steady state and steady-state experiments was done randomly using a mixture of donor and acceptor fluorophores. The acceptor fluorophore was added in excess, to minimize the amount of protein molecules labeled only with donor fluorophore. The protein stock solutions were kept in a buffer containing 2-mercaptoethanol, which had to be removed prior to labeling reaction. This was done using a HiTrap^{TM} Desalting column (GE Healthcare) as described in chapter 2.2.5.1.

Conformational changes following substrate binding and/or cleavage was monitored by mixing double labeled BsoBI with unlabeled DNA. For this purpose, mixture of donor and acceptor fluorophore, in a ratio of 1:10 respectively, was added to the protein and allowed to react for 30 min at room temperature. Unreacted fluorophore was removed using a HiTrap^{TM} Desalting column.

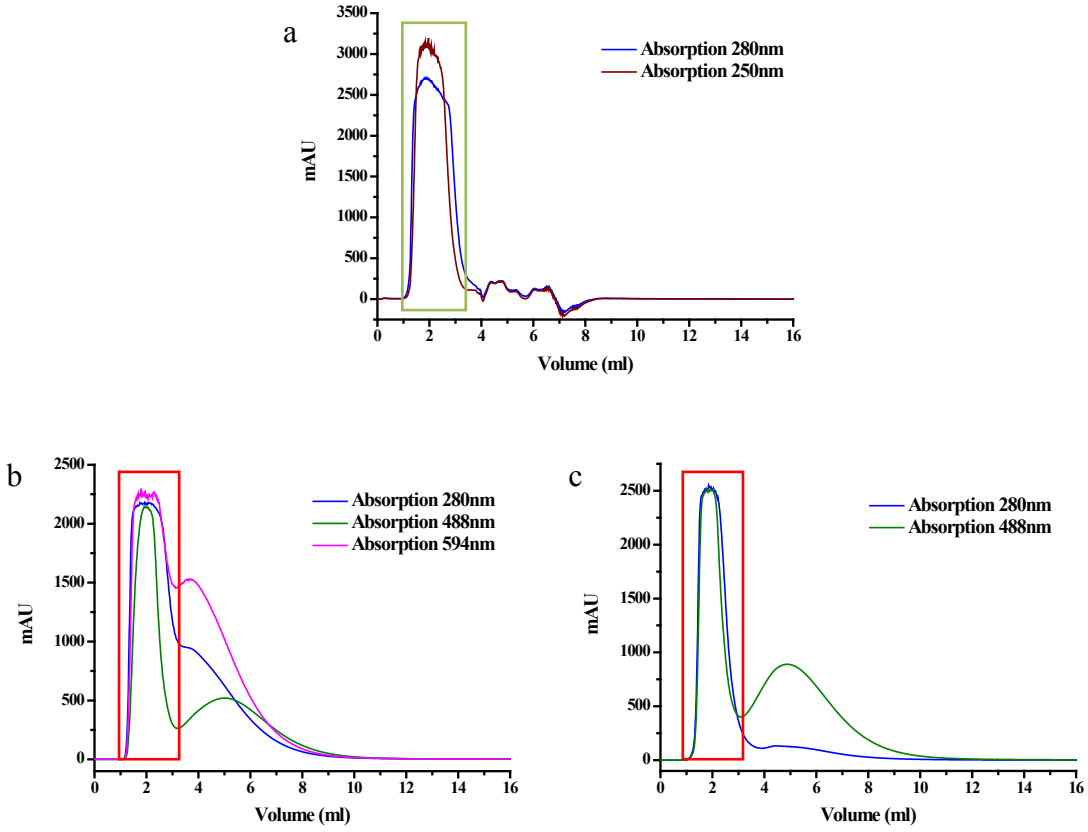

Figure 3.6 Chromatography steps during random BsoBI labeling. *a) Chromatogram of removal of 2-ME from protein stock solution, b) Chromatogram of removal of excess of Alexa488 and Alexa594, c) Chromatogram of removal of excess of Alexa488. The green box represents the portion of eluted protein used for further labeling. Red boxes represent the portions of eluted protein used in experiments*

The kinetics of binding and/or cleavage of substrate was monitored using single labeled BsoBI and single labeled DNA. In this case, BsoBI was labeled with donor fluorophore, and excess of unreacted fluorophore was removed as previously described, while DNA was labeled with acceptor fluorophore. Figure 3.6 shows chromatograms of 2-ME and free fluorophore removal.

The chromatogram in Figure 3.6.a shows co-elution of species that absorb at 280 nm (maximal absorption for protein) and 250 nm (maximal absorption for 2-ME). However, protein also absorbs at 250 nm, so this 250 nm absorption does not represent 2-ME still bound to BsoBI.

Figure 3.6.b shows co-elution of species that absorb at 280 nm (maximal absorption for protein), 488 nm (maximal absorption for Alexa488) and 594 nm (maximal absorption for Alexa594). It is clearly visible that the protein is labeled with both donor and acceptor fluorophore, and that the majority of free fluorophore can be removed using this chromatography step. The amount of free flurophores still present after this purification is removed after o/n dialysis against storage buffer.

Figure 3.6.c shows the removal of free Alexa488 fluorophore after BsoBI labeling. Again, it is clear that protein and Alexa488 co-elute, suggesting that the protein is labeled, and that most of the unreacted fluorophore can be removed.

Red boxes in Figure 3.6.b and c show the elution fractions that were collected and dialysed o/n against storage buffer, and used in further experiments.

The purity of the labeled protein was confirmed using SDS-PAGE (chapter 2.2.2.1.1.). Figure 3.7 shows one example of the double labeled BsoBI A153C variant before and after removing the unreacted fluorophore. The gel was photographed under UV light, prior to staining, in order to observe the fluorescence of labeled protein and unreacted fluorophore, and then washed and stained as described in chapter 2.2.2.1.1.

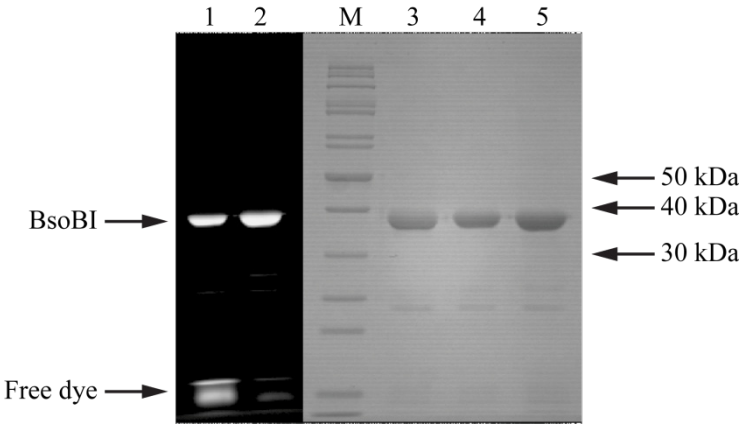

Figure 3.7 SDS-PAGE of double labeled BsoBI A153C variant. *1) Double labeled BsoBI A153C before removing the free dye, 2) Double labeled BsoBI A153C after removing the free dye, 3) Unlabeled BsoBI A153C stained with Coomassie Brilliant Blue, 4) Double labeled BsoBI A153C before removing the free dye stained with Coomassie Brilliant Blue, 5) Double labeled BsoBI A153C after removing the free dye stained with Coomassie Brilliant Blue, M – PageRuler™ Protein Ladder (Fermentas)*

Unreacted fluorophore (free dye) can be seen only in lane 1, in the sample of double labeled BsoBI before purification. BsoBI appears as a single band, which represents one subunit with the size of approximately 38 kDa.

Table 8 shows one example of labeling efficiencies and concentrations of BsoBI and fluorophores after this labeling protocol. The degree of labeling was calculated as described in chapter 2.2.5.3, using the correction factor for fluorophore absorption at 280 nm, and taking into account that there are two positions for labeling per homodimeric A153C.

Table 8

		Concentration	DOL	
A153C **A488**/**A594** 235 µM	**A488**	**138 µM**	**20 %**	81 %
	A594	**285 µM**	**61 %**	
A153C **A488** 128 µM	**A488**	**155 µM**	**61 %**	

DOL: degree of labeling; A488: Alexa488; A594: Alexa594

The introduction of the labels should not influence binding or cleavage of specific DNA, and therefore all labeled proteins were analyzed for cleavage activity. The procedure for determination of cleavage activity is explained in chapter 2.2.3.6.2. Figure 3.8 shows the result of the cleavage assays for BsoBI A153C labeled with Alexa488 and Alexa647, unlabeled BsoBI A153C and BsoBI wild type (wt).

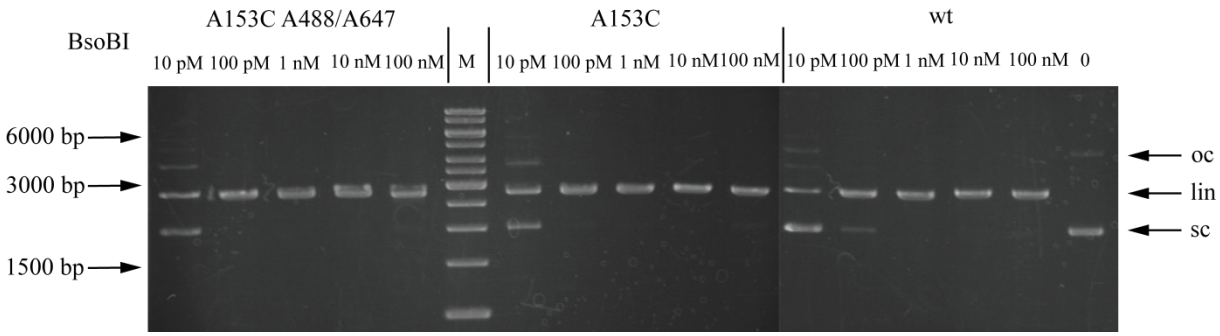

Figure 3.8 Activity test of double labeled BsoBI A153C, unlabeled BsoBI A153C and BsoBI wt. *Cleavage of the pDGS plasmid, with one BsoBI recognition site, results in appearance of linear DNA in the electropherogram. M: GeneRuler™ 1kb DNA ladder (Fermentas); oc: open circle; lin: linear plasmid DNA; sc: supercoiled plasmid DNA*

The plasmid used in the activity test has one BsoBI recognition site, and the cleavage activity is reflected in appearance of linear DNA, and disappearance of supercoiled plasmid. The activity assay shows that neither the introduction of cysteines nor fluorophores influences the cleavage activity of BsoBI (partial cleavage at 10 pM BsoBI, full cleavage at 100 pM BsoBI).

3.3.2. Double labeling of BsoBI used in single-molecule experiments

BsoBI is a homodimer, so introduction of cysteine in one of the subunits leads to introduction of cysteine at the same position in the second subunit. To improve the labeling procedure, which would lead to BsoBI homodimer labeled with donor fluorophore on one subunit, and acceptor fluorophore on the other subunit, a two-step labeling procedure was used. Chromatography steps during this process are presented in Figure 3.9.

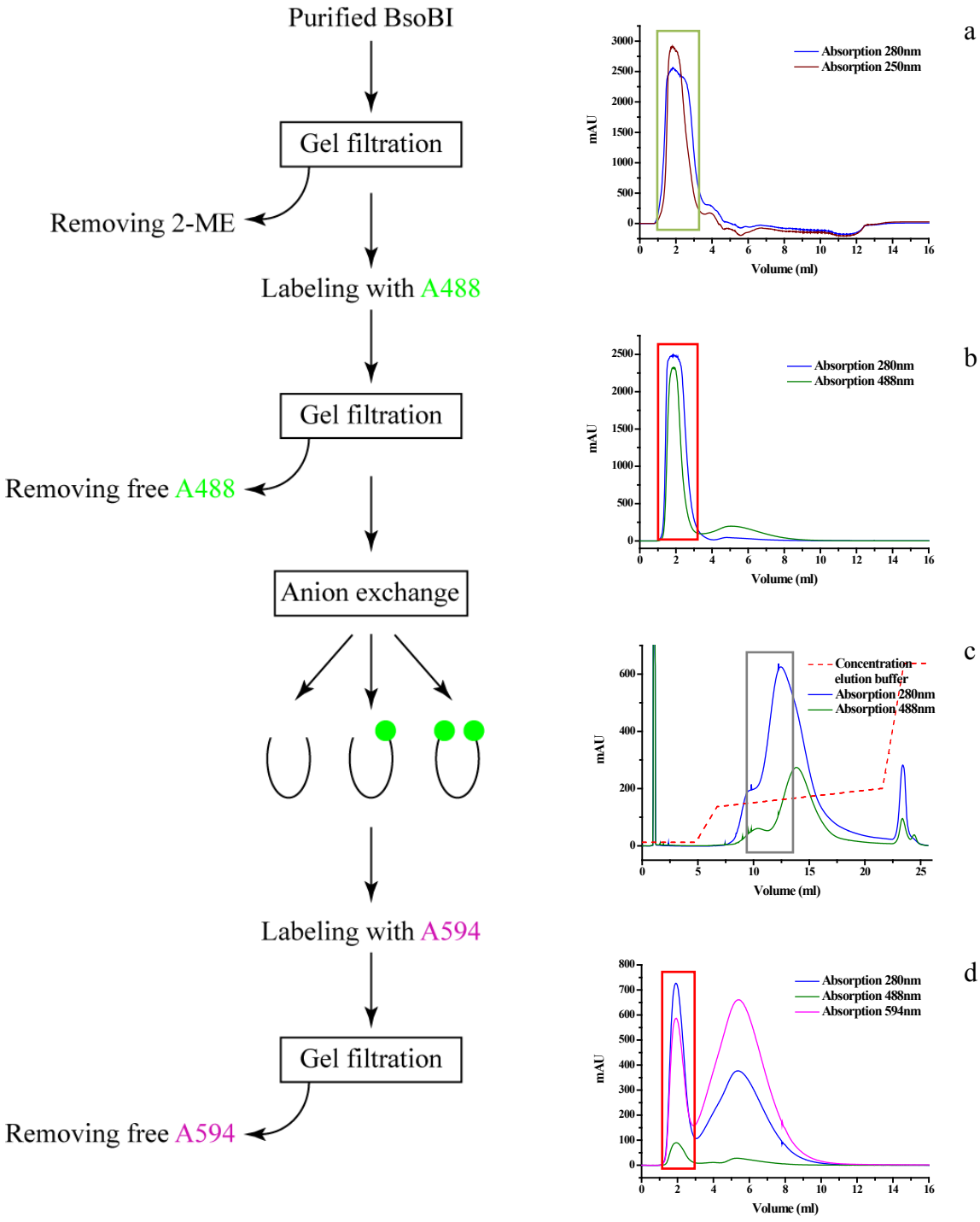

Figure 3.9 Chromatography steps during the two-step double labeling of BsoBI A153C. *a) Chromatogram of removal of 2-ME from protein stock solution, b) Chromatogram of removal of excess of Alexa488, c) Chromatogram of separation of differently labeled proteins, d) Chromatogram of removal of excess of Alexa594. The green box represents the portion of eluted protein used for further labeling. Red boxes represent the portions of eluted protein used in further experiments. The gray box represents the portion of eluted protein used for labeling with Alexa594.*

As described previously, 2-ME was removed from the protein stock solution, and the eluted protein was labeled with donor fluorophore added in molar excess of 1-fold over BsoBI dimer (in stoichiometric amounts to the cysteines). The excess of unreacted fluorophore was removed as previously described.

Figure 3.9.c shows the chromatogram of separating differently labeled protein molecules, carried out using a ResourceQ^{TM} column. The first peak (around 10 ml elution volume) represents BsoBI molecules that are not labeled with Alexa488 fluorophore. The second peak (between 12 and 15 ml elution volume) shows the co-elution of species that absorbs at 280 nm and 488 nm, namely protein and Alexa488 fluorophore. This peak represents BsoBI molecules labeled with one and two fluorophores. However, the separation of the two differently labeled populations is not complete, and the gray box represents the portion of eluted protein that was used for labeling with acceptor fluorophore. Most of the protein used has none or one fluorophore attached to cysteine, but some of the molecules also have two fluorophores, since the separation was not complete. This can be seen in single-molecule experiments, where the population labeled only with donor appears in the double labeled sample.

Subsequently, the portion of eluted protein marked with a gray box in Figure 3.9.c was labeled with a 10-fold molar excess of acceptor fluorophore, either Alexa594 or Alexa647. Also, 200 µl of the chosen eluted portion was kept labeled only with donor fluorophore, and dialysed against storage buffer, to serve as single (donor) labeled sample. Figure 3.9.d shows the chromatogram of removing the excess of unreacted Alexa594 fluorophore via gel filtration.

In Table 9 two examples of labeling efficiencies for double and single labeled BsoBI A153C are shown, obtained after the purification described, using the correction factor for fluorophore absorption at 280 nm (Chapter 2.2.5.3), and taking into account that there are two positions for labeling per homodimeric A153C.

Table 9

		Concentration	DOL	
A153C **A488**/**A594** 14.2 µM	**A488**	**4.2 µM**	**9 %**	90.7 %
	A594	**23.2 µM**	**81.7 %**	
A153C **A488** 33.4 µM	**A488**	**8.3 µM**	**12.4 %**	

DOL: degree of labeling; A488: Alexa488; A594: Alexa594

3.4. DNA binding induces conformational changes in the catalytic domain of BsoBI

Conformational changes induced by substrate binding and cleavage were monitored in steady-state ensemble experiments by mixing different double labeled BsoBI variants with unlabeled DNA. The variant A153C has cysteines introduced in the catalytic domain, and variant E100C has cysteines introduced in the helical domain. The effect of DNA binding was investigated in the presence of different divalent metal ions, namely Ca^{2+} and Mg^{2+}. Mg^{2+} ion is the natural metal ion cofactor which supports specific binding and cleavage of the DNA substrate. In contrast, Ca^{2+} ions enable only specific binding of the substrate, but not cleavage. Conformational changes observed in the presence of Ca^{2+} represent the changes the protein undergoes while binding to the specific DNA site. Conformational changes observed in the presence of Mg^{2+} represent the changes the protein undergoes while binding and cleaving the specific DNA substrate.

First, double labeled BsoBI variant A153C was diluted in buffer containing $CaCl_2$ (chapter 2.1.4), to give a concentration of 50 nM, and the fluorescence spectrum, after excitation at 470 nm, was recorded (Figure 3.10.a). Then an excess of the specific 39 bp long oligonucleotide was added to the cuvette, and the measurement was repeated. The same experiment was done in the presence of $MgCl_2$ (Figure 3.10.b).

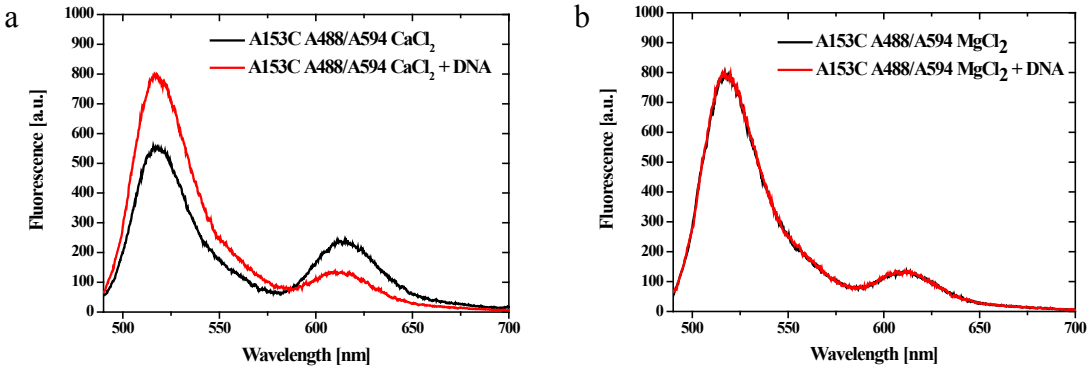

Figure 3.10 Influence of DNA binding on the conformation of the catalytic domain of BsoBI. *a) Conformational changes upon specific DNA binding (in the presence of $CaCl_2$); black line: protein alone, red line: addition of the 39 bp long oligonucleotide, b) conformational changes upon specific DNA binding and cleavage (in the presence of $MgCl_2$); black line: protein alone, red line: addition of the 39 bp long oligonucleotide.*

It can be seen that the addition of specific DNA to the double labeled A153C variant, in the presence of $CaCl_2$, causes a decrease of the FRET signal and increase of the donor signal,

which reflects the movement of two fluorophores away from each other. In contrast, the addition of specific DNA to the double labeled A153C variant, in the presence of $MgCl_2$, does not induce a FRET change. Due to the fact that BsoBI is able to cleave DNA in the presence of $MgCl_2$, this ensemble experiment shows the average signal originating from molecules bound to DNA and molecules that released the product of cleavage, and thus it cannot resolve different species. Also, in the time between mixing the enzyme and DNA, and recording the spectrum (1-2 min), most of the enzyme already had cleaved the substrate, and only enzyme bound to the product and/or free enzyme can be detected.

In the control experiment, the double labeled BsoBI variant E100C was used, and mixed with DNA in the presence of $CaCl_2$ (Figure 3.11.a) or $MgCl_2$ (Figure 3.11.b).

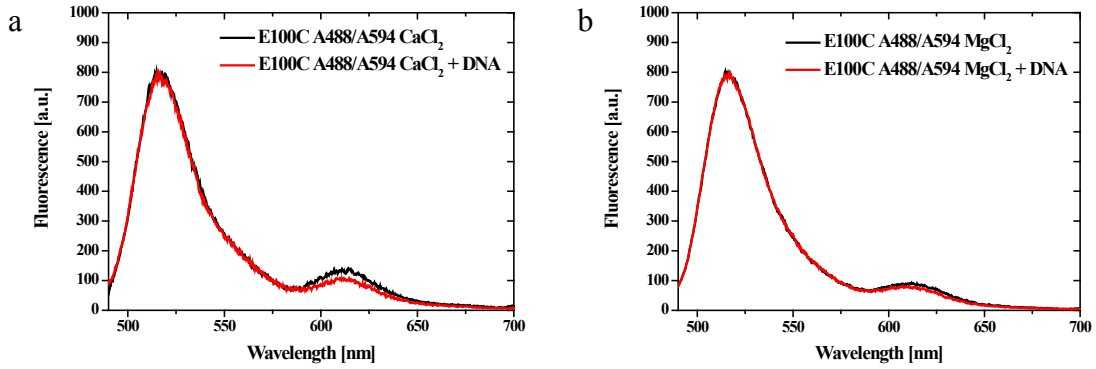

Figure 3.11 Influence of DNA binding on the conformation of the helical domain of BsoBI. *a) Conformational changes upon specific DNA binding (in the presence of $CaCl_2$); black line: protein alone, red line: addition of the 39 bp long oligonucleotide, b) conformational changes upon specific DNA binding and cleavage (in the presence of $MgCl_2$); black line: protein alone, red line: addition of the 39 bp long oligonucleotide.*

The addition of unlabeled specific DNA substrate to the double labeled BsoBI variant E100C, either in the presence of $CaCl_2$ or $MgCl_2$, did not induce a significant FRET change, implying that there is no major movement of the fluorophores placed in the helical domain of BsoBI upon DNA binding and cleavage.

Based on the spectra obtained in previously described experiments, and using the equations described in chapter 2.2.6.2. the efficiency of FRET signal and the distance between two fluorophores for different experiments was calculated. The average of three measurements for different BsoBI variants, as well as different metal ions used, is presented in Figure 3.12.

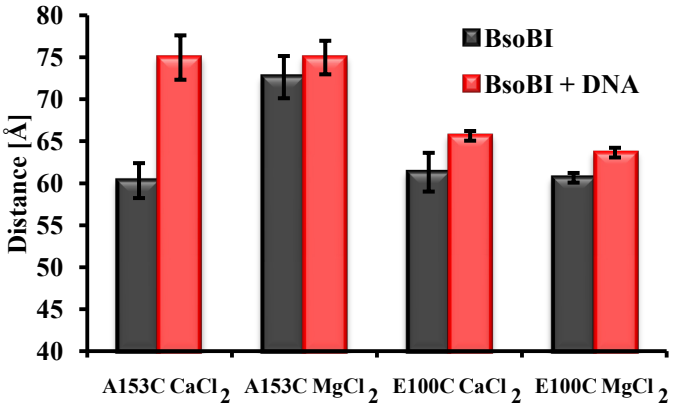

Figure 3.12 Distances between two fluorophores for different BsoBI variants and different buffer conditions as estimated using FRET data. *Gray bars: double labeled BsoBI without DNA; Red bars: double labeled BsoBI with specific DNA*

The distance between the two symmetry related residues A153, measured on the basis of the co-crystal structure, is 77 Å, which is in good agreement with the distance obtained in FRET measurements done in the presence of $CaCl_2$ and specific DNA. Distances calculated for BsoBI alone could not be compared with those from crystal structure, since there is no crystal structure without DNA available.

The distance between the two E100 residues based on the co-crystal structure is 46 Å, while distances calculated from FRET measurements are in the range between 60 Å and 65 Å. However, the position of these cysteines, which suggests that the fluorophores are positioned away from the enzyme, (Figure 3.5.c) and the fact that fluorophores are linked to the protein via a C_5 linker, may explain the differences between calculated and theoretical values.

3.5. Ca^{2+} and Mg^{2+} ions have a different influence on the catalytic domain of BsoBI

Previously described experiments revealed a different behaviour of free BsoBI A153C in the presence of $CaCl_2$ and $MgCl_2$ (Figure 3.12). In order to study in more detail this effect, the double labeled BsoBI variant A153C was diluted into three different buffers, and the FRET was measured. The buffers contained 5 mM $CaCl_2$ or 5 mM $MgCl_2$ or 0.5 mM EDTA (Figure 3.13.a). The same experiments were repeated with the double labeled BsoBI variant E100C as a control, to study the effect of divalent metal ions on the helical domain (Figure 3.13.b).

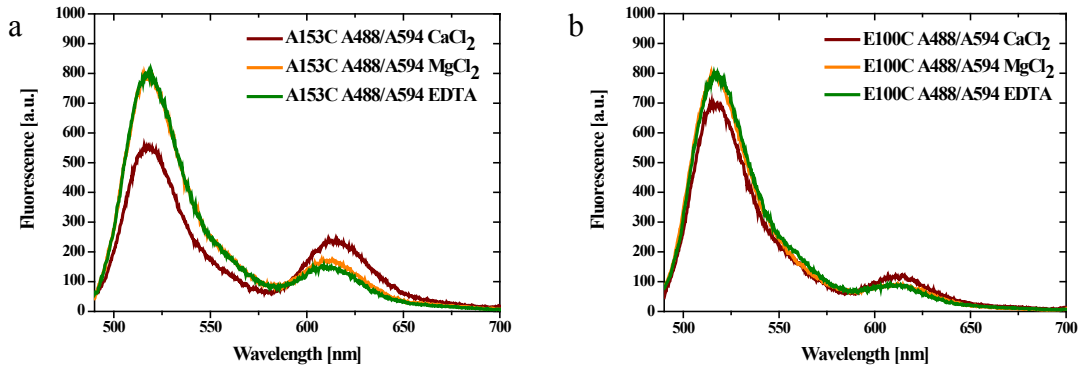

Figure 3.13 Influence of different divalent metal ions on the structure of BsoBI. *a) Influence of Ca^{2+} and Mg^{2+} on the catalytic domain of BsoBI, b) Influence of Ca^{2+} and Mg^{2+} on the helical domain of BsoBI; All experiments were done in the absence of DNA. Brown line: BsoBI in the presence of $CaCl_2$; Orange line: BsoBI in the presence of $MgCl_2$; Green line: BsoBI in the absence of metal ions and in the presence of EDTA.*

It could be seen that the addition of $CaCl_2$ induces a conformational change in the catalytic domain of BsoBI which brings two fluorophores attached to the cysteines at the position 153 closer together. In the control experiment, in which double labeled BsoBI variant E100C was used, no significant change could be seen after measuring the FRET signal in the presence of $MgCl_2$ or EDTA.

In addition, FRET values were determined for different $CaCl_2$ concentrations in the buffer, using the double labeled variant A153C. The results are presented in Figure 3.14 as the influence of the $CaCl_2$ concentrations on the F_A/F_D ratio. This ratio is calculated by dividing the maximum fluorescence of the FRET signal (F_A) by the maximum fluorescence of the donor signal (F_D) in the double labeled protein.

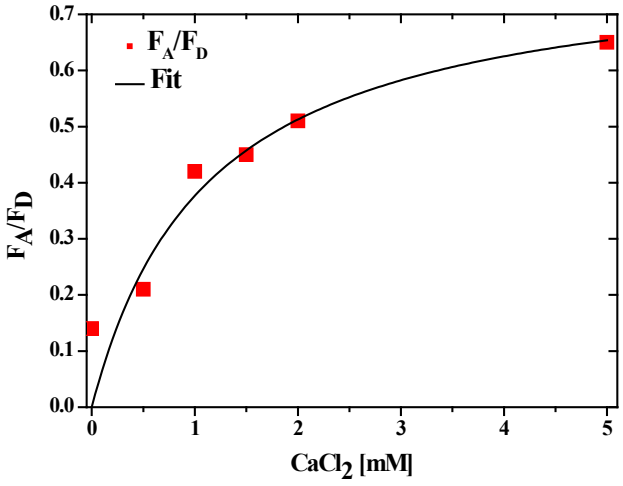

Figure 3.14 Influence of different $CaCl_2$ concentrations on the conformation of double labeled A153C variant. *All experiments were done in the absence of DNA*

Based on the curve obtained, the estimated value for the binding constant (K_D) for Ca^{2+} ions to the protein is 1.1 ± 0.5 mM.

3.6. Pre-steady state experiments reveal different enzyme kinetics in the presence of Ca^{2+} and Mg^{2+} ions

In order to study the kinetics of conformational changes in BsoBI, a series of pre-steady state experiments was done. The experiments were carried out using either double labeled BsoBI and unlabeled DNA, or single labeled BsoBI and labeled DNA. All experiments were done at room temperature, and using the same buffers used in the steady-state and single-molecule measurements.

3.6.1. Kinetics of conformational changes induced by DNA binding to the double labeled BsoBI A153C variant

In order to study the kinetics of conformational changes in BsoBI induced by DNA binding, a series of stopped-flow experiments was done using double labeled BsoBI and an unlabeled specific oligonucleotide (39 bp). Double labeled BsoBI A153C variant was diluted to 100 nM in buffer containing $CaCl_2$, to give a final concentration of 50 nM enzyme in the mixing chamber. The use of $CaCl_2$ allows only specific binding, but not cleavage of DNA. The second syringe contained 800 nM unlabeled DNA, diluted in same buffer, to give a final concentration of 400 nM in the mixing chamber. This solution was diluted with buffer, in

order to achieve four additional DNA concentrations (200 nM, 100 nM, 75 nM and 50 nM). The changes were observed during 100 s, in three time intervals with different number of data points collected: 0-5 s each 10 ms (501 data points), 5-50 s each 50 ms (900 data points) and 50-100 s each 100 ms (500 data points) (Figure 3.15). Bandpass filter D515/30m (LOT Oriel) was used in order to monitor changes in the donor signal.

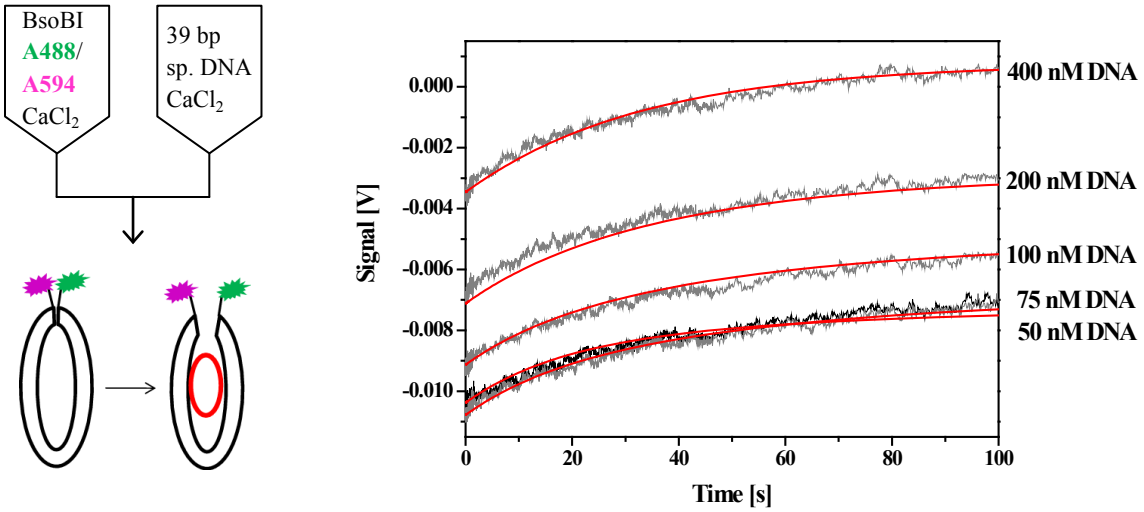

Figure 3.15 Kinetics of conformational changes induced by DNA binding. *Double labeled BsoBI A153C variant was diluted with buffer containing $CaCl_2$, to a final concentration in the mixing chamber of 50 nM. Experimental time traces are shown in gray, and fitted curves are shown in red. On the left a scheme of the stopped flow reaction is shown.*

Binding of DNA to the double labeled BsoBI A153C variant induces an increase in the donor signal (and consequently a decrease in the FRET signal), suggesting that the conformational change in the catalytic domain of BsoBI moves the two fluorophores further apart. Experimental traces were analyzed using the DynaFit (Biokin) program [69], which performs a nonlinear least-squares regression of the kinetic data. The program performed a global analysis, i.e. fitted all experimental curves simultaneously to the same set of rate constants. The curves obtained are shown in red in Figure 3.15. The result of the global analysis is presented in the following scheme:

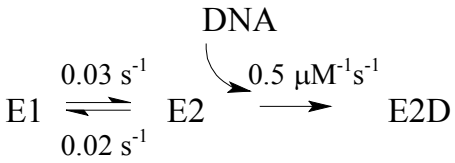

It can be seen that the enzyme exists in at least two different conformations (E1 and E2), one of which (E2) is slightly favored (equilibrium constant 1.5), and able to bind DNA. DNA

binding can be therefore described as a two step reaction: a first order conformational change followed by a second order association of DNA to the binding competent BsoBI, with a rate constant of 0.5 $\mu M^{-1}s^{-1}$. The errors for the rate constants obtained were between 1 % and 6 %.

3.6.2. Kinetics of DNA binding to the BsoBI A153C variant using fluorescently labeled DNA and labeled protein

The kinetics of DNA binding was monitored in the stopped-flow setup, using donor labeled BsoBI and acceptor labeled 39 bp long specific oligonucleotide. Both protein and DNA were diluted in buffer containing Ca^{2+} ions, which enables specific binding but not the cleavage of DNA. BsoBI was diluted to 100 nM in one syringe, making the end concentration in the mixing chamber 50 nM. The first DNA concentration was 800 nM (400 nM in mixing chamber), and this solution was diluted for further experiments to make four additional concentrations (200 nM, 100 nM, 75 nM and 50 nM). Since the concentration of acceptor labeled DNA was varied during the experiments, the changes in donor signal were monitored (Figure 3.16).

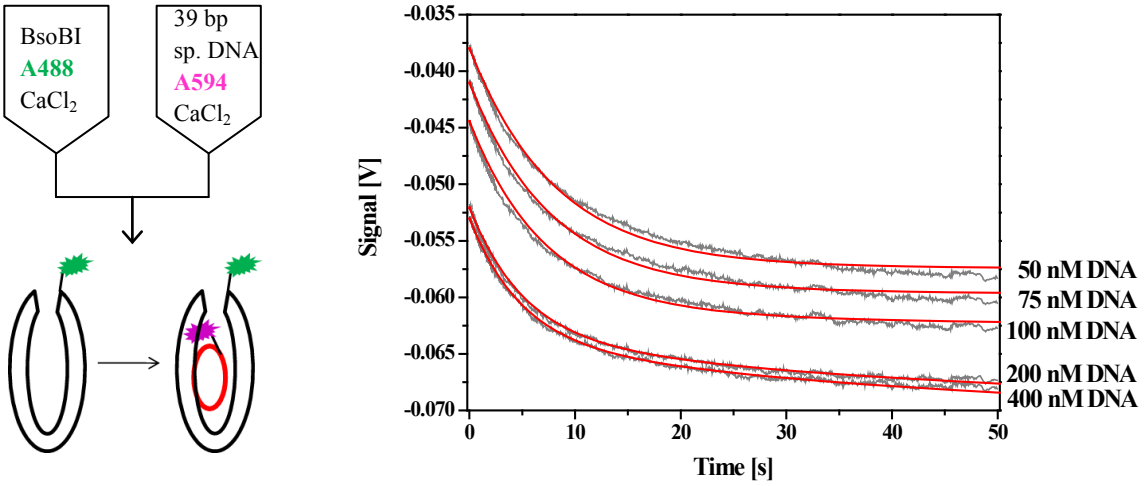

Figure 3.16 Kinetics of DNA binding in the presence of Ca^{2+} ions. *Single (donor) labeled BsoBI was diluted with buffer containing $CaCl_2$, to a final concentration in the mixing chamber of 50 nM. Experimental time traces of the donor signal are shown in gray, and fitted curves are shown in red. On the left a scheme of the stopped flow reaction is shown.*

As the result of the acceptor labeled DNA binding to the donor labeled BsoBI, donor signal decreased. The obtained experimental traces were analyzed using the DynaFit (Biokin) program, performing a global analysis. The resulted fits are shown in red in Figure 3.16, and also presented in the following scheme:

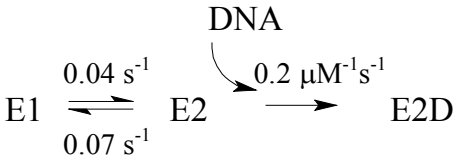

As in the experiment with double labeled protein, BsoBI exists in at least two conformations before binding the DNA, although the equilibrium constant is slightly different compared to the previous experiment, which is not too surprising, since in the two sets of experiments differently labeled reaction partners were used. DNA binding is described as a second order association, with a rate constant of 0.2 $\mu M^{-1}s^{-1}$.

3.6.3. Kinetics of DNA binding and cleavage in the presence of Mg^{2+} ions

In order to monitor the kinetics of binding and cleavage of specific DNA by BsoBI, donor labeled BsoBI and acceptor labeled 39 bp long specific oligonucleotide were mixed in the presence of Mg^{2+} ions, and the donor signal was monitored. After DNA binding, the donor signal decreases due to association of the acceptor labeled DNA and thus appearance of FRET. After DNA cleavage and product release, the donor signal increases due to dissociation of the acceptor labeled product. The concentration of BsoBI in the syringe was 100 nM, which made the concentration in the mixing chamber 50 nM. The start concentration of DNA was 800 nM, making the concentration in the mixing chamber 400 nM. This solution was subsequently diluted to give four additional concentrations (200 nM, 100 nM, 75 nM and 50 nM, in the mixing chamber). The reactions were monitored after mixing 100 μl of each species in the mixing chamber. For each concentration 10-20 curves were obtained, and averaged using the Biokine 2.07 software (Figure 3.17).

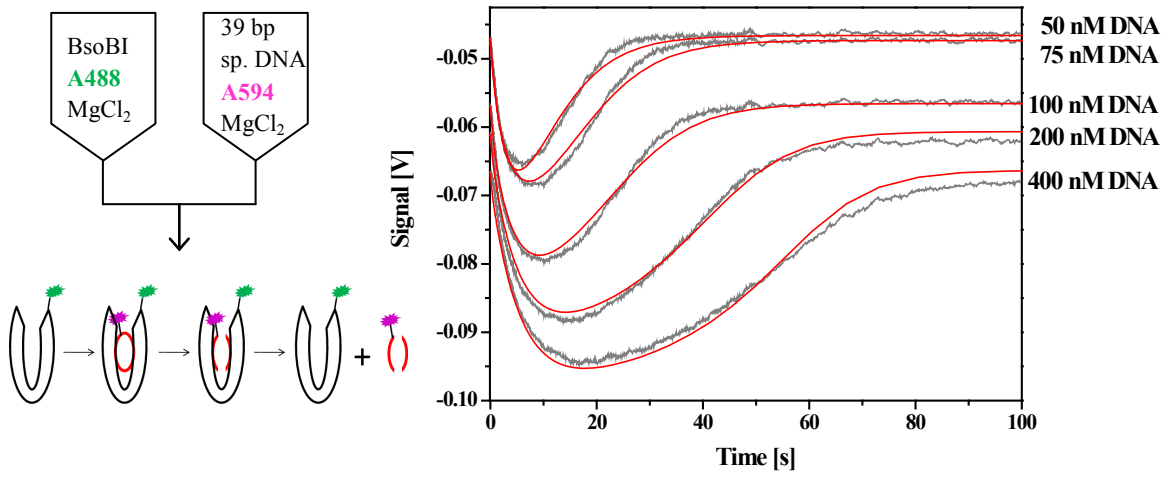

Figure 3.17 Kinetics of DNA binding and cleavage in the presence of Mg^{2+} ions. *Single (donor) labeled BsoBI was diluted with buffer containing $MgCl_2$, to give a final concentration in the mixing chamber of 50 nM. Experimental time traces of the donor signal are shown in gray, and fitted curves are shown in red. On the left a scheme of the stopped flow reaction is shown.*

The experimental data (gray in Figure 3.17) obtained were analyzed using the DynaFit (Biokin) program, performing a global analysis, and presented in red in Figure 3.17 and as a scheme below:

As can be seen, BsoBI exists in two conformations before binding the DNA, one of which is slightly more favored (E2 in the scheme). DNA binding is described as a second order association reaction, with a rate constant of 4.8 $\mu M^{-1}s^{-1}$, approximately 20 times higher than in the binding experiments using Ca^{2+} ions.

3.6.4. Influence of Ca^{2+} and Mg^{2+} ions on the conformation of the catalytic domain of BsoBI

The observed influence of different metal ions on the conformation of the catalytic domain of BsoBI was analyzed in the stopped-flow setup, using double labeled BsoBI and buffers with different concentrations of Ca^{2+} or Mg^{2+} ions.

First, double labeled BsoBI A153C variant was diluted with a buffer containing 5.5 mM $CaCl_2$, and mixed with buffer containing increasing concentrations of $MgCl_2$. The bandpass

filter D630/30 (LOT Oriel) was used in order to monitor the changes in acceptor signal (Figure 3.18). The changes were monitored for 100 s, in three time intervals, with different number of data points collected: 0-5 s each 10 ms (501 data points), 5-50 s each 50 ms (900 data points) and 50-100 s each 100 ms (500 data points). Double labeled BsoBI was diluted to 100 nM with a buffer containing 5.5 mM $CaCl_2$. After mixing equal volumes of labeled protein and a $MgCl_2$ containing buffer, the final concentrations in mixing chamber were half of the starting concentrations (50 nM BsoBI, 2.75 mM $CaCl_2$, 2.75-27.5 mM $MgCl_2$).

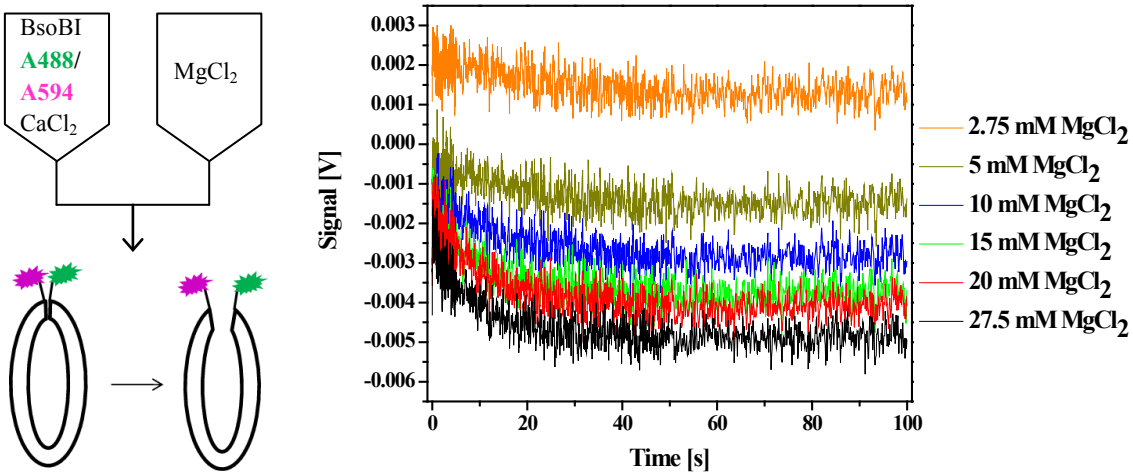

Figure 3.18 Kinetics of the conformational changes of the catalytic domain of BsoBI induced by replacing Ca^{2+} ions by Mg^{2+} ions. *The double labeled BsoBI A153C variant (50 nM) was diluted with buffer containing $CaCl_2$, and mixed with buffer containing different concentrations of $MgCl_2$. The acceptor signal was monitored. On the left a scheme of the stopped flow reaction is shown.*

It can be seen that the FRET signal decreases when Mg^{2+} ions replace Ca^{2+} ions in the double labeled BsoBI A153C variant, suggesting that the conformational changes in the catalytic domain of BsoBI move the two fluorophores further apart. The traces obtained were fitted with first order exponential curves, and one example of the fitted curve is presented in Figure 3.19.

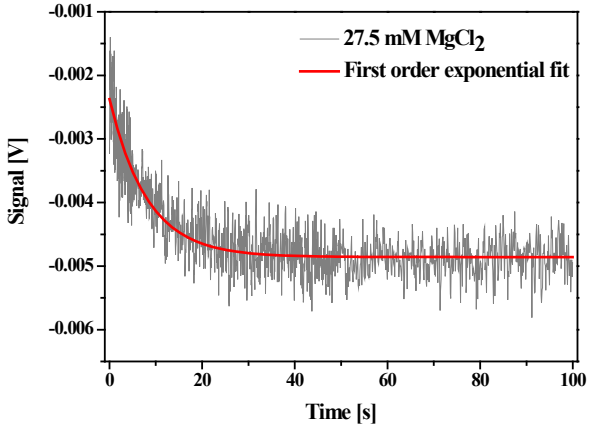

Figure 3.19 Influence of the highest $MgCl_2$ concentration on the conformation of BsoBI. *The time trace of the acceptor signal is fitted with a first order exponential curve, resulting in a rate constant of 0.085 ± 0.002 s^{-1}.*

All traces were fitted in the same way, and the resulting rate constants were plotted as a function of $MgCl_2$ concentrations (Figure 3.20).

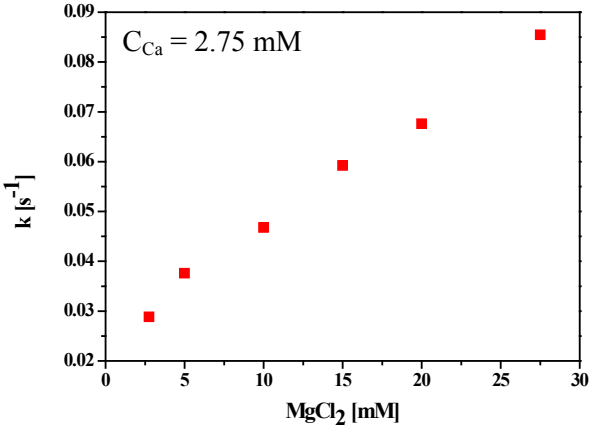

Figure 3.20 Observed apparent rate constants for the conformational changes as a function of $MgCl_2$ concentrations.

As can be seen in Figure 3.20, the rate of the conformational changes in the catalytic domain of BsoBI are dependent on the concentration of Mg^{2+} ions used, namely, with the increase of $MgCl_2$ concentration, the apparent rate constant is increasing.

In order to study the influence of Ca^{2+} ions replacing Mg^{2+} ions on the conformation of the catalytic domain of BsoBI, double labeled BsoBI A153C variant was diluted with buffer containing 5.5 mM $MgCl_2$ and mixed with increasing concentrations of $CaCl_2$. The concentrations of double labeled protein, as well as metal ions used, were the same as the

ones used in the previously described experiments. As in the previous case, the changes in acceptor signal were monitored (Figure 3.21).

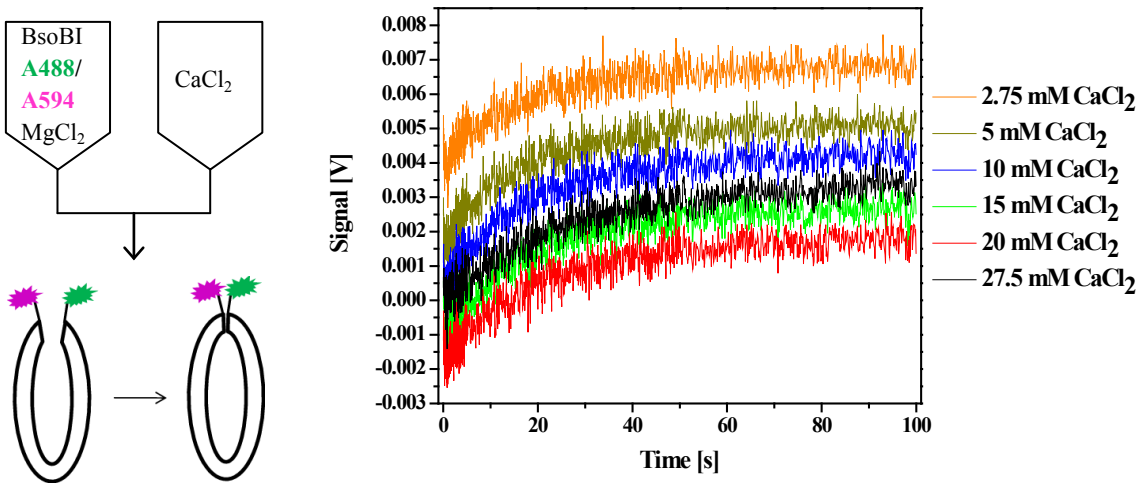

Figure 3.21 Kinetics of conformational changes of catalytic domain of BsoBI induced by replacing Mg^{2+} ions by Ca^{2+} ions. *The double labeled BsoBI A153C variant (50 nM) was diluted with buffer containing $MgCl_2$, and mixed with a buffer containing different concentrations of $CaCl_2$. The acceptor signal was monitored. On the left a scheme of the stopped flow reaction is shown.*

The Figure 3.21 shows the increase in FRET signal after replacing Mg^{2+} ions with Ca^{2+} ions, suggesting that the conformational change in the catalytic domain of BsoBI moves the two fluorophores closer together. As previously described, all traces were fitted with first order exponential curves, and examples of one $CaCl_2$ concentration and the dependence of the apparent rate constant on the $CaCl_2$ concentration is shown in Figure 3.22 and Figure 3.23, respectively.

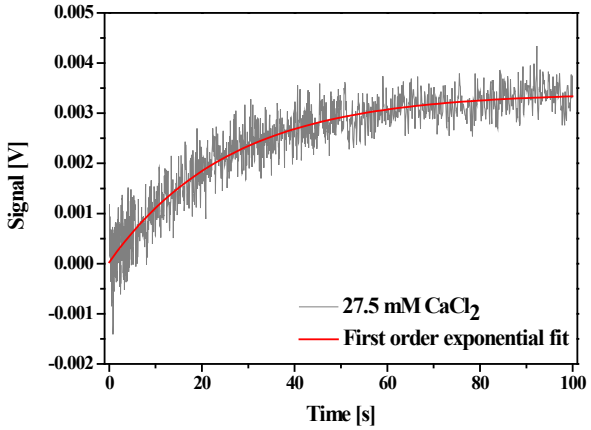

Figure 3.22 Influence of the highest $CaCl_2$ concentration on the rate of the conformational change of BsoBI. *The time trace of the acceptor signal is fitted with a first order exponential curve, resulting in a rate constant of 0.0267 ± 0.0006 s^{-1}.*

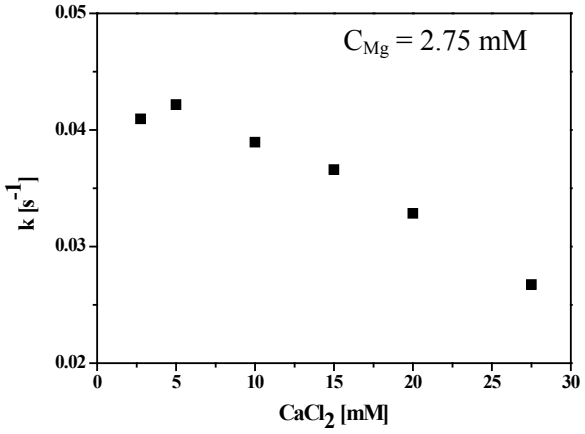

Figure 3.23 Observed apparent rate constants for the conformational change as a function of $CaCl_2$ concentrations.

In contrast to the results of the previous experiments, the rate constant is decreasing with the increase of $CaCl_2$ added, although the change is not as pronounced as in the case of the $MgCl_2$ addition (Figure 3.24).

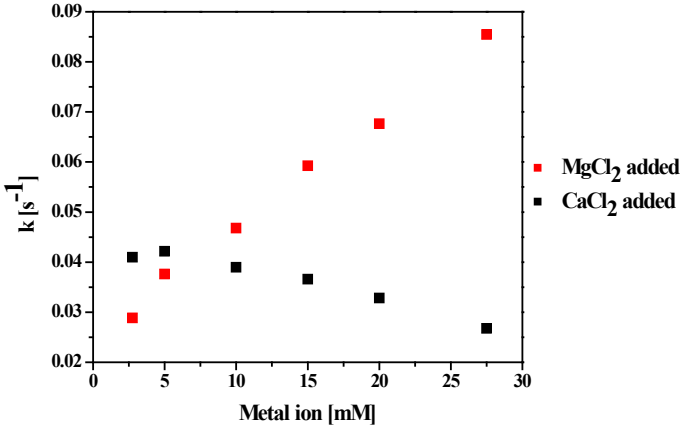

Figure 3.24 Comparison of the influence of the metal ion used on the apparent rate constant of the conformational change of the BsoBI catalytic domain.

If the exchange of Ca^{2+} is faster than the one of Mg^{2+}, the signal monitored is the exchange of Mg^{2+}, since this is the rate limiting step, and the description of the exchange rates can be presented by the following equation (detailed calculations are presented in Supplementary information) describing the relationship between the apparent rate constant k in terms of the association and dissociation rate constants for Mg^{2+} and Ca^{2+} and their concentrations:

$$k = k_{-1} + \frac{k_1 \cdot k_{-2}}{k_2} \cdot \frac{[Mg^{2+}]}{[Ca^{2+}]}$$

Where k_1 and k_{-1} are the association and dissociation rate constants of Mg^{2+}, respectively, while k_2 and k_{-2} are the association and dissociation rate constants of Ca^{2+}, respectively. It is clear that the increase of the $CaCl_2$ concentration will cause the decrease of the exchange rates. Vice versa, the increase of the $MgCl_2$ concentration will cause the increase of the exchange rates.

The influence of different metal ions was also studied by mixing the double labeled BsoBI A153C variant diluted in a buffer containing 0.5 mM EDTA with buffers containing either 5.5 mM $CaCl_2$ or 5.5 mM $MgCl_2$ (Figure 3.25). The final concentration of BsoBI in the mixing chamber was 50 nM, while the concentrations of all divalent metal ions and EDTA were half of the starting values. The change in acceptor signal was monitored for 100 s, in time intervals described in previous experiments.

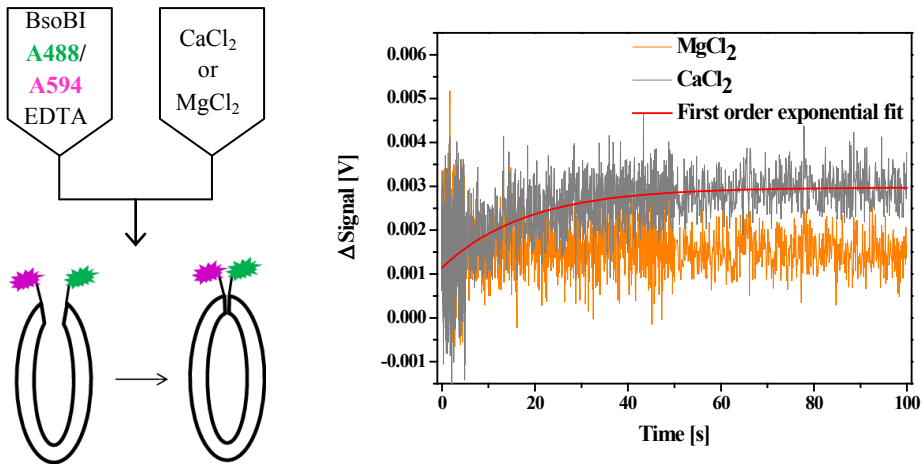

Figure 3.25 Kinetics of the conformational changes of the catalytic domain of BsoBI induced by replacing EDTA by Ca^{2+} or Mg^{2+} ions. *The double labeled BsoBI A153C variant (50 nM) was diluted with buffer containing 0.5 mM EDTA, and mixed with a buffer containing 5.5 mM $CaCl_2$ or $MgCl_2$. The first order exponential fit of $CaCl_2$ addition resulted in rate constant of 0.038 ± 0.003 s^{-1}. The acceptor signal was monitored. On the left a scheme of the stopped flow reaction is shown.*

The replacement of EDTA by Ca^{2+} ions induces an increase in the FRET signal, suggesting a conformational change in the catalytic domain of BsoBI that moves the two fluorophores closer together. In contrast, the addition of $MgCl_2$ containing buffer did not induce any change in acceptor (FRET) signal, suggesting no conformational change in the catalytic domain of BsoBI.

3.6.5. Influence of Ca^{2+} and Mg^{2+} ions on the catalytic activity of BsoBI

In order to further study the influence of different divalent metal ions on BsoBI, a series of pre-steady state experiments was done using different mixtures of Ca^{2+} and Mg^{2+} ions:

1. Donor labeled BsoBI and acceptor labeled specific DNA pre-mixed in the presence of EDTA + 5.5 mM $CaCl_2$ *versus* 5.5 mM $MgCl_2$ or 5.5 mM $CaCl_2$ *versus* 55 mM $MgCl_2$

First, the donor labeled BsoBI A153C variant and the acceptor labeled 39 bp long specific oligonucleotide were pre-mixed in the presence of EDTA. The concentration of BsoBI was 100 nM (giving a 50 nM final concentration in the mixing chamber), while the concentration of DNA was 150 nM (75 nM in the mixing chamber). This complex was mixed with buffers containing 5.5 mM $CaCl_2$ and either 5.5 mM or 55 mM $MgCl_2$ (Figure 3.26). The donor signal was monitored for 100 s in time intervals described in previous experiments. The

cleavage and release of acceptor labeled DNA causes an increase in the donor signal, as the result of the disappearance of FRET.

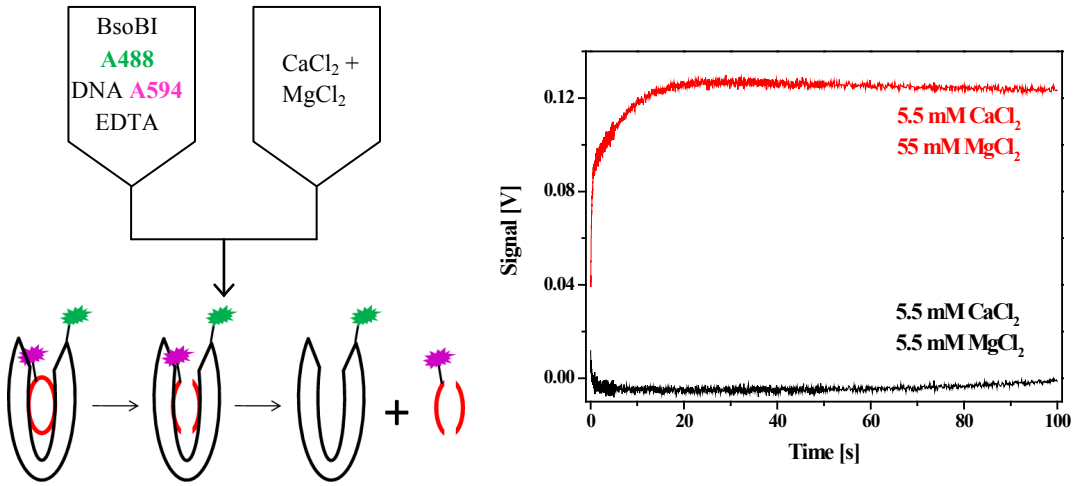

Figure 3.26 Kinetics of DNA cleavage in the presence of Ca^{2+} and Mg^{2+} ions. *Donor labeled BsoBI and acceptor labeled DNA were pre-mixed in buffer containing EDTA, and then mixed with buffers containing 5.5 mM $CaCl_2$ and either 5.5 mM $MgCl_2$ (black curve) or 55 mM $MgCl_2$ (red curve). On the left a scheme of the stopped flow reaction is shown.*

From Figure 3.26 it can be seen that the mixture of equal concentrations of $CaCl_2$ and $MgCl_2$ causes residual substrate binding (decrease of the signal at the beginning of the black curve) and then very slow cleavage of specific DNA (increase of the signal at the end of the black curve). In contrast, the 10-fold excess of $MgCl_2$ over $CaCl_2$ causes fast cleavage of specific DNA pre-bound to BsoBI in the presence of EDTA.

2. Donor labeled BsoBI and acceptor labeled specific DNA pre-mixed in the presence of EDTA + 5.5 mM $MgCl_2$ or 55 mM $MgCl_2$

Next, the donor labeled BsoBI A153C variant was pre-mixed with the acceptor labeled 39 bp long specific oligonucleotide in the presence of EDTA, in the same concentrations as in the previous experiment. This complex was mixed with buffer containing different concentrations of $MgCl_2$ (Figure 3.27). Donor signal was monitored for 50 s, in the time intervals described previously. Again, the cleavage and release of donor labeled DNA causes an increase of donor signal.

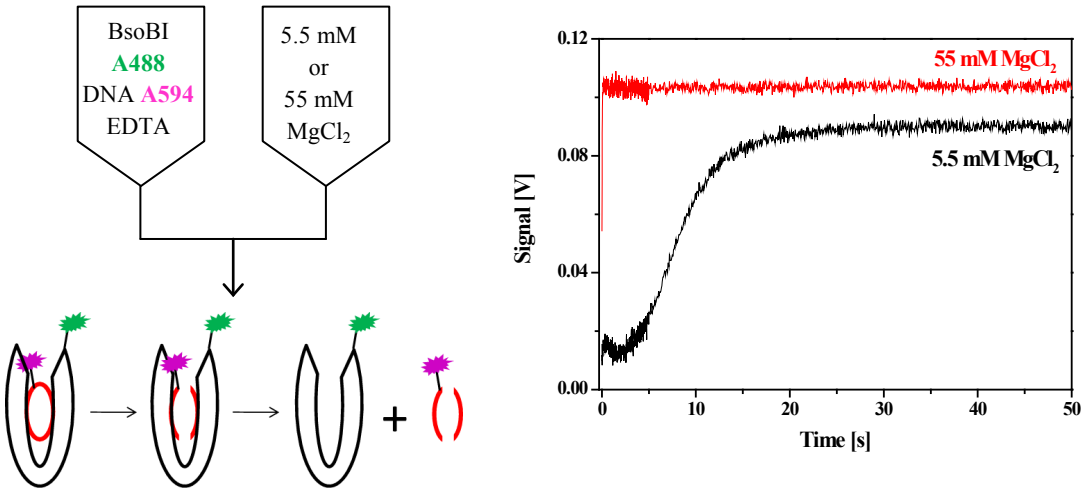

Figure 3.27 Kinetics of DNA cleavage in the presence of different $MgCl_2$ concentrations. *Donor labeled BsoBI and acceptor labeled DNA were pre-bound in the presence of 0.5 mM EDTA and mixed with buffers containing either 5.5 mM $MgCl_2$ (black curve) or 55 mM $MgCl_2$ (red curve). On the left a scheme of the stopped flow reaction is shown.*

After mixing BsoBI-DNA complex pre-bound in 0.5 mM EDTA with 5.5 mM $MgCl_2$, there is a lag phase in the signal, and possibly certain residual substrate binding (small decrease of the signal in black curve in Figure 3.27), after which the cleavage and product release is happening. In contrast, when 55 mM of $MgCl_2$ was used, the cleavage and release of the product is much faster, and the first part of the signal is lost in the dead-time of the stopped-flow machine (red curve in Figure 3.27).

3. Donor labeled BsoBI and acceptor labeled specific DNA pre-mixed in the presence of 5.5 mM $CaCl_2$ + 5.5 mM $MgCl_2$ or 55 mM $MgCl_2$

Finally, the donor labeled BsoBI A153C variant was pre-mixed with the acceptor labeled 39 bp long specific oligonucleotide, in the presence of 5.5 mM $CaCl_2$, using the same concentrations as in the previous experiments. This complex was mixed with buffers containing either 5.5 mM $MgCl_2$ or 55 mM $MgCl_2$ (Figure 3.28). The donor signal was monitored for 100 s, in the time intervals previously described. The increase of this signal indicated the cleavage and release of acceptor labeled DNA.

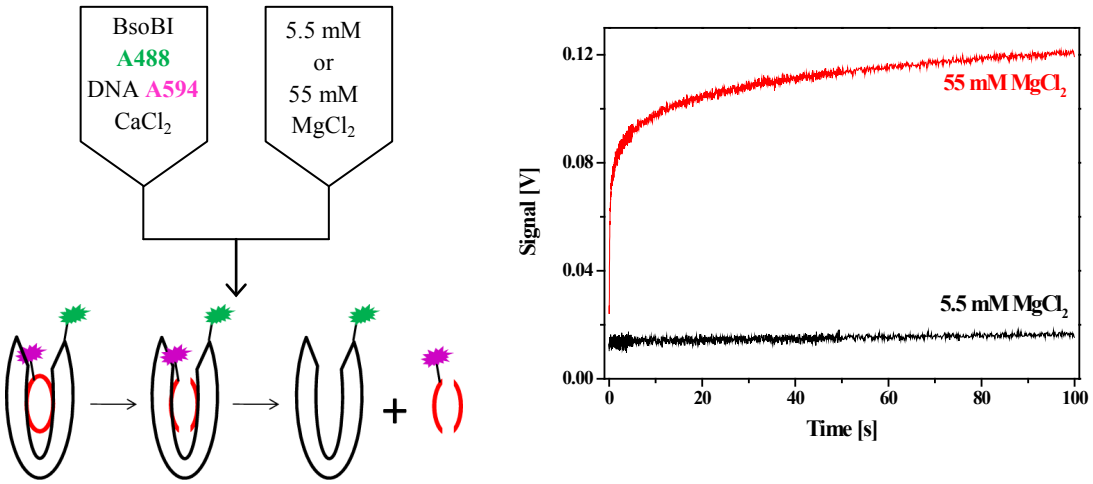

Figure 3.28 Kinetics of DNA cleavage in the presence of different $MgCl_2$ concentrations. *Donor labeled BsoBI and acceptor labeled DNA were pre-bound in the presence of 5.5 mM $CaCl_2$ and mixed with buffers containing either 5.5 mM $MgCl_2$ (black curve) or 55 mM $MgCl_2$ (red curve). On the left a scheme of the stopped flow reaction is shown.*

Equimolar concentrations of $CaCl_2$ and $MgCl_2$ cause very slow cleavage of DNA (black curve in Figure 3.28). After addition of a 10-fold excess of $MgCl_2$ over $CaCl_2$, there is fast cleavage of DNA pre-bound to BsoBI in the presence of 5.5 mM $CaCl_2$ (red curve in Figure 3.28).

3.7. Single-molecule experiments reveal the existence of two conformations of free BsoBI

In order to investigate in more detail the conformational changes during DNA binding by BsoBI, a series of single-molecule experiments were done using smMFD (single-molecule multiparameter fluorescence detection). These experiments allowed for separation of subpopulations present in the sample, which are hidden during the ensemble experiments. The results obtained are presented in 2D frequency histograms of S_G/S_R *vs.* $\tau_{D(A)}$. S_G/S_R represents the ratio between green and red fluorescence, corrected for background, detection efficiencies and crosstalk, and $\tau_{D(A)}$ represents the donor lifetime in the presence of acceptor. Figure 3.29 shows a theoretical example of this kind of data representation.

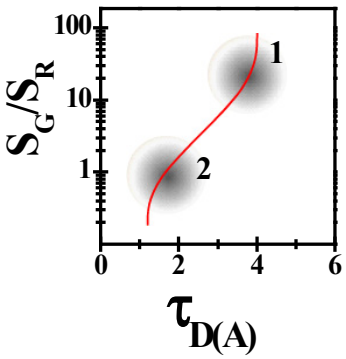

Figure 3.29 2D frequency histogram of S_G/S_R *vs.* $\tau_{D(A)}$. *1 – Low FRET / donor only population; 2 – High FRET population; number of bursts increases from white to black. Detailed explanation in the text.*

Two populations in Figure 3.29 represent examples of a low FRET or donor only population (population 1) and a high FRET population (population 2). With the appearance of FRET, the ratio between green and red fluorescence (S_G/S_R) decreases (due to the increase of red fluorescence). At the same time, the lifetime of the donor also decreases (due to the energy transfer to the acceptor), resulting in the movement of the FRET population along the sigmoidal curve (red in Figure 3.29), i.e. toward the lower donor lifetime and lower S_G/S_R ratio.

3.7.1. Conformational changes during DNA binding in the presence of Ca^{2+} ions

Conformational changes during DNA binding were first monitored using the double labeled BsoBI E290C variant and the 12 bp long specific or unspecific oligonucleotide, in the presence of Ca^{2+} ions. The results obtained are presented in Figure 3.30, as 2D frequency histogram of S_G/S_R vs. $\tau_{D(A)}$. Full trace data underwent a burst selection process, in which only the bursts containing >20 photons in the red channel were selected. This selection allowed for excluding red bursts not originating from FRET, and it is commonly used to remove significant amount of donor-only population. As can be seen in Figure 3.30, this analysis did not influence the properties of the FRET species (compare red lines with black and orange filled histograms).

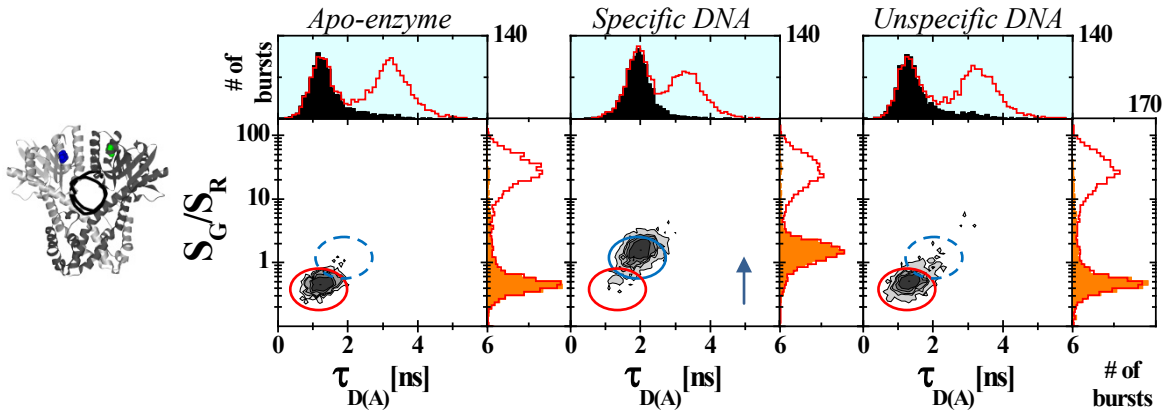

Figure 3.30 Double labeled BsoBI E290C in the presence of $CaCl_2$ with 12 bp long DNA. *The ratio between green and red fluorescence (S_G/S_R) was corrected for background, detection efficiencies and crosstalk. Red lines in single histograms represent full trace data; black and orange filled histograms represent bursts selected based on the number of photons in the red channel – only bursts with more than 20 photons were selected. Red circle – high FRET; blue circle – middle FRET. The structure on the left indicates the labeling positions.*

Double labeled (Alexa488/Alexa647) BsoBI E290C was diluted to 50 pM in buffer containing $CaCl_2$, and measured in the absence of DNA for 1,5 h. The results obtained presented in Figure 3.30 show that BsoBI E290C has one favored conformation in the absence of DNA (left panel), with a second conformation present in low proportion (around 7 %, according to the probability distribution analysis – PDA [71]). This population has the same distance between the fluorophores as the enzyme with the specific substrate bound. The addition of specific DNA (Figure 3.30, middle panel) causes a significant change in conformation of BsoBI E290C, which results in almost complete movement (indicated by the arrow) of high FRET species to lower FRET value (approximately 12 % of the protein, according to the PDA analysis, is still in the high FRET population). The binding of unspecific DNA (Figure 3.30, right panel) causes no significant change compared to the FRET species of protein alone.

The same experiments were done using a 39 bp long specific or unspecific DNA, and the results are presented in Figure 3.31. As in the previous case, burst selection was performed in order to remove donor-only population.

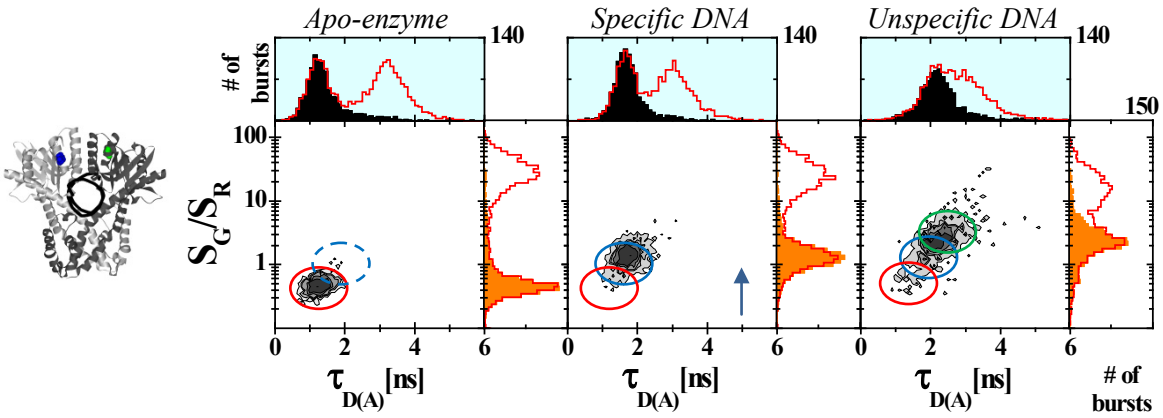

Figure 3.31 Double labeled BsoBI E290C in the presence of $CaCl_2$ with 39 bp long DNA. *The ratio between green and red fluorescence (S_G/S_R) was corrected for background, detection efficiencies and crosstalk. Red lines in single histograms represent full trace data; black and orange filled histograms represent bursts selected based on the number of photons in the red channel – only bursts with more than 20 photons were selected. Red circle – high FRET; blue circle – middle FRET; green circle – lowest FRET. The structure on the left indicates the labeling positions.*

The binding to the 39 bp specific oligonucleotide (Figure 3.31, left panel) caused similar conformational changes as in the case of the 12 bp oligonucleotide, namely the movement of high FRET species to the lower values. However, binding to longer unspecific DNA showed some significant differences. Three different FRET populations can be seen in the presence of unspecific DNA (Figure 3.31, right panel). The highest FRET population (approximately 17 %, according to the PDA analysis) corresponds to the same FRET population present in the case of the protein alone. The middle FRET population is the most populated (approximately 61 %, according to the PDA analysis) and corresponds to the population present also in the case of protein binding to specific DNA. The lowest FRET population (approximately 22 %, according to the PDA analysis) is present only in the case of unspecific DNA binding.

In order to get more insight into conformational changes in the helical domain of BsoBI, the same experiments were done using the double labeled (Alexa488/Alexa647) variant A153C. Figure 3.32 represents the results of the measurements performed in the presence of $CaCl_2$, using short (12 bp) and long (39 bp) specific or unspecific DNA.

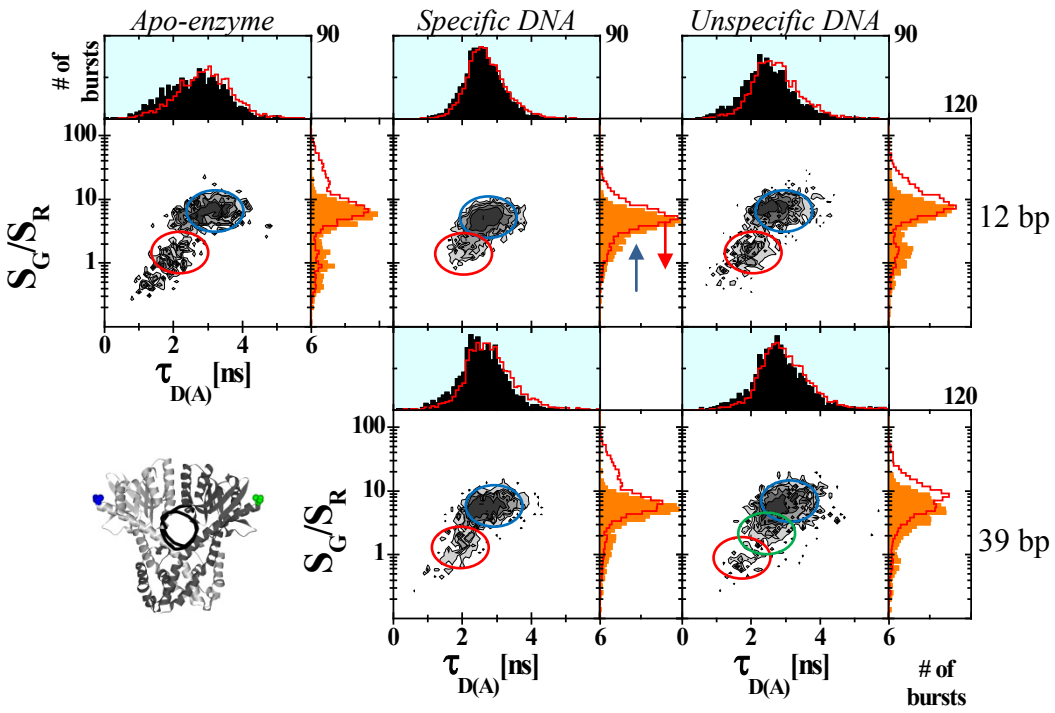

Figure 3.32 Double labeled BsoBI A153C in the presence of $CaCl_2$ with 12 bp and 39 bp long DNA. *The ratio between green and red fluorescence (S_G/S_R) was corrected for background, detection efficiencies and crosstalk. Red lines in single histograms represent full trace data; black and orange filled histograms represent bursts selected based on the number of photons in the red channel – only bursts with more than 20 photons were selected. Red circle – high FRET; green circle – middle FRET; blue circle – lowest FRET. The structure on the left indicates the labeling positions.*

Similar to the experiments using the E290C variant, the A153C variant was diluted to 80 pM concentration (the difference in concentrations between two variants was caused by different labeling efficiencies) in buffer containing $CaCl_2$, and measured in the absence or presence of specific or unspecific short or long DNA. As can be seen in Figure 3.32, left panel, BsoBI exists in two conformations in the absence of DNA, one of which is more populated (approximately 80 % according to the PDA analysis; lower FRET population). After the addition of short specific DNA (Figure 3.32, upper row, middle panel), the high FRET population is moved toward the lower value, while the low FRET population is slightly moved toward the higher value, making mostly single FRET population position in the middle between previously existing populations. The addition of short unspecific DNA (Figure 3.32, upper row, right panel), does not lead to a significant change, compared to the apo-enzyme (Figure 3.32, left panel).

The addition of long specific DNA (Figure 3.32, bottom row, left panel) caused a slight movement of the high FRET population toward the lower value, as well as low FRET

population toward the higher value, although this change is not as pronounced as in the case of short DNA, or the variant E290C. The addition of long unspecific DNA (Figure 3.32, bottom row, right panel), caused the appearance of a third FRET population, with middle FRET efficiency value, present only in the case of long unspecific substrate, similar to the results obtained with the variant E290C.

As a control experiment, the double labeled BsoBI variant E100C was used (Figure 3.33).

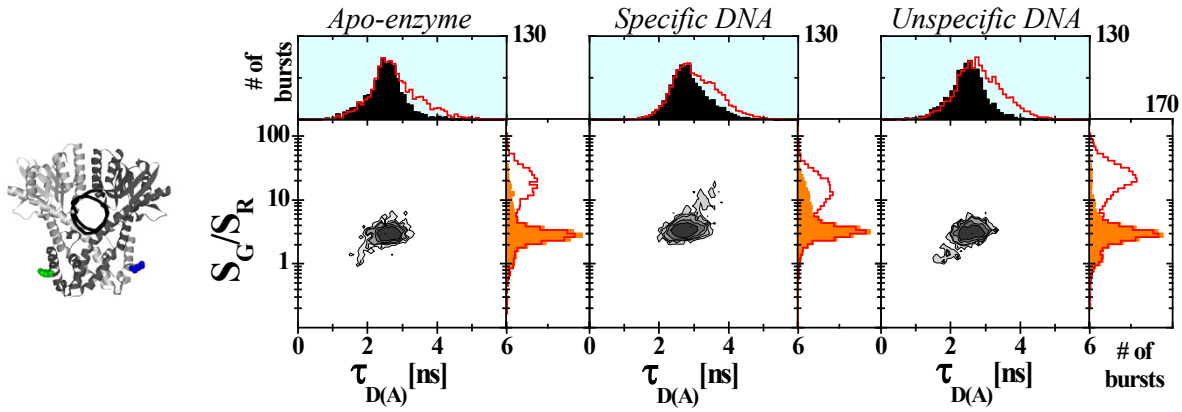

Figure 3.33 Double labeled BsoBI E100C in the presence of $CaCl_2$ with 12 bp long DNA. *The ratio between green and red fluorescence (S_G/S_R) was corrected for background, detection efficiencies and crosstalk. Red lines in single histograms represent full trace data; black and orange filled histograms represent bursts selected based on the number of photons in the red channel – only bursts with more than 20 photons were selected. The structure on the left indicates the labeling positions.*

It can be seen that the addition of either specific or unspecific short DNA does not cause significant changes in the conformation of the helical domain of BsoBI.

3.7.2. Conformational changes during DNA binding and cleavage in the presence of Mg^{2+} ions

Conformational changes during binding and cleavage were monitored using the double labeled (Alexa488/Alexa594) BsoBI variants E290C (Figure 3.34) and A153C (Figure 3.35). The protein was diluted with a buffer containing Mg^{2+} ions, which support specific DNA cleavage. After measuring the protein alone, excess of specific or unspecific, short or long DNA was added, and the measurements were repeated.

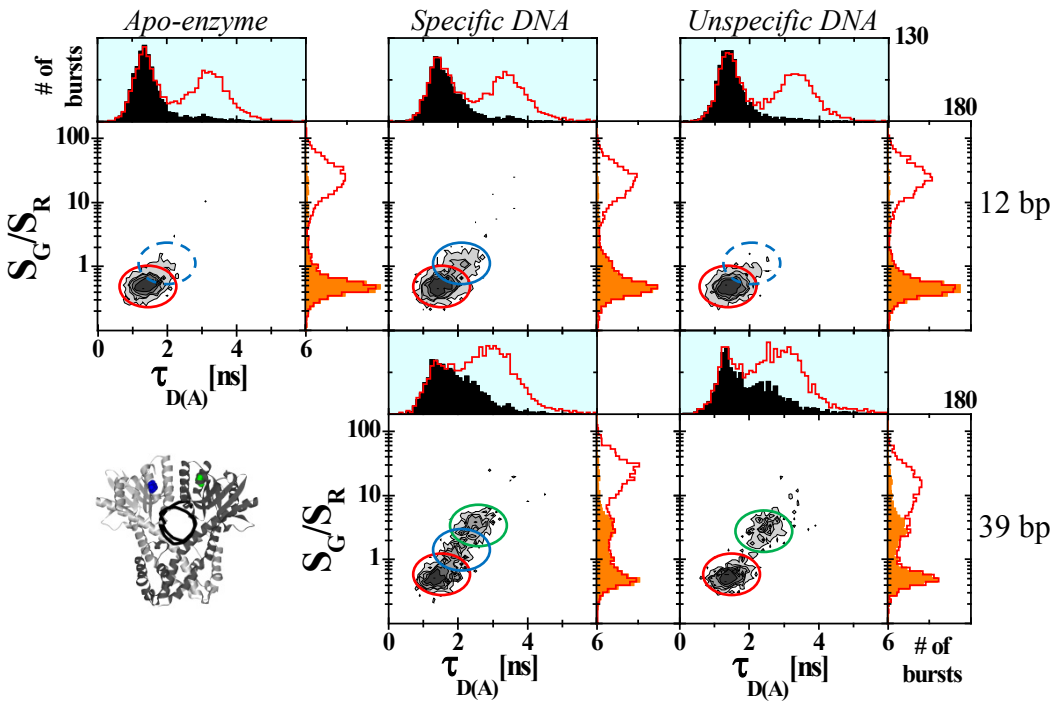

Figure 3.34 Double labeled BsoBI E290C in the presence of $MgCl_2$ with 12 bp and 39 bp long DNA. *The ratio between green and red fluorescence (S_G/S_R) was corrected for background, detection efficiencies and crosstalk. Red lines in single histograms represent full trace data; black and orange filled histograms represent bursts selected based on the number of photons in the red channel – only bursts with more than 20 photons were selected. Red circle – high FRET; blue circle – middle FRET; green circle – lowest FRET. The structure on the left indicates the labeling positions.*

In the experiment using protein alone (Figure 3.34, left panel), similar to the case when $CaCl_2$ was used, two FRET populations can be seen. However, when $MgCl_2$ is present in the buffer, the lower FRET population is slightly more populated (19 % compared to previous 7 %, according to the PDA analysis). The largest difference between the two metal ions is seen when short specific DNA is added (Figure 3.34, upper row, middle panel): in the case of Mg^{2+} the change in FRET populations is minor, and the lower FRET population is increased from 19 % to 23 %, according to the PDA analysis. Similar to the Ca^{2+} measurement, after the addition of unspecific short DNA (Figure 3.34, upper row, right panel), there is no significant change in FRET populations.

The addition of long specific DNA (Figure 3.34, bottom row, left panel) causes the appearance of three FRET populations. The high and the middle FRET populations correspond to the populations seen with protein alone and protein with short specific DNA, and the low FRET population is not present in the case of short DNA, but only with the long DNA. When unspecific long DNA is added (Figure 3.34, bottom row, right panel), the middle FRET population seen in the case of long specific DNA is disappearing.

The same experiments were repeated with double labeled BsoBI A153C variant, using $MgCl_2$ and specific or unspecific, short or long DNA (Figure 3.35).

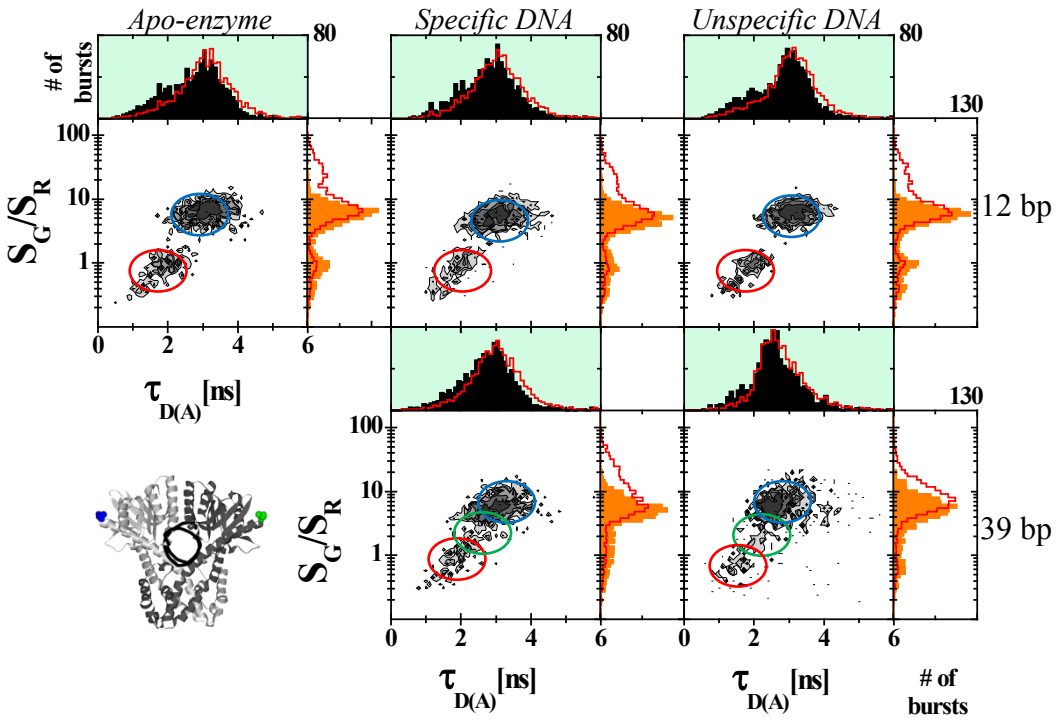

Figure 3.35 Double labeled BsoBI A153C in the presence of $MgCl_2$ with 12 bp and 39 bp long DNA. *The ratio between green and red fluorescence (S_G/S_R) was corrected for background, detection efficiencies and crosstalk. Red lines in single histograms represent full trace data; black and orange filled histograms represent bursts selected based on the number of photons in the red channel – only bursts with more than 20 photons were selected. Red circle – high FRET; green circle – middle FRET; blue circle – lowest FRET. The structure on the left indicates the labeling positions.*

BsoBI A153C apo-enzyme diluted in buffer containing $MgCl_2$ exists in at least two populations, with different FRET values, similarly to the previously described experiments in the presence of $CaCl_2$. As in the case of variant E290C, the addition of short specific DNA does not cause significant changes in FRET populations, when Mg^{2+} ions are present in the buffer. Also, the addition of short unspecific DNA does not cause a significant change.

The addition of long specific DNA causes the appearance of a third FRET population, with the value between the values seen in the apo-enzyme. This middle value FRET population is also present in the case of long unspecific DNA, although it is less populated.

The control experiment using BsoBI E100C variant did not show any significant difference in FRET populations when different substrates were added to the protein (Figure 3.36).

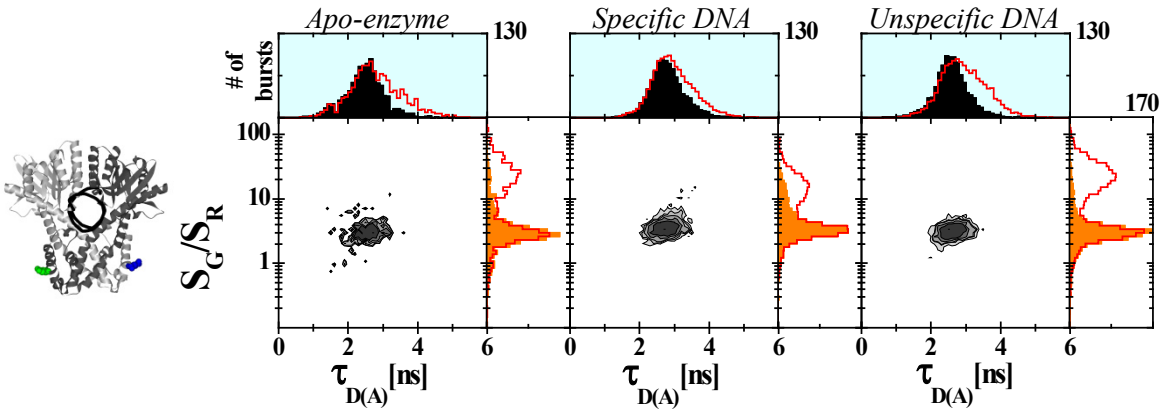

Figure 3.36 Double labeled BsoBI E100C in $MgCl_2$ with 12 bp long DNA. *The ratio between green and red fluorescence (S_G/S_R) was corrected for background, detection efficiencies and crosstalk. Red lines in single histograms represent full trace data; black and orange filled histograms represent bursts selected based on the number of photons in the red channel – only bursts with more than 20 photons were selected. The structure on the left indicates the labeling positions.*

An overview of conformational changes in BsoBI A153C and E290C during DNA binding and cleavage, studied on the single-molecule level is presented in Figure 3.37.

	Apo-enzyme		Specific DNA		Unspecific DNA	
	$CaCl_2$	$MgCl_2$	$CaCl_2$	$MgCl_2$	$CaCl_2$	$MgCl_2$
A153C	Two populations; high FRET population competent for binding		High FRET population is shifted towards lower FRET value	No significant change with short substrate; additional populations with long substrate	No significant change with short substrate	Additional populations with long substrate
E290C	Two conformations with the same FRET efficiency		High FRET population is almost completely shifted towards lower FRET value	No significant change with short substrate; additional populations with long substrate	No significant change with short substrate	Additional populations with long substrate

Figure 3.37 Overview of the single-molecule experiments.

4. Discussion

Restriction endonucleases are important for every day laboratory work, as they are essential for all genetic engineering techniques. Along with their practical use, they are also model systems for studying protein/DNA interactions, and one of the best studied families of proteins/enzymes. The ability to control their activity, change the specificities or selectively activate/deactivate restriction enzymes could be one of the approaches to gene targeting and gene therapy. In order to do that, we have to understand all aspects of their functions, including the means of finding their recognition site or possible conformational changes in enzyme and/or DNA during the substrate binding and cleavage. The main aim of this work was to investigate conformational changes of the thermostable Type IIP restriction enzyme BsoBI, during substrate binding and cleavage. Different fluorescence techniques were chosen, because of their high sensitivity and possibility to observe distance changes in the range that is relevant for most of the biological functions. These techniques also allowed the monitoring of BsoBI conformational dynamics during the catalytic process.

4.1. Creating catalytically inactive single-cysteine BsoBI variants

The influence of DNA binding without cleavage in the presence of Mg^{2+} ions can be studied using different approaches, e.g. using an unspecific (non-cleavable) substrate or creating a cleavage inactive but binding active variant of the enzyme. In order to create cleavage inactive variants, certain residues in the catalytic center of the enzyme have to be mutated. Based on available literature data [36] two positions were chosen: aspartic acid at position 212 and histidine at position 253. The role of histidine as a putative catalytic residue [38] was not seen in any other restriction enzyme so far. Newly created BsoBI variants D212N, D212A and H253Q were checked for binding and cleavage activity, and it was shown that exchange of histidine at the position 253 to glutamine leads to loss in both binding (Figure 3.2) and cleavage activity (Figure 3.3). On the contrary, the exchange of aspartic acid at position 212 to asparagine resulted in preservation of the binding activity (Figure 3.2), but caused a loss of the cleavage activity (Figure 3.3).

Thus, the newly created BsoBI variant D212N could be used to examine the binding of specific DNA in the presence of Mg^{2+} ions without cleavage occurring. However, the mutation was introduced in the active site, the place most likely involved in metal ion binding. As was shown previously, and will be discussed in the next chapters, there is a strong influence of different divalent metal ions on the structure of BsoBI, as well as on the kinetics of its catalytic cycle. For this reason, the use of a variant with modified metal ion binding site

would be inappropriate, since it would not give a clear picture of the catalytic properties of the wild type enzyme.

4.2. Michaelis-Menten kinetics

Michaelis-Menten kinetics describe the rate of enzyme catalyzed reactions, when the product does not bind to the enzyme, and the concentration of the substrate is higher than the concentration of the enzyme. In order to accurately determine kinetic parameters, the substrate concentration is increased until a constant rate of product formation is achieved (maximum velocity, V_{max}). Different factors can affect the rate of enzymatic reactions, such as pH or temperature. In this study, the effect of different temperatures on the kinetic parameters of BsoBI was analyzed. BsoBI is a thermostable restriction enzyme, with an optimal catalytic activity at 65 °C. However, all ensemble and single-molecule experiments were carried out at room temperature (25 °C). The kinetic parameters were calculated for three different temperatures, 25 °C, 37 °C and 65 °C, in order to determine how the kinetic constants were affected by the change in temperature.

As can be seen in Figure 3.4 and Table 7, the change in temperatures did not significantly influence the cleavage rate (k_{cat}) of BsoBI. In contrast, the value of the Michaelis constant (K_M) decreased with the increase of temperature. The Michaelis constant is a measure of the affinity of an enzyme to the substrate; the higher K_M is, the lower the affinity of the enzyme for its substrate. This result suggests that the temperature affects the conformation of BsoBI, by slowing down the conformational changes prior to substrate binding at lower temperatures. The observed behavior can explain the existence of two distinct FRET populations seen in single-molecule experiments (Chapter 4.6.). At higher temperatures conformational changes of BsoBI would be faster, and different FRET subpopulations might not be resolved, because of their short lifetime. Since the single-molecule experiments were carried out at room temperature, the speed of conformational changes was slow enough to allow the observation of distinct subpopulations.

4.3. Site-specific fluorescent labeling of selected single-cysteine BsoBI variants

In order to perform the desired experiments, a set of single-cysteine variants of BsoBI had to be created, and labeled with different fluorophores using maleimide chemistry. The distance between these positions and the fluorophores chosen had to be suitable for ensemble as well as for single-molecule FRET experiments. The positions chosen had to be surface exposed and mutations at these positions or the introduction of fluorophores should not influence the

binding or cleavage activity of the enzyme. It was shown that exchange of amino acids at positions chosen to cysteines (Figure 3.1) or fluorescent labeling at these positions (Figure 3.8) did not influence the cleavage activity of BsoBI.

Based on previous cross-linking data (see below), it was suggested that BsoBI undergoes conformational changes in its catalytic domain. Therefore, two positions were chosen in this part of the enzyme, with suitable distances, to monitor the conformational changes upon substrate binding and cleavage: A153 and E290 (Figure 3.5). These positions are located in different protein axes, and by combining the results from both positions it was possible to resolve the directions of conformational changes. In addition to these positions, two more positions were chosen for exchange into cysteines, namely S298 and R318. In the case of the single-cysteine variant S298C no significant change in FRET signal was observed upon DNA binding. The FRET change of the double labeled R318C variant was the same as in the case of the A153C variant. Therefore, the variants A153C and E290C were chosen as the best representatives to study the conformational change of BsoBI. As a control, one position on the helical domain of the enzyme was chosen (E100, Figure 3.5), because it was assumed that this part of the enzyme does not change its conformation upon substrate binding or cleavage.

The choice of fluorophores depended on the distance between the labeling positions, as well as their suitability for different experiments. Initially, Alexa488 C_5 maleimide and Alexa594 C_5 maleimide were chosen as donor and acceptor fluorophores, respectively. After initial single-molecule experiments it was suggested that, based on the set-up available, Alexa647 C_2 maleimide is used as acceptor, since the cross-talk between donor and acceptor is smaller, and the quality of the results would be better.

Since BsoBI is a homodimer, the introduction of cysteine in one subunit leads to the introduction of the cysteine to the same position in the other subunit. Random labeling with the mixture of donor and acceptor fluorophore would give the ratio of 1:2:1 of donor labeled : donor/acceptor labeled : acceptor labeled molecules. Single-molecule experiments required better labeling quality, preferably only molecules with donor fluorophore on one subunit and acceptor fluorophore on the other subunit, although single-molecule measurements allow separation of different species, and thus it could be possible to separate differently labeled enzymes. If the sample has too much donor only labeled molecules, the measurements should be performed for longer times, in order to achieve satisfactory statistics, which is not always possible if the enzyme is not stable. Also, the excess of unreacted fluorophore had to be removed after the labeling reaction. The labeling protocol was modified from the one available in the literature [72]. The enzyme was first labeled with the donor fluorophore, and

differently labeled molecules (single, double or unlabeled) were separated using anion exchange chromatography. An important step in this process was choosing the optimal pH value, at which the protein binds to a positively charged anion exchanger. This pH value had to be higher than the isoelectric point (pI) of the protein, which was estimated to be around 7.5. Since the fluorophores are negatively charged, introduction of one or two fluorophores introduces one or two additional negative charges to the protein, respectively. During elution from the anion exchange column, molecules with the lowest negative charge are eluted first (unlabeled protein), followed by protein labeled with one and two fluorophores. The elution was done by increasing the ionic strength (salt concentration) of the buffer, allowing the salt ions to compete for charges on the column with bound components, and thus eluting them from the column. Although no complete separation was achieved (Figure 3.9c), the removal of most of the donor only double labeled molecules was successful. Also, certain amounts of acceptor only double labeled molecules was produced, but this population was not "visible" in single-molecule experiments, since the excitation was done at the wavelength of the donor fluorophore.

This labeling protocol produced enough material for single-molecule experiments, but not for stopped-flow experiments. Since the pure double labeled protein was not needed for these experiments, BsoBI was randomly labeled with mixture of donor and acceptor fluorophore, and the anion exchange chromatography was excluded from the protocol, since it is the step during which most of the material is lost.

4.4. DNA binding induces conformational change in the catalytic domain of BsoBI

Based on the available co-crystal structure it was clear that the helical domain of BsoBI is more compact than the catalytic domain, and that the catalytic domain probably undergoes large conformational change in order to allow DNA entry. This was confirmed in previous cross-linking experiments (Diploma thesis Katja Welsch, Justus-Liebig-University Gießen, 2006). However, the directions of conformational changes, as well as their kinetics, were not known. After producing the single-cysteine variant A153C, it was expected that the distance between two fluorophores decreases after DNA binding, if the conformational change was simple "opening" (in a scissor-like movement) of the catalytic domain. However, steady-state FRET experiments showed that upon DNA binding the FRET efficiency decreases in comparison to the apoenzyme (Figure 3.10a). This result showed that two fluorophores at the

position A153 move apart upon specific DNA binding, in the presence of Ca^{2+} ions, which support only specific substrate binding, but not cleavage.

The binding of unlabeled specific DNA to the double labeled BsoBI variant E100C did not cause a significant change in the FRET signal (Figure 3.11a). This result showed that there is no major movement of the helical domain of BsoBI upon substrate binding in the presence of Ca^{2+} ions.

Steady-state FRET experiments revealed an unusual influence of different divalent metal ions on the conformation of the catalytic domain of BsoBI. It was shown that the presence of Ca^{2+} ions induces an increase of the FRET signal of the double labeled BsoBI apoenzyme, in comparison to the presence of Mg^{2+} or EDTA (Figure 3.13a). This suggested that the fluorophores at the position A153 move closer together when Ca^{2+} is present in the solution, while in the presence of Mg^{2+} or EDTA they move apart. In the case of the position E100, no significant change in FRET values was observed in the presence of either metal ion (Figure 3.13b). The influence of Ca^{2+} ions on the conformation of catalytic domain of BsoBI was also studied by titrating different $CaCl_2$ concentrations to the double labeled BsoBI A153C apoenzyme. This allowed determining the binding constant of Ca^{2+} to BsoBI, which was estimated to be ~ 1 mM (Figure 3.14).

4.5. Kinetic studies of BsoBI substrate binding and cleavage – influence of Ca^{2+} and Mg^{2+} ions

The observed changes in the catalytic domain of BsoBI after DNA binding were monitored in pre-steady state experiments, using the double labeled BsoBI variant A153C and unlabeled DNA, mixed in the presence of Ca^{2+} ions. This allowed monitoring the kinetics of the conformational changes upon specific DNA binding. After mixing double labeled BsoBI with unlabeled DNA, and monitoring the change in the donor signal, it was seen that the donor signal increases over time, as expected based on previous steady-state experiments (Figure 3.15). Different concentrations of DNA were used, in order to globally analyze the kinetic traces and resolve different steps during DNA binding. Specific DNA binding in the presence of Ca^{2+} can be described as a two step reaction: a first order conformational change prior to DNA binding (with an equilibrium constant of 1.5), followed by a second order association of DNA (with a rate constant of 0.5 $\mu M^{-1}s^{-1}$). These experiments also revealed the presence of two conformations of BsoBI in the solution, only one of which is believed to be binding competent (referred to as E2).

The kinetics of DNA binding was also monitored using single (donor) labeled BsoBI and single (acceptor) labeled specific DNA, in the presence of Ca^{2+} ions. As in the previous experiment, the enzyme concentration was kept constant while the DNA concentration varied. The changes in donor signal were monitored, since the concentration of donor labeled species was constant during the series of experiments. The binding of acceptor labeled DNA to donor labeled enzyme caused appearance of FRET and subsequent decrease of donor signal over time (Figure 3.16). Again, the experimental curves obtained were fitted globally in order to resolve single steps during specific DNA binding. The analysis showed the presence of two conformations of BsoBI (with an equilibrium constant of 0.6), one of which is competent to bind DNA (E2), and DNA binding is described by a second order association with a rate constant of 0.2 $\mu M^{-1}s^{-1}$. The rate constants for DNA binding obtained in these experiments slightly differ from the rate constants obtained in the experiments with double labeled BsoBI, which could be explained by fluorophores now being on both enzyme and DNA.

The full catalytic cycle of DNA binding, cleavage and product release was monitored using single (donor) labeled BsoBI and single (acceptor) labeled specific DNA. They were mixed in the presence of Mg^{2+}, i.e. conditions that allow specific DNA binding and cleavage. The protein concentration was constant, while DNA concentration was varied during the series of experiments, so the changes in donor signal were monitored. After rapid mixing of donor labeled enzyme and acceptor labeled DNA, there is a decrease in donor signal over time, due to DNA binding and appearance of FRET. After DNA cleavage, acceptor labeled product is released, which results in the disappearance of FRET and the concomitant increase in donor signal (Figure 3.17). The experimental curves obtained were fitted globally in order to resolve single steps of DNA binding, cleavage and product release. The analysis showed the presence of two conformations of BsoBI before DNA binding, similar to the previously described experiments. This time, the changes are faster than in the presence of Ca^{2+}, which can be explained by different influences of these two metal ions already observed in steady-state experiments. DNA binding is described as a second order association, with a rate constant of 4.8 $\mu M^{-1}s^{-1}$, approximately 20 times faster than in the presence of Ca^{2+}. These results show that binding of DNA in the presence of Ca^{2+} is slower than in the presence of Mg^{2+}, presumably by Mg^{2+} favoring a binding competent conformation of BsoBI. The observed rate constant of cleavage of 0.6 s^{-1} is in good agreement with rates usually observed for other restriction enzymes (REBASE Kinetics Data, http://rebase.neb.com/cgi-bin/kinlist). Cleavage of DNA is slower than the product release (estimated 2.2 s^{-1}), suggesting that cleavage, and

not the product release, is the rate limiting step in the BsoBI catalytic cycle under these conditions.

The exchange of different divalent metal ions causes a conformational change in the apo-enzyme, which is reflected in the change of the FRET signal of the double labeled BsoBI A153C variant. The addition of $MgCl_2$ to BsoBI diluted in buffer containing $CaCl_2$ causes a decrease in the FRET signal (Figure 3.18), suggesting conformational changes that move two fluorophores at the 153 positions further apart. In contrast, the addition of $CaCl_2$ to BsoBI diluted in buffer containing $MgCl_2$ causes an increase in FRET signal (Figure 3.21), suggesting a conformational change of the double labeled apo-enzyme that moves the two fluorophores at the 153 positions closer together. While the lowest concentration of $MgCl_2$ (orange curve in Figure 3.18) does not cause significant changes in the acceptor signal, the lowest concentration of $CaCl_2$ (orange curve in Figure 3.21) causes significant changes in the FRET signal of the apo-enzyme previously diluted in buffer containing the same concentration of $MgCl_2$. This result suggests that the affinity of Ca^{2+} ions to the BsoBI apo-enzyme is greater than the one of Mg^{2+} ions.

The influence of Mg^{2+} and Ca^{2+} ions on DNA cleavage by BsoBI was further investigated using different mixtures of these two ions. When donor labeled BsoBI and acceptor labeled DNA were pre-bound in the presence of 0.5 mM EDTA and mixed with different ratios of $CaCl_2$ and $MgCl_2$, two effects were observed (Figure 3.26). After addition of equal concentrations of both metal ions, residual substrate binding followed by very slow cleavage was observed. This result showed that in the presence of the same concentrations of metal ions, Ca^{2+} ions bind firmly to the enzyme, preventing Mg^{2+} ion binding, and consequently interfering with (or at least slowing down) DNA cleavage. In contrast, when excess of Mg^{2+} over Ca^{2+} ions is present, fast cleavage of DNA is observed, showing that higher concentrations of $MgCl_2$ (in comparison to $CaCl_2$) are needed for Mg^{2+} to bind to the enzyme and for cleavage of the DNA to occur. So far, without more experiments that would include different ratios of $CaCl_2$ and $MgCl_2$, it is not possible to resolve different steps in the metal ion exchange reaction. A possible scheme of this reaction is presented below, showing the binding of both metal ions to the enzyme/substrate complex, although from the experiments described it cannot be concluded if dissociation of substrate is necessary before binding of different metal ions.

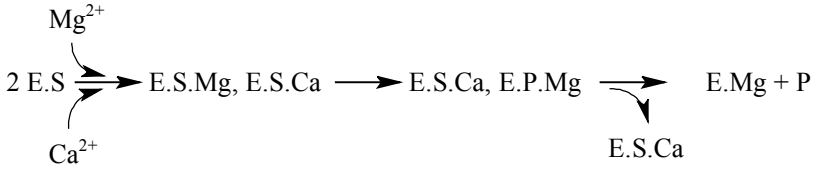

The influence of different $MgCl_2$ concentrations on the cleavage of DNA pre-bound to BsoBI in the presence of EDTA is shown in Figure 3.27. The lowest concentration of $MgCl_2$ (5.5 mM) causes a lag of the monitored signal, during which Mg^{2+} ions bind to the enzyme/DNA complex. After this, the cleavage of DNA and subsequent product release can occur, which is reflected in the increase of the donor signal (black curve in Figure 3.27). The addition of higher $MgCl_2$ concentration causes very fast DNA cleavage, which is unresolved in the dead-time of the machine. Again, without additional $MgCl_2$ concentrations it is not possible to resolve different reaction steps, but one possible reaction scheme is presented below. It is also unclear if the dissociation of substrate is necessary for the Mg^{2+} ions to bind and allow DNA cleavage to occur.

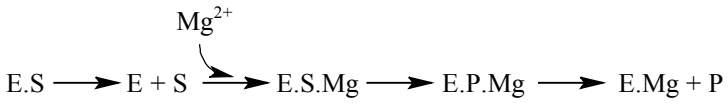

Finally, the influence of different $MgCl_2$ concentrations on DNA cleavage was monitored after pre-mixing BsoBI and specific DNA in the presence of 5.5 mM $CaCl_2$ (Figure 3.28). The addition of equal concentrations of $MgCl_2$ (black curve in Figure 3.28) was not enough to replace all Ca^{2+} ions, and caused only very slow DNA cleavage, confirming previous observations that Ca^{2+} ions have a greater affinity for BsoBI than Mg^{2+} ions. Only when excess of $MgCl_2$ was added, it was possible to replace Ca^{2+} ions from the enzyme/DNA complex and allow DNA cleavage (red curve in Figure 3.28). Like in previous experiments, the lack of data with different $MgCl_2$ concentrations limits the possibility to resolve different reaction steps and to predict different rate constants. It remains unclear if the dissociation of substrate is a necessary step in this reaction, and a possible scheme is presented below.

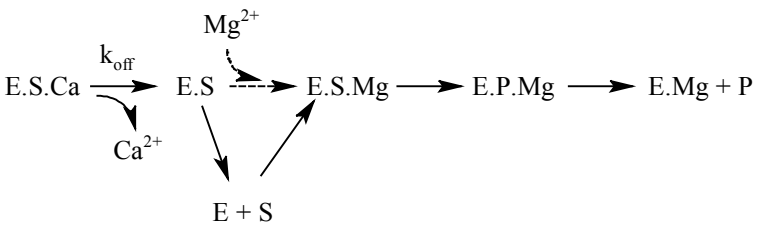

The experiments described clearly show different effects of Mg^{2+} and Ca^{2+} ions on the catalytic activity of BsoBI. The presence of Mg^{2+} speeds up the equilibrium between two

BsoBI conformations, as well as faster DNA binding. The different metal ions also showed an unusual influence on the conformation of the apo-enzyme, which could be followed as the change of FRET efficiency of double labeled BsoBI. These experiments also revealed unusual differences in affinities of Ca^{2+} and Mg^{2+} ions, showing that the affinity of Ca^{2+} ions to BsoBI is greater than the one of Mg^{2+}. The confirmation of these findings was shown in the experiments analyzing the influence of mixtures of two metal ions on the DNA cleavage, which needs to be looked at in greater detail. Moreover, the use of mixtures of two metal ions causes the presence of enzymes containing both metal ions bound to the metal ion binding sites at the same time, which additionally complicates the analysis and interpretation of the results obtained.

4.6. Conformational changes in BsoBI during DNA binding and cleavage studied on the single-molecule level

Previously observed influences of DNA binding or metal ions on the conformation of BsoBI were the result of different ensemble experiments. In these experiments subpopulations present in the sample cannot be seen, and all effects are the result of averaging of different signals. In order to resolve the subpopulations hidden in the average signal, several series of single-molecule experiments were done using single-molecule multiparameter fluorescence detection (smMFD). In these experiments, double labeled BsoBI molecules were freely diffusing through the solution, and 8 different fluorescence parameters were monitored: excitation spectrum, fluorescence spectrum, fundamental anisotropy, fluorescence lifetime, FRET, fluorescence quantum yield, fluorescence intensity and time. Combination of different parameters allowed for separating subpopulations of molecules present in the sample.

The single-molecule measurements of the double labeled BsoBI A153C variant, in the presence of $CaCl_2$, revealed the existence of at least two populations of apo-enzyme, with different FRET values (Figure 3.32). These two populations are most likely the same as those observed in pre-steady state experiments, described as DNA binding competent and DNA binding incompetent conformations. The addition of a short specific DNA causes a shift in FRET populations, so that the population with lower FRET is more populated (Figure 3.32). This suggests that the two fluorophores at the positions 153 move apart after DNA binding, as it was shown in the steady-state ensemble measurements. The addition of short unspecific DNA did not cause any significant change in FRET populations, presumably because of the low affinity of BsoBI for the short unspecific substrate. These results suggest that the lower FRET population represents a binding incompetent conformation of BsoBI, as well as DNA

occupied conformation, while the population with higher FRET represents a binding competent conformation. Similarly to the experiments using short substrate, the addition of long specific DNA causes the movement of FRET species towards the lower value, although not as pronounced as with short DNA (Figure 3.32). However, the addition of long unspecific DNA causes the appearance of additional FRET populations. These subpopulations represent different binding modes of BsoBI to the long unspecific substrate, where it can bind to several different positions on the DNA and take up slightly different conformations.

In contrast to the variant A153C, the apo-enzyme E290C apparently exists in mainly one FRET population in the presence of $CaCl_2$ (Figure 3.30). However, this result does not mean that the BsoBI variant E290C exists in only one conformation, but that two conformations seen with the A153C variant have the same FRET value when 290 position is chosen for labeling. The addition of short specific DNA caused a shift in FRET populations towards the lower FRET value, suggesting conformational changes of the catalytic domain of BsoBI that moves two fluorophores at the position 290 further apart. The addition of a short unspecific DNA, similar to the variant A153C, did not cause the significant change in FRET populations. The binding of a long specific substrate (Figure 3.31) caused the same conformational change as the short specific substrate, i.e. a shift towards the lower FRET value. However, the addition of long unspecific substrate caused the appearance of an additional FRET population, with the lowest FRET value. These populations represent different binding modes of BsoBI to the long unspecific substrate, presumably the conformations of the enzyme while searching for its recognition site.

In order to investigate the conformational changes during substrate binding and cleavage, single-molecule experiments were carried out in the presence of $MgCl_2$, the metal ion which allows specific DNA cleavage to occur. Under these conditions, the observed conformations of BsoBI represent different states of the enzyme, i.e. substrate or product bound states, or free enzyme. That substrate bound states are seen at all is due to the fact that substrate is in large excess over enzyme, which is present at very low concentration.

The FRET populations of the BsoBI E290C apo-enzyme did not change significantly when $MgCl_2$ is used instead of $CaCl_2$ (Figure 3.34). In contrast, the most striking difference is seen when the substrate is added to the enzyme in the presence of Mg^{2+} ions. The addition of short specific DNA caused a small shift in FRET populations, towards the lower FRET value, in contrast to the $CaCl_2$ conditions, when the shift is almost complete. As previously mentioned, in the presence of $MgCl_2$, different enzyme-substrate complexes can be observed. However, the affinity of BsoBI for the product derived from the short substrate cleavage is very low,

and thus this conformation is not very populated, and the predominant conformation seen in this experiment is that of the free enzyme. As in the case of $CaCl_2$ conditions, the addition of short unspecific DNA does not cause a significant change in FRET populations compared to the apo-enzyme. The addition of a long specific DNA causes the appearance of a new population, with the lowest FRET value observed in this experiment (Figure 3.34). This population may represent one of the binding modes of BsoBI to the long substrate, not present in the case of a short substrate, where BsoBI has only one binding position. In addition to this population, the populations of free enzyme (high FRET value) and substrate/product bound enzyme are also present (middle FRET value). In the presence of long unspecific DNA, as expected, the population of product bound enzyme (middle FRET value) is not present, and only populations of free enzyme and of the unspecific complex are present.

The BsoBI A153C apo-enzyme measured in the presence of Mg^{2+} ions exists in at least two populations (Figure 3.35), with the lower FRET population slightly more populated compared to the $CaCl_2$ conditions. As in the case of the E290C variant, the addition of a short specific DNA does not cause a significant shift in FRET populations (as was also shown in the steady-state ensemble experiments [Figure 3.10b]), presumably because of the low affinity of BsoBI to the product of the cleavage of a short substrate. Also, the addition of a short unspecific substrate did not cause significant changes in FRET values compared to the apo-enzyme. The addition of a long specific substrate, in the presence of Mg^{2+} ions, causes the appearance of a middle FRET value population, presumably representing a product bound state of the enzyme. This population is not as pronounced when the unspecific substrate is present, although several FRET populations are visible, representing different binding modes of BsoBI to the long unspecific substrate.

As a control, single-molecule experiments were performed using the double labeled BsoBI E100C variant, which has single cysteines introduced in the helical domain of the enzyme. Based on previous experiments and available literature data, it was expected that this part of the enzyme does not change its conformation upon substrate binding. The single-molecule experiments confirmed this assumption (Figure 3.33, Figure 3.36), since there is no significant shift in the FRET population after adding specific or unspecific substrate.

The single-molecule experiments confirmed the influence of substrate binding to the conformation of the catalytic domain of BsoBI. Also, they revealed the existence of at least two subpopulations of the apo-enzyme, which could be quantitatively analyzed. It was shown that the binding of long unspecific substrate induces the appearance of more subpopulations,

representing different binding modes to the long substrate, presumably during the search for the recognition site.

Based on the single-molecule experiments described, a model for conformational changes ocurring in BsoBI upon divalent metal and DNA binding can be proposed (Figure 4.1), which assumes a complex "twisting" motion of two subunits, which leads to a closer distance between residues 153 and 290 in the apo-enzyme compared to the substrate bound complex. The results obtained suggest that the "simple" scissor-like movement of BsoBI subunits is not likely, since the distances between residues 153 and 290 would be larger in the apo-enzyme.

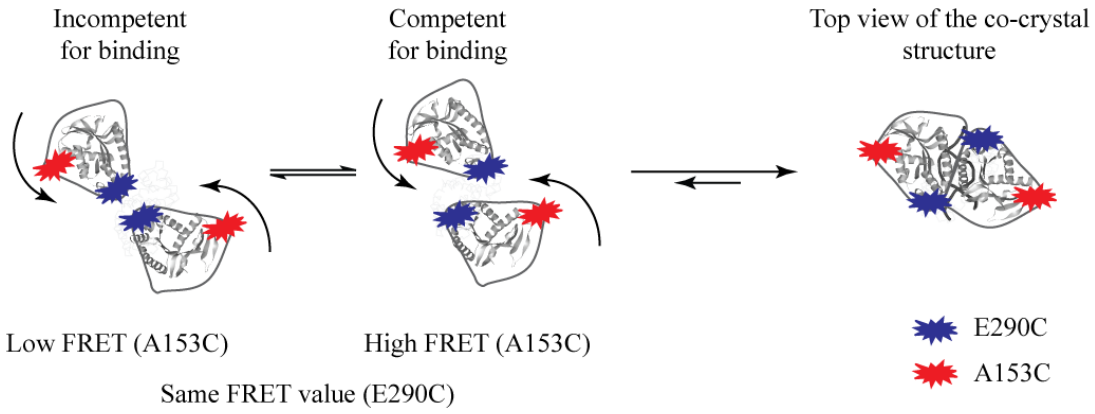

Figure 4.1 A scheme illustrating BsoBI conformational changes. *The apo-enzyme exists in at least two conformations, binding competent and binding incompetent. The distances between residues 153 of the two subunits and 290 of the two subunits are shorter in the apo-enzyme than in the DNA-bound complex.*

The combination of single-molecule experiments and ensemble steady-state and pre-steady state experiments, allowed the determination of individual steps in the catalytic cycle of BsoBI, and the analysis of the effects of different metal ions on this process. However, more detailed experiments are needed to fully describe the influence of Ca^{2+} and Mg^{2+} metal ions. Also, the use of more single-cysteine variants will allow a more accurate modeling of the conformational changes in the catalytic domain of BsoBI.

5. Summary

Enzyme flexibility is known to be crucial for various enzymatic functions: allosteric regulation, catalysis or ligand binding induced conformational changes. Conformational rearrangements have wide range of timescales, and are considered intrinsic features of all proteins. X-ray crystallography has provided important insight into different enzymatic conformations, but it can only give a snapshot of a complex protein life cycle. Fluorescence spectroscopy methods are becoming the primary methods in investigating protein structural dynamics, especially when combined with different single-molecule techniques.

Restriction endonucleases are important tools for every day laboratory work, being essential for all genetic engineering techniques. They are also model systems for studying protein/DNA interactions and one of the best studied families of proteins/enzymes. The main aim of this study was to investigate conformational changes of restriction enzyme BsoBI, during substrate binding and cleavage. Fluorescence resonance energy transfer (FRET) was used to determine the changes in distances between donor and acceptor fluorophores during substrate binding and cleavage, in steady-state or pre-steady state ensemble, as well as in single-molecule experiments. These fluorophores were attached to single cysteine residues introduced to BsoBI subunits at specific positions.

BsoBI is a thermostable restriction enzyme, with optimal catalytic activity at 65 °C. Crystallographic studies had shown that BsoBI exists as a homodimer, which completely encircles specific DNA. The substrate is enclosed in a 20 Å long tunnel formed by the protein, which excludes access of water molecules from the solvent. Up to date, only the co-crystal structure of BsoBI with specific DNA is known, and there are no data indicating the conformational changes required for substrate binding and cleavage. The crystallographic data had shown that the interface between the catalytic domains of BsoBI is much weaker than the one between the helical domains, and it was proposed that the major conformational changes happen in the catalytic domain of the enzyme.

Steady-state experiments using double labeled BsoBI confirmed that the binding of DNA causes a conformational change in the catalytic domain of the enzyme. The addition of unlabeled specific DNA to the double labeled BsoBI variant A153C (positioned at the catalytic domain) caused a decrease in FRET signal. This result unexpectedly suggested that the fluorophores at the 153 position move apart upon specific substrate binding. The addition of DNA to the double labeled BsoBI variant E100C (positioned at the helical domain) did not cause change in the FRET signal, suggesting that this part of the enzyme does not change its conformation upon substrate binding. Suggested conformational change in the catalytic

domain of BsoBI does not involve expected scissor-like motion of two subunits, but more complex “twisting” motion. These experiments also showed the influence of Ca^{2+} and Mg^{2+} ions on the conformation of the catalytic domain of BsoBI. The presence of Ca^{2+} induced a conformational change of the catalytic domain of the enzyme that moved two fluorophores at the positions 153 closer together, while the presence or the absence of Mg^{2+} did not cause any effect on the BsoBI conformation.

The conformational changes during substrate binding and cleavage, as well as the influence of different metal ions were analysed in pre-steady state experiments, using double labeled BsoBI and unlabeled DNA, or single labeled BsoBI and DNA. These experiments also confirmed the influence of DNA binding on the conformation of the catalytic domain of BsoBI. In addition, the kinetic model of DNA binding and cleavage revealed the existence of at least two conformations of the free enzyme before DNA binding. These two conformations were proposed to be substrate binding competent and substrate binding incompetent. The kinetic models also suggested that BsoBI binds Ca^{2+} and Mg^{2+} with different affinity, namely that Ca^{2+} binding is stronger and faster than Mg^{2+} binding.

The single-molecule experiments confirmed the existence of at least two different conformations of the apo-enzyme, and allowed quantifying the relative proportions of these subpopulations. The analysis of single-molecule experiments using different time windows demonstrated slow dynamics of different conformations of apo-enzyme, which was expected based on the observed influence of temperature on the K_M value of BsoBI. Also, it was shown that the enzyme has more than one conformation when bound to the unspecific long substrate, suggesting different binding modes to the unspecific DNA.

By combining different fluorescence techniques, as well as different single cysteine variants, it was possible to explain and model single the conformational dynamics of substrate binding and cleavage by BsoBI. These experiments showed unexpected mechanism of the conformational changes, as well as the influence of different metal ions on the conformation of BsoBI.

6. Zusammenfassung

Die Flexibilität von Enzymen ist essentiell für verschiedene enzymatische Aufgaben, z.B. die allosterische Regulation, die Liganden- und Substratbindung sowie die eigentliche Katalyse. Diese Konformationsänderungen können dabei unterschiedliche Zeitskalen aufweisen, und werden als eine intrinsische Eigenschaft aller Proteine angesehen. Die Röntgenstrukturanalyse hat wichtige Erkenntnisse über diese unterschiedlichen Konformationen verschiedenster Enzyme geliefert, sie ermöglicht jedoch immer nur eine Momentaufnahme im komplexen Katalyseprozess. Es werden daher heutzutage vermehrt fluoreszenzspektroskopische Methoden, insbesondere moderne Einzelmolekültechniken eingesetzt, um die strukturelle Dynamik von Proteinen zu untersuchen.

Restriktionsendonukleasen sind wichtige Werkzeuge im molekularbiologischen Labor und essentiell für Anwendungen in der Gentechnik. Sie dienen jedoch auch als Modelsystem um Protein / DNA- Wechselwirkungen zu untersuchen und gehören deshalb zu den am besten untersuchten Enzymfamilien. Das Ziel dieser Arbeit war es, die Konformationsänderungen der Restriktionsendonuklease BsoBI beim Binden und Spalten der DNA zu untersuchen. Hierzu wurden ortsspezifisch einzelne Cysteinreste in beide Untereinheiten des Proteins eingebracht und diese mit spezifischen Fluoreszenzfarbstoffen modifiziert. Untersuchungen des Fluoreszenz-Resonanzenergietransfers (FRET) zwischen Donor- und Akzeptorfluorophor ermöglichten, die Abstandsänderungen der Proteinuntereinheiten beim Binden und Spalten der DNA zu detektieren. Die kinetischen *steady-state* und *pre-steady-state* Experimente wurden dabei im Ensemble durchgeführt und durch fluoreszenzspektroskopische Einzelmolekülmessungen ergänzt.

BsoBI ist ein thermostabiles Restriktionsenzym mit einem Temperaturoptimum für die katalytische Aktivität von 65 °C. Die Röntgenstrukturanalyse eines BsoBI x DNA-Komplexes hat gezeigt, dass das Protein als Homodimer die spezifische DNA vollständig umschließt. Das Substrat liegt dabei in einem 20 Å langen Tunnel, der durch das Protein gebildet wird und die Aufnahme von Wasser aus dem Lösungsmittel verhindert. Bis heute ist nur die Kokristallstruktur des BsoBI x DNA-Komplexes bestimmt worden, aus der jedoch keine Hinweise auf die notwendigen Konformationsänderungen des Enzyms beim Binden und Spalten der DNA gezogen werden können. Die kristallographischen Daten zeigen nur, dass das Interface zwischen den beiden katalytischen Domänen, im Vergleich zu den beiden helikalen Domänen, wesentlich schwächer ausgebildet ist. Aufgrund dessen wurde vermutet, dass hauptsächlich Konformationsänderungen der beiden katalytischen Domänen die Substratbindung ermöglichen.

Steady-state FRET-Experimente mit doppelt markierten BsoBI bestätigten, dass die Bindung an die spezifische DNA eine Konformationsänderung zwischen den beiden katalytischen Domänen bewirkt. Die Zugabe von spezifischer DNA zu der in der katalytischen Domäne doppelt markierten BsoBI Variante A153C verursacht dabei eine Abnahme des FRET-Effekts. Dieses Ergebnis weist darauf hin, dass sich beim Binden der spezifischen DNA die Fluorophore an Position 153 voneinander entfernen. Bei der in der helikalen Domäne markierten BsoBI Variante E100C ändert sich der FRET-Effekt bei der Zugabe spezifischer DNA nicht; dies deutet darauf hin, dass in diesem Bereich keine Konformationsänderung stattfindet. Die *steady-state* FRET-Experimente machen auch den Einfluss der zweiwertigen Metallionen Ca^{2+} und Mg^{2+} auf die Konformation der katalytischen Domäne deutlich. Ca^{2+} induziert eine Konformationsänderung der katalytischen Domäne, so dass sich die Fluorophore an Position 153 näher kommen. Die Zugabe von Mg^{2+} hat keinen Effekt auf die Konformation von BsoBI.

Die Konformationsänderung bei der Substratbindung und Spaltung, wie auch der Einfluss der Metallionen, wurden darüber hinaus mittels *pre-steady-state* Experimenten untersucht, bei denen doppelt markiertes Protein und unmarkierte DNA oder aber markierte DNA und einfach markierte BsoBI Varianten eingesetzt wurden. Diese Experimente bestätigen den beobachteten Einfluss der DNA-Bindung auf die Konformation der katalytischen Domäne. Des Weiteren konnte mit Hilfe des entwickelten kinetischen Models der DNA-Bindung und Spaltung das Vorliegen von mindestens zwei Konformationen des freien Enzyms aufgedeckt werden. Eine dieser Konformationen wurde als kompetent, die andere als inkompetent für die Substratbindung eingestuft. Die Ergebnisse der *pre-steady-state* Experimente zeigen auch, dass die zweiwertigen Metallionen Ca^{2+} und Mg^{2+} mit unterschiedlicher Affinität gebunden werden, dabei bindet Ca^{2+} im Vergleich zu Mg^{2+} fester und schneller.

Anschließende fluoreszenzspektroskopische Einzelmolekülmessungen bestätigten schließlich die Existenz von zwei unterschiedlichen Konformationen des BsoBI Apoenzyms und ermöglichten weiterhin, die relative Größe der beiden Subpopulationen zu quantifizieren. Die Analyse der Einzelmolekülmessungen mit Hilfe verschiedener Zeitfenster zeigte eine langsame Umwandlung der beiden Konformationen des Apoenzyms bei Raumtemperatur an, dies steht im Einklang mit dem beobachtete Einfluss der Temperatur auf die K_M-Werte bei der Michaelis-Menten-Analyse. Ferner konnten die Einzelmolekülmessungen mehr als eine Konformation und somit unterschiedliche Bindungsmodi nachweisen, wenn BsoBI an unspezifische DNA bindet.

Durch die Kombination unterschiedlicher fluoreszenzspektroskopischer Techniken und die gezielte Auswahl geeigneter modifizierter BsoBI Varianten war es so möglich, die Konformationsdynamik bei der Bindung und Spaltung der Substrat-DNA von BsoBI aufzuklären und zu modellieren. Dabei waren vor allem die Richtung der Konformationsänderung bei der DNA-Bindung sowie der Einfluss der Metallionen auf die Konformation überraschend.

7. References

1. Arber, W., *Host controlled variation*, In *The Bacteriophage Lambda*, A.D. Hershey, Editor. 1971, Cold Spring Harbor Lab. Press: New York. p. 83-96.
2. Wood, W.B., *Host specificity of DNA produced by Escherichia coli: bacterial mutations affecting the restriction and modification of DNA.* J Mol Biol, 1966. **16**(1): p. 118-33.
3. Wilson, G.G.,N.E. Murray, *Restriction and modification systems.* Annu Rev Genet, 1991. **25**: p. 585-627.
4. Arber, W., *Promotion and limitation of genetic exchange.* Science, 1979. **205**(4404): p. 361-5.
5. Pingoud, A., M. Fuxreiter, V. Pingoud,W. Wende, *Type II restriction endonucleases: structure and mechanism.* Cell Mol Life Sci, 2005. **62**(6): p. 685-707.
6. Pingoud, A.,A. Jeltsch, *Structure and function of type II restriction endonucleases.* Nucleic Acids Res, 2001. **29**(18): p. 3705-27.
7. Bickle, T.A.,D.H. Kruger, *Biology of DNA restriction.* Microbiol Rev, 1993. **57**(2): p. 434-50.
8. Raleigh, E.A., Brooks, J.E., *Restriction modification systems: where they are and what they do*, In *Bacterial genomes : physical structure and analysis*, F.J.d. Bruijn, J.R. Lupski, and G.M. Weinstock, Editors. 1998, Chapman & Hall: New York. p. 78-92.
9. Van Etten, J.L., *Unusual life style of giant chlorella viruses.* Annu Rev Genet, 2003. **37**: p. 153-95.
10. Roberts, R.J., T. Vincze, J. Posfai,D. Macelis, *REBASE--enzymes and genes for DNA restriction and modification.* Nucleic Acids Res, 2007. **35**(Database issue): p. D269-70.
11. Stein, D.C., J.S. Gunn, M. Radlinska,A. Piekarowicz, *Restriction and modification systems of Neisseria gonorrhoeae.* Gene, 1995. **157**(1-2): p. 19-22.
12. Jeltsch, A., *Maintenance of species identity and controlling speciation of bacteria: a new function for restriction/modification systems?* Gene, 2003. **317**(1-2): p. 13-6.
13. Marinus, M.G., *DNA methylation in Escherichia coli.* Annu Rev Genet, 1987. **21**: p. 113-31.
14. Barras, F.,M.G. Marinus, *The great GATC: DNA methylation in E. coli.* Trends Genet, 1989. **5**(5): p. 139-43.
15. Jones, M., R. Wagner,M. Radman, *Mismatch repair of deaminated 5-methyl-cytosine.* J Mol Biol, 1987. **194**(1): p. 155-9.
16. Lieb, M., *Bacterial genes mutL, mutS, and dcm participate in repair of mismatches at 5-methylcytosine sites.* J Bacteriol, 1987. **169**(11): p. 5241-6.
17. Roberts, R.J*., et al.*, *A nomenclature for restriction enzymes, DNA methyltransferases, homing endonucleases and their genes.* Nucleic Acids Res, 2003. **31**(7): p. 1805-12.
18. Dryden, D.T., N.E. Murray,D.N. Rao, *Nucleoside triphosphate-dependent restriction enzymes.* Nucleic Acids Res, 2001. **29**(18): p. 3728-41.
19. Murray, N.E., *Type I restriction systems: sophisticated molecular machines (a legacy of Bertani and Weigle).* Microbiol Mol Biol Rev, 2000. **64**(2): p. 412-34.
20. Meisel, A*., et al.*, *Type III restriction endonucleases translocate DNA in a reaction driven by recognition site-specific ATP hydrolysis.* EMBO J, 1995. **14**(12): p. 2958-66.
21. Stewart, F.J., D. Panne, T.A. Bickle,E.A. Raleigh, *Methyl-specific DNA binding by McrBC, a modification-dependent restriction enzyme.* J Mol Biol, 2000. **298**(4): p. 611-22.

22. Sutherland, E., L. Coe,E.A. Raleigh, *McrBC: a multisubunit GTP-dependent restriction endonuclease.* J Mol Biol, 1992. **225**(2): p. 327-48.
23. Pingoud, A.,A. Jeltsch, *Recognition and cleavage of DNA by type-II restriction endonucleases.* Eur J Biochem, 1997. **246**(1): p. 1-22.
24. Perona, J.J., *Type II restriction endonucleases.* Methods, 2002. **28**(3): p. 353-64.
25. Imhof, P., S. Fischer,J.C. Smith, *Catalytic mechanism of DNA backbone cleavage by the restriction enzyme EcoRV: a quantum mechanical/molecular mechanical analysis.* Biochemistry, 2009. **48**(38): p. 9061-75.
26. Williams, R.J., *Restriction endonucleases: classification, properties, and applications.* Mol Biotechnol, 2003. **23**(3): p. 225-43.
27. Gowers, D.M., S.R. Bellamy,S.E. Halford, *One recognition sequence, seven restriction enzymes, five reaction mechanisms.* Nucleic Acids Res, 2004. **32**(11): p. 3469-79.
28. Chandrasegaran, S.,H.O. Smith, *Amino acid sequence homologies among twenty-five restriction endonucleases and methylases*, In *Structure and Expression. From proteins to ribosomes*, R.H. Sarma and M.H. Sarma, Editors. 1988, Adenine Press: New York. p. 149-156.
29. Lauster, R., T.A. Trautner,M. Noyer-Weidner, *Cytosine-specific type II DNA methyltransferases. A conserved enzyme core with variable target-recognizing domains.* J Mol Biol, 1989. **206**(2): p. 305-12.
30. Bestor, T., A. Laudano, R. Mattaliano,V. Ingram, *Cloning and sequencing of a cDNA encoding DNA methyltransferase of mouse cells. The carboxyl-terminal domain of the mammalian enzymes is related to bacterial restriction methyltransferases.* J Mol Biol, 1988. **203**(4): p. 971-83.
31. Lauster, R., *Evolution of type II DNA methyltransferases. A gene duplication model.* J Mol Biol, 1989. **206**(2): p. 313-21.
32. Posfai, J., A.S. Bhagwat, G. Posfai,R.J. Roberts, *Predictive motifs derived from cytosine methyltransferases.* Nucleic Acids Res, 1989. **17**(7): p. 2421-35.
33. Klimasauskas, S., J.L. Nelson,R.J. Roberts, *The sequence specificity domain of cytosine-C5 methylases.* Nucleic Acids Res, 1991. **19**(22): p. 6183-90.
34. Wilke, K.*, et al.*, *Sequential order of target-recognizing domains in multispecific DNA-methyltransferases.* EMBO J, 1988. **7**(8): p. 2601-9.
35. Ruan, H.*, et al.*, *Cloning and sequence comparison of AvaI and BsoBI restriction-modification systems.* Mol Gen Genet, 1996. **252**(6): p. 695-9.
36. Ruan, H., K.D. Lunnen, J.J. Pelletier,S. Xu, *Overexpression of BsoBI restriction endonuclease in E. coli, purification of the recombinant BsoBI, and identification of catalytic residues of BsoBI by random mutagenesis.* Gene, 1997. **188**(1): p. 35-9.
37. Roberts, R.J.,D. Macelis, *REBASE--restriction enzymes and methylases.* Nucleic Acids Res, 1996. **24**(1): p. 223-35.
38. van der Woerd, M.J., J.J. Pelletier, S. Xu,A.M. Friedman, *Restriction enzyme BsoBI-DNA complex: a tunnel for recognition of degenerate DNA sequences and potential histidine catalysis.* Structure, 2001. **9**(2): p. 133-44.
39. Aggarwal, A.K., *Structure and function of restriction endonucleases.* Curr Opin Struct Biol, 1995. **5**(1): p. 11-9.
40. Xie, X.S.,J.K. Trautman, *Optical studies of single molecules at room temperature.* Annu Rev Phys Chem, 1998. **49**: p. 441-80.
41. Lakowicz, J.R., *Principles of fluorescence spectroscopy*. 3rd ed. 2006, New York: Springer. xxvi, 954 p.
42. Mukhopadhyay, S.,A.A. Deniz, *Fluorescence from diffusing single molecules illuminates biomolecular structure and dynamics.* J Fluoresc, 2007. **17**(6): p. 775-83.

43. Moerner, W.E.,M. Orrit, *Illuminating single molecules in condensed matter.* Science, 1999. **283**(5408): p. 1670-6.
44. Xie, X.S., *Single-Molecule Spectroscopy and Dynamics at Room Temperature.* Accounts of Chemical Research, 1996. **29**(12): p. 598-606.
45. Weiss, S., *Fluorescence spectroscopy of single biomolecules.* Science, 1999. **283**(5408): p. 1676-83.
46. Roy, R., S. Hohng,T. Ha, *A practical guide to single-molecule FRET.* Nat Methods, 2008. **5**(6): p. 507-16.
47. Lakowicz, J.R.,G. Weber, *Quenching of protein fluorescence by oxygen. Detection of structural fluctuations in proteins on the nanosecond time scale.* Biochemistry, 1973. **12**(21): p. 4171-9.
48. Wagner, G., *Characterization of the distribution of internal motions in the basic pancreatic trypsin inhibitor using a large number of internal NMR probes.* Q Rev Biophys, 1983. **16**(1): p. 1-57.
49. Englander, S.W.,N.R. Kallenbach, *Hydrogen exchange and structural dynamics of proteins and nucleic acids.* Q Rev Biophys, 1983. **16**(4): p. 521-655.
50. Benkovic, S.J.,S. Hammes-Schiffer, *Biochemistry. Enzyme motions inside and out.* Science, 2006. **312**(5771): p. 208-9.
51. Hammes-Schiffer, S.,S.J. Benkovic, *Relating protein motion to catalysis.* Annu Rev Biochem, 2006. **75**: p. 519-41.
52. Frauenfelder, H., S.G. Sligar,P.G. Wolynes, *The energy landscapes and motions of proteins.* Science, 1991. **254**(5038): p. 1598-603.
53. Winkler, F.K.*, et al.*, *The crystal structure of EcoRV endonuclease and of its complexes with cognate and non-cognate DNA fragments.* EMBO J, 1993. **12**(5): p. 1781-95.
54. Newman, M.*, et al.*, *Structure of restriction endonuclease bamhi phased at 1.95 A resolution by MAD analysis.* Structure, 1994. **2**(5): p. 439-52.
55. Viadiu, H.,A.K. Aggarwal, *The role of metals in catalysis by the restriction endonuclease BamHI.* Nat Struct Biol, 1998. **5**(10): p. 910-6.
56. Boehr, D.D., H.J. Dyson,P.E. Wright, *An NMR perspective on enzyme dynamics.* Chem Rev, 2006. **106**(8): p. 3055-79.
57. Th. Förster, *Zwischenmolekulare Energiewanderung und Fluoreszenz.* Annalen der Physik, 1948. **437**(1-2): p. 55-75.
58. Stryer, L.,R.P. Haugland, *Energy transfer: a spectroscopic ruler.* Proc Natl Acad Sci U S A, 1967. **58**(2): p. 719-26.
59. Selvin, P.R., *Fluorescence resonance energy transfer.* Methods Enzymol, 1995. **246**: p. 300-34.
60. Selvin, P.R., *The renaissance of fluorescence resonance energy transfer.* Nat Struct Biol, 2000. **7**(9): p. 730-4.
61. Ha, T.*, et al.*, *Probing the interaction between two single molecules: fluorescence resonance energy transfer between a single donor and a single acceptor.* Proc Natl Acad Sci U S A, 1996. **93**(13): p. 6264-8.
62. Nie, S.,R.N. Zare, *Optical detection of single molecules.* Annu Rev Biophys Biomol Struct, 1997. **26**: p. 567-96.
63. Yang, H.*, et al.*, *Protein conformational dynamics probed by single-molecule electron transfer.* Science, 2003. **302**(5643): p. 262-6.
64. Hanson, J.A.*, et al.*, *Illuminating the mechanistic roles of enzyme conformational dynamics.* Proc Natl Acad Sci U S A, 2007. **104**(46): p. 18055-60.
65. Rothwell, P.J.*, et al.*, *Multiparameter single-molecule fluorescence spectroscopy reveals heterogeneity of HIV-1 reverse transcriptase:primer/template complexes.* Proc Natl Acad Sci U S A, 2003. **100**(4): p. 1655-60.

66. Weiss, S., *Measuring conformational dynamics of biomolecules by single molecule fluorescence spectroscopy.* Nat Struct Biol, 2000. **7**(9): p. 724-9.
67. Kirsch, R.D.,E. Joly, *An improved PCR-mutagenesis strategy for two-site mutagenesis or sequence swapping between related genes.* Nucleic Acids Res, 1998. **26**(7): p. 1848-50.
68. Clegg, R.M., *Fluorescence resonance energy transfer and nucleic acids.* Methods Enzymol, 1992. **211**: p. 353-88.
69. Kuzmic, P., *Program DYNAFIT for the analysis of enzyme kinetic data: application to HIV proteinase.* Anal Biochem, 1996. **237**(2): p. 260-73.
70. Widengren, J*., et al.*, *Single-molecule detection and identification of multiple species by multiparameter fluorescence detection.* Anal Chem, 2006. **78**(6): p. 2039-50.
71. Antonik, M., S. Felekyan, A. Gaiduk,C.A. Seidel, *Separating structural heterogeneities from stochastic variations in fluorescence resonance energy transfer distributions via photon distribution analysis.* J Phys Chem B, 2006. **110**(13): p. 6970-8.
72. Allen, W.J., P.J. Rothwell,G. Waksman, *An intramolecular FRET system monitors fingers subdomain opening in Klentaq1.* Protein Sci, 2008. **17**(3): p. 401-8.

Supplementary information

The sequence of the wild type BsoBI restriction enzyme, without the His-tag is given below:

L N T Q K P F E N H L K S V D D L K T T Y E E Y R A G F I A F A L E K N K R S T P Y
I E R A R A L K V A A S V A K T P K D L L Y L E D I Q D A L L Y A S G I S D K A K K
F L T E D D K K E S I N N L I E N F L E P A G E E F I D E L I F R Y L L F Q G D S L G
G T M R N I A G A L A Q Q K L T R A I I S A L D I A N I P Y K W L D S R D K K Y T N
W M D K P E D D Y E L E T F A K G I S W T I N G K H R T L M Y N I T V P L V K K N
V D I C L F N C E P E I Y T P Q K V H Q Q P E K Y L L L G E L K G G I D P A G A D E
H W K T A N T A L T R I R N K F S E K G L S P K T I F I G A A I E H S M A E E I W D
Q L Q S G S L T N S A N L T K T E Q V G S L C R W I I N I

The sequence of the wild type BsoBI restriction enzyme, with the His-tag is given below. The His-tag (5 histidines) is shown in red. The His-tagged variant has five additional amino acids, as well as serine residue introduced instead of the N-terminal leucine, in order to create a BamHI cleavage site. Additional amino acids are shown in green.

M K H H H H H M H A K G S N T Q K P F E N H L K S V D D L K T T Y E E Y R A G
F I A F A L E K N K R S T P Y I E R A R A L K V A A S V A K T P K D L L Y L E D I Q
D A L L Y A S G I S D K A K K F L T E D D K K E S I N N L I E N F L E P A G E E F I D
E L I F R Y L L F Q G D S L G G T M R N I A G A L A Q Q K L T R A I I S A L D I A N I
P Y K W L D S R D K K Y T N W M D K P E D D Y E L E T F A K G I S W T I N G K H
R T L M Y N I T V P L V K K N V D I A L F N S E P E I Y T P Q K V H Q Q P E K Y L L
L G E L K G G I D P A G A D E H W K T A N T A L T R I R N K F S E K G L S P K T I F
I G A A I E H S M A C E I W D Q L Q S G S L T N S A N L T K T E Q V G S L A R W I I
N I

Oligonucleotides used for steady state and stopped-flow experiments are presented in Table 10.

Table 10

	Sequence
Tri-sub-up	5’-GACCACACCCGTCAGCTGATATCTCGAGGCCGGACGCAT-3’
Tri-sub-low	5’-ATGCGTCCGGCCTCGAGATATCAGCTGACGGGTGTGGTC-3’
wt2006 upper	5’-TCTATGTCGGGTGCGGAGAAAGAGGTAATGAAATGGCAG-3’
wt2006 lower	5’-CTGCCATTTCATTACCTCTTTCTCCGCACCCGACATAGA-3’

Tri-sub-up/low is a specific oligonucleotide, with one BsoBI recognition site (marked in red box in Table 10), while wt2006 upper/lower is an unspecific oligonucleotide, with no BsoBI recognition site. For production of labeled oligonucleotides, lower strands were labeled at the 5’ end with the Alexa594 fluorophore, annealed with unlabeled upper strand, and used in stopped flow experiments.

Oligonucleotides used for single molecule experiments are presented in Table 11.

Table 11

	Sequence
BsoBI sub12	5’-ATACTCGAGTAT-3’ 3'-TATGAGCTCATA-5'
RV-A11	5'-AAAGATATCTT-3' 3'- TTCTATAGAAA-5'

BsoBI sub12 is a specific, self-complementary oligonucleotide, with one BsoBI recognition site, while RV-A11 is an unspecific oligonucleotide, without BsoBI recognition site.

Primers used for site specific mutagenesis are presented in Table 12.

Table 12

	Sequence	Marker enzyme
BsoBI_S298C	5’-TATGGGACCAACTGCAG TGCGGTTCATTAACAAAC-3’	PstI
BsoBI_S54C	5’-CATTAAAAGTTGCTGCA TGCGTTGCAAAAACACCA-3’	SphI
BsoBI_E108C	5’-CTTTTTGGAACCTGCCG GCTGCGAGTTTATAGACG-3’	NaeI
BsoBI_E100C	5’-AGGAGTCTATAAATAATCTCA	NdeI

	TATGTAACTTTTTGGAACCTGC-3’	
BsoBI_A153C	5’-ATAATCTCTGCCTTGGACATA TGTAATATCCCTTATAAATGG-3’	NdeI
BsoBI_R318C	5’-ACTGAACAAGTAGGGTCTCTCG CGTGTTGGATAATTAATATATAA-3’	BsaI
BsoBI_E290C	5'-ATTGAGCATAGTATGGCATG CGAAATATGGGACCAACTT-3’	SphI
BsoBI_D212N	5’-GTTCCACTTGTAAAAAAGA ACGTTAATATCGCGTTATTT-3’	AclI
BsoBI_D212A	5‘-GTTCCACTTGTAAAAAAGA ACGTTGCTATCGCGTTATTT-3‘	AclI
BsoBI_H253Q	5‘-CCTGCTGGAGCGGATGAG CAATGGAAAACAGCAAATACT-3‘	BsrDI

Primers used to create the 237 bp long PCR fragment (using the plasmid pAT153 triple as a template), used in EMSA experiments, are listed in Table 13.

Table 13

	Sequence
lin diff kurz 3'	5'-ATAGGCGCCAGCAACCGCACCTGTG-3'
lin diff 1.5 for	5'-ATCGCCAGTCACTATGGCGTGC-3'

Primers used to amplify the region of BsoBI containing mutations for screenings are listed in Table 14.

Table 14

	Sequence
pQEfor	5'-GTATCACGAGGCCCTTTCGTCT-3'
pQErev	5'-CATTACTGGATCTATCAACAGGAG-3'

All unlabeled oligos were purchased from Biomers, while labeled oligos were purchased from IBA.

The model of metal ion exchange, with the assumption that the exchange of Mg^{2+} is slow and the exchange of Ca^{2+} is fast, is presented in the following equations:

$$E + Mg \underset{k_{-1}}{\overset{k_1}{\rightleftharpoons}} EMg \qquad E + Ca \underset{k_{-2}}{\overset{k_2}{\rightleftharpoons}} ECa$$

$[EMg] = x$

$E_0 = [EMg] + [ECa] + [E]\ ;\ [E] \ll E_0$

$\Rightarrow [ECa] = E_0 - x$

$$\frac{dx}{dt} = k1\cdot[E]\cdot Mg - k_{-1}\cdot x \qquad (1)$$

$$\frac{d(E_0 - x)}{dt} = k_2\cdot[E]\cdot Ca - k_{-2}\cdot(E_0 - x) = k_2\cdot[E]\cdot Ca - k_{-2}\cdot E_0 + k_{-2}\cdot x$$

$$\frac{dx}{dt} = -k_2\cdot[E]\cdot Ca + k_{-2}\cdot E_0 - k_{-2}\cdot x \qquad (2)$$

(1) + (2) $k_1\cdot[E]\cdot Mg - k_{-1}\cdot x = -k_2\cdot[E]\cdot Ca + k_{-2}\cdot E_0 - k_{-2}\cdot x$

$[E]\cdot(k_1\cdot Mg + k_2\cdot Ca) = k_{-2}\cdot E_0 + x\cdot(k_{-1} - k_{-2})$

$$[E]\cdot Mg = \frac{1}{k_1 + \frac{Ca}{Mg}}\cdot[k_{-2}\cdot E_0 + x\cdot(k_{-1} - k_{-2})] \qquad (3)$$

(1) + (3) $$\frac{dx}{dt} = \frac{k_1}{k_1 + \frac{Ca}{Mg}}\cdot[k_{-2}\cdot E_0 + x\cdot(k_{-1} - k_{-2})] - k_{-1}\cdot x$$

$$\frac{dx}{dt} = \frac{k_1\cdot k_{-2}\cdot E_0}{k_1 + k_2\cdot\frac{Ca}{Mg}} + x\cdot\left[\frac{k_1\cdot(k_{-1} - k_{-2})}{k_1 + k_2\cdot\frac{Ca}{Mg}} - k_{-1}\right]$$

$$\frac{dx}{dt} = \frac{k_1\cdot k_{-2}\cdot E_0}{k_1 + k_2\cdot\frac{Ca}{Mg}} + x\cdot\frac{1}{k_1 + k_2\cdot\frac{Ca}{Mg}}\cdot(k_1\cdot k_{-1} - k_1\cdot k_{-2} - k_1\cdot k_{-1} - k_{-1}\cdot k_2\cdot\frac{Ca}{Mg})$$

$$\frac{dx}{dt} + \frac{k_1\cdot k_{-2} + k_{-1}\cdot k_2\cdot\frac{Ca}{Mg}}{k_1 + k_2\cdot\frac{Ca}{Mg}}\cdot x = \frac{k_1\cdot k_{-2}\cdot E0}{k_1 + k_2\cdot\frac{Ca}{Mg}}$$

$$\Rightarrow\ k = \frac{k_1\cdot k_{-2} + k_{-1}\cdot k_2\cdot\frac{Ca}{Mg}}{k_1 + k_2\cdot\frac{Ca}{Mg}} \qquad (4)$$

Hypothesis 1: the binding of Mg^{2+} to the enzyme is faster than the binding of Ca^{2+}; then: $k_1 >> k_2$, and equation (4) becomes:

$$k = \frac{k_1\cdot k_{-2} + k_{-1}\cdot k_2\cdot\frac{Ca}{Mg}}{k_1}$$

$$k = k_{-2} + \frac{k_{-1} \cdot k_2}{k_1} \cdot \frac{Ca}{Mg}$$

When the concentration of Ca^{2+} increases, and the concentration of Mg^{2+} is constant, the rate constant would increase; vice versa, with the increase of the Mg^{2+} concentration, the rate constant would decrease. However, the experimental data show a different metal ion influence on the rate constant (Figure 3.24).

Hypothesis 2: the binding of Ca^{2+} to the enzyme is faster than the binding of Mg^{2+}; then: $k_2 >> k_1$, and equation (4) becomes:

$$k = \frac{k_1 \cdot k_{-2} + k_{-1} \cdot k_2 \cdot \frac{Ca}{Mg}}{k_2 \cdot \frac{Ca}{Mg}}$$

$$k = \frac{k_1 \cdot k_{-2} \cdot Mg + k_{-1} \cdot k_2 \cdot Ca}{k_2 \cdot Ca}$$

$$k = k_{-1} + \frac{k_1 \cdot k_{-2}}{k_2} \cdot \frac{Mg}{Ca}$$

When the concentration of Ca^{2+} increases, and the concentration of Mg^{2+} is constant, the rate constant would decrease; vice versa, with the increase of the Mg^{2+} concentration, the rate constant would increase. This dependence is shown in Figure 3.24.

Publications

J. Dikic, K. Welsch, E. Sisamakis, P. Rothwell, S. Felekyan, W. Wende, C. Seidel, and A. Pingoud, *"Conformational dynamics of the restriction endonuclease BsoBI involved in DNA binding and cleavage – analyzed by ensemble and single molecule experiments"* , in preparation

Poster presentations

2008 (August): Gordon Research Conference "Single molecule approaches to biology", New London, New Hampshire, USA; "The conformational changes accompanying substrate binding and cleavage by the Type IIP restriction endonucleases"

2008 (December): 3rd Marie Curie Workshop "Single-molecule techniques", University of York, York, England; "The conformational changes accompanying substrate binding and cleavage by the Type IIP restriction endonucleases"

Oral presentations

2006 (September): 1st Annual Marie Curie Meeting, University of Bristol, Bristol, England

2007 (March): 1st Marie Curie Off-Spring Meeting, University of Giessen, Giessen, Germany

2007 (September): 2nd Annual and Mid-Term Marie Curie Meeting, Vilnius, Lithuania

2008 (April): 2nd Marie Curie Off-Spring Meeting, University of Newcastle, Newcastle, England

2008 (September): 3rd Annual Marie Curie Meeting, Berlin, Germany

2008 (December): 3rd Marie Curie Workshop "Single-molecule techniques", University of York, York, England

2009 (September): Final Annual Marie Curie Meeting, Budapest, Hungary